UNIVERSIDAD AUTÓNOMA DE MADRID

Facultad de Ciencias

Sección de Ingeniería Química

NANOPARTÍCULAS SINTETIZADAS EN MICROEMULSIÓN AGUA/AOT/ISOOCTANO Y SU APLICACIÓN EN HIDROTRATAMIENTOS EN FASE ACUOSA

NANOPARTICLES SYNTHESIZED IN WATER/AOT/ISOOCTANE MICROEMULSION FOR THEIR APPLICATION IN WATER HYDROTREATMENT REACTIONS

Tesis Doctoral

ANA MARÍA PÉREZ CORONADO

Madrid, 2017

UNIVERSIDAD AUTÓNOMA DE MADRID

Facultad de Ciencias

Sección de Ingeniería Química

NANOPARTÍCULAS SINTETIZADAS EN MICROEMULSIÓN AGUA/AOT/ISOOCTANO Y SU APLICACIÓN EN HIDROTRATAMIENTOS EN FASE ACUOSA

NANOPARTICLES SYNTHESIZED IN WATER/AOT/ISOOCTANE MICROEMULSION FOR THEIR APPLICATION IN WATER HYDROTREATMENT REACTIONS

MEMORIA

Para optar al grado de

Doctor
Mención Internacional

presenta

Ana María Pérez Coronado

Directores: Dra. Luisa Calvo Hernández
Dr. Miguel Ángel Gilarranz Redondo

Madrid, 2017

Dña. Luisa Calvo Hernández, Profesora Titular de Universidad, y **D. Miguel Ángel Gilarranz Redondo**, Profesor Titular de Universidad, ambos profesores de la Sección de Ingeniería Química perteneciente al Departamento de Química-Física Aplicada de la Universidad Autónoma de Madrid.

HACEN CONSTAR: que el presente trabajo, titulado "*Nanopartículas sintetizadas en microemulsion agua/AOT/isooctano y su aplicación en hidrotratamientos en fase acuosa",* presentado por D. Ana María Pérez Coronado, ha sido realizado bajo su dirección, en los laboratorios de la Sección de Ingeniería Química, en la Universidad Autónoma de Madrid, y que a su juicio reúne los requisitos de originalidad y rigor científico necesarios para ser presentado como Tesis Doctoral.

Y para que conste a efectos oportunos, firmamos el presente informe en Madrid, a 23 de mayo de 2017.

Luisa Calvo Hernández

Miguel Ángel Gilarranz Redondo

La realización de este trabajo ha sido posible gracias al apoyo económico prestado a través de los proyectos SusFuelCat, dentro del Séptimo Programa Marco de la Unión Europea para el desarrollo tecnológico y en el marco del acuerdo de subvención nº 310490, CTQ2012-32821 del Ministerio de Economía y Competitividad y CTQ2015-65491-R del Ministerio de Economía, Industria y Competitividad.

A mi familia y amigos

"La magia de librar batallas más allá de lo humanamente soportable se basa en lo mágico que resulta arriesgarlo todo por un sueño que nadie más alcanza a ver excepto tú"

Contents

List of Figures

List of Tables

Abbreviations

AC	activated carbon
AOT	sodium bis(2-ethylhexyl) sulfosuccinate
d_s	average mean diameters
IWI	incipient wetness impregnation
N_A	constant of Avogadro
NPs	nanoparticles
ME	microemulsion
MeOH	methanol
Pd	palladium
S_{Pd}	surface occupied by one Pd-atom
SSA_{Pd}	specific surface area of Pd
TEM	transmission electron microscopy
TGA	thermogravimetric analysis
THF	tetrahydrofuran
TFE	tri-fluoroethanol
TOF	turn-over-frequency
w_0	water-to-surfactant ratio
w/o	water-in-oil
XPS	X-Ray Photoelectron Spectroscopy
σ_s	standard deviation

OBJETIVOS Y RESUMEN

El objetivo principal de este trabajo es el estudio de la aplicación de nanopartículas (NPs) sintetizadas por el método de microemulsión (ME), para el desarrollo de catalizadores activos y selectivos en reacciones de hidrotratamiento en fase acuosa. Las aplicaciones seleccionadas para evaluar la actividad de estos catalizadores fueron la reducción con H_2 del ión nitrato (NO_3^-), nitrito (NO_2^-) —la especie intermedia en la reducción de NO_3^-— y bromato (BrO_3^-). Los catalizadores seleccionados para estos tratamientos se basaron en NPs de Pd y de Cu. La síntesis de NPs de Pd se optimizó con el objetivo de diseñar catalizadores basados en NPs de tamaños controlados para evaluar la sensibilidad estructural en las reacciones de hidrotratamiento, que es una de las bases para el diseño de catalizadores. Además, se estudió el efecto de la síntesis de las NPs y los soportes utilizados para inmovilizar las NPs en las reacciones.

La tesis comprende varios capítulos que se resumen a continuación. El *Capítulo I* describe los principales contaminantes del agua y su diferente clasificación según su naturaleza u origen. Se presta especial atención a los NO_3^-, NO_2^- y BrO_3^- y a sus principales fuentes de contaminación en las aguas superficiales y subterráneas. Por otra parte, se resumen los sistemas de tratamientos propuestos en bibliografía para la eliminación de estos contaminantes. De todos ellos, la reducción catalítica con H_2 se destaca como método prometedor que opera en condiciones suaves. En particular, se ha propuesto la hidrogenación catalítica con catalizadores basados en Pd para tratar NO_3^- y otros oxianiones (por ejemplo, NO_2^-, BrO_3^-, ClO_4^-). Por otra parte, se estudiaron las propiedades necesarias para sintetizar catalizadores diseñados racionalmente, con el fin de desarrollar NPs de tamaño controlado y evaluar su actividad en procesos de hidrotratamientos. En este *capítulo* también se analizan los procedimientos usuales para la síntesis de NPs metálicas, y las principales características del método de ME.

En el *Capítulo II* se describen los materiales utilizados para la síntesis de las NPs metálicas, así como los diferentes procedimientos llevados a cabo para la

preparación de los catalizadores. Además, se detallan las técnicas empleadas para la caracterización de los catalizadores y se describe el procedimiento experimental llevado a cabo en las reacciones de hidrotratamientos para la eliminación de NO_3^-, NO_2^- y BrO_3^-. Asimismo, se definen los métodos utilizados para el análisis de los reactivos y los productos de reacción.

En el *Capítulo III* se aborda el estudio de la síntesis de NPs de Pd mediante el método de ME de agua en aceite (w/o). La síntesis se lleva a cabo usando el sistema de ME de agua/sodio bis (2-etilhexil) sulfosuccinato (AOT)/isooctano. Se realizó un estudio de las principales variables que influyen en la síntesis y el control del tamaño de las NPs de Pd. Además, se estudió la influencia de diferentes métodos de purificación de las NPs en el tamaño de las mismas. La novedad de este procedimiento radica en la estrategia basada en el control de las operaciones físicas durante la síntesis, lo que proporciona conocimiento sobre: la influencia de la etapa de purificación de las NPs, el tiempo de reacción (reducción) y la temperatura durante la concentración de las NPs de Pd. Además, se evaluó el efecto cruzado entre las variables más comunes de la síntesis, como son: la relación agua-surfactante (w_0), la concentración de surfactante, la naturaleza del agente reductor y la relación molar agente reductor-metal. Los tamaños medios de NPs que se obtuvieron variaron entre 6,2 y 11,7 nm, observándose que el factor que más influye sobre el tamaño de las NPs es la relación w_0.

En el *Capítulo IV* se lleva a cabo la síntesis y uso como catalizador modelo de NPs de Pd de distintos tamaños sin soportar, en la reducción de NO_2^- en fase acuosa. En el rango de tamaños de NPs estudiadas (6,2-11,6 nm), se observó que las NPs de menor tamaño conducían a una menor velocidad de reacción y actividad (TOF). Esta aparente sensibilidad estructural es debida al bloqueo de la superficie de las NPs producida por la interacción del AOT, como se evidenció en la purificación de las NPs con varios disolventes, que proporcionó una eliminación diferente del AOT. La pérdida de actividad en la reducción de NO_2^- fue acompañada de una insignificante selectividad hacia NH_4^+. Las NPs de mayor

tamaño probadas en la reducción de NO_2^- en medio tamponado con CO_2 provocó una insignificante producción de NH_4^+ para altos valores de conversión de NO_2^-. El control de selectividad se atribuyó al bloqueo preferencial de los sitios responsables de la generación de NH_4^+. Los resultados mostraron que la interacción entre el AOT y las NPs es una herramienta para controlar la selectividad catalítica.

En el *Capítulo V*, las NPs de Pd sintetizadas controlando el tamaño por el método basado en el ME se soportaron en carbón activado (AC) y se usaron en la reducción de NO_2^-. El efecto bloqueante del AOT se atenuó por la inmovilización de las NPs en el soporte. Esto condujo a catalizadores con una actividad ligeramente inferior a la observada en los catalizadores de Pd/C preparados por impregnación de humedad incipiente (IWI). Sin embargo, la interacción entre las NPs de Pd y el AOT permitió el bloqueo de centros activos responsables de la generación de NH_4^+ y estos catalizadores produjeron una selectividad insignificante hacia el NH_4^+. Para conocer mejor el papel del AOT, se aplicaron algunos tratamientos térmicos a los catalizadores para eliminar el AOT y aumentar la actividad, aunque también se observó una mayor producción de NH_4^+.

El *Capítulo VI* estudia la viabilidad de la reducción de NO_3^- mediante el empleo de las NPs de Pd-AOT soportadas, dado que tienen la propiedad característica de reducir la especie intermedia NO_2^- con una selectividad despreciable a NH_4^+. Los catalizadores bimetálicos de Pd:Cu y los monometálicos de Pd y Cu, todos ellos soportados sobre AC, fueron preparados siguiendo diferentes métodos. Los catalizadores que contenían una fase de Pd que había sido expuesta al AOT en algún momento de su preparación, mostraron una actividad más baja que aquellos que fueron sintetizados mediante IWI. No obstante, estos catalizadores demostraron ser altamente activos en la reducción de NO_2^-. La fuerte interacción entre el Pd y el AOT bloquea la reacción del par redox Pd:Cu, impidiendo la formación del Cu en su estado metálico. Esto provoca la disminución de la actividad en la reducción de NO_3^-.

En el *Capítulo VII* se aborda la síntesis de NPs de Pd, mediante ME agua/AOT/isooctano usando diferentes relaciones de w_0, como catalizadores en la reacción de reducción de BrO_3^-. Con el fin de minimizar la influencia del AOT, las NPs de Pd se inmovilizaron en diferentes soportes: AC, nanotubos de carbono de pared múltiple (CNT) y dióxido de titanio (TiO_2). Además, estos catalizadores fueron sometidos a diferentes tratamientos térmicos en aire y N_2. La inmovilización de las NPs de Pd sobre TiO_2 condujo a una mayor actividad que la obtenida para los soportes basados en carbono. El tratamiento térmico de los catalizadores a 673 K en aire eliminó exitosamente el AOT y los residuos generados por su descomposición, dando lugar a un aumento significativo de la actividad. Por otra parte, el TiO_2 fue sometido a un tratamiento térmico en atmósfera de aire a 773 K provocando una variación en las proporciones de la fase rutilo y anatasa respecto al TiO_2. La actividad de las NPs inmovilizadas sobre el TiO_2 tratado térmicamente se vio afectada. Los experimentos realizados a cabo con las NPs de Pd sintetizadas con diferente relación de w_0 y soportadas no evidenciaron sensibilidad a la estructura.

El capítulo *Conclusiones* y *Trabajos Futuros* se recogen las principales conclusiones recabadas durante el progreso de la tesis. Además se detallan una serie de previsiones futuras de investigación para avanzar en los conocimientos generados durante el desarrollo de la presente tesis.

OBJECTIVES AND SUMMARY

The main objective of this work is to study the application of nanoparticles (NPs) synthesized by the microemulsion method (ME) in the development of active and selective catalysts for the hydrotreatment of water. The applications selected to evaluate the performance of the catalysts prepared were the reduction with H_2 of nitrate (NO_3^-), nitrite (NO_2^-)— the intermediate species in the reduction of NO_3^-—- and bromate (BrO_3^-). The catalysts selected for these applications were based on Pd NPs, including also Cu in the case of the reduction of NO_3^-. The synthesis of Pd NPs was optimized in order to prepare catalysts based on NPs of different size suitable to evaluate the structure sensitiveness of the reactions, which is one of the basis for the design of catalysts. The role of the reagents used during the synthesis of the NPs and the supports used to immobilize the NPs was also studied.

The thesis comprises several chapters that are summarized below. *Chapter I* describes the main water pollutants and their different classification according to their nature or origin. Special attention is given to NO_3^-, NO_2^- and BrO_3^-, and to their sources in relation to surface and ground water pollution. The treatments proposed for the removal of these pollutants are also revised. The catalytic reduction with H_2 is highlighted as a promising method operating at mild conditions. In particular, catalytic hydrogenation with Pd-based bimetallic catalysts has been widely proposed for treating NO_3^- and other oxyanions (e.g. NO_2^-, BrO_3^-, ClO_4^-). The characteristics demanded for efficient catalysts to be applied in the hydrotreatment of water and the potential of rationally designed catalysts, i.e. those based in growth controlled NP, are commented. This chapter also revises the usual procedures for the synthesis of metallic NPs, and the main features of the ME method.

Chapter II describes the experimental methods, including the materials used, the procedures for the synthesis and characterization of metallic NPs and catalysts

preparation, the experimental set-up used in the experiments for the hydrotreatment of NO_3^-, NO_2^- and BrO_3^-; and the methods for the analysis of reagents and reaction products.

In *Chapter III* the control of the characteristics of Pd NPs via w/o ME synthesis is evaluated. The Pd NPs were synthesized using the water/sodium bis(2-ethylhexyl) sulfosuccinate (AOT)/isooctane microemulsion system. A multiple approach for the control and assessment of the size of Pd NPs was designed, including the variables affecting the synthesis and the purification of the NPs. The novelty of the strategy lays on the control of the physical operations during the synthesis, which provides knowledge about the influence of the NPs purification stage, the reaction (reduction) time and the temperature during the concentration of the Pd NPs. Moreover, the crossed effect of the most common variables, such as water-to-surfactant ratio (w_o), surfactant concentration, nature of the reducing agent and reducing agent-to-metal molar ratio was also evaluated. NPs with a mean size between 6.2 and 11.7 nm were obtained, being w_o the most influencing factor.

Chapter IV deals with the application of unsupported Pd NPs as model catalysts for the reduction of NO_2^-. In the NP size range studied (6.2-11.6 nm) a lower reaction rate and turn-over frequency (TOF) were observed for small NPs. This apparent structure sensitiveness results from blockage due to interaction of AOT with the surface of nanoparticles, as evidenced by purification with several solvents providing different removal of AOT. The activity loss was accompanied by negligible selectivity to ammonium. Large NPs in a reaction medium buffered with CO_2 produced insignificant amount of ammonium ion for high NO_2^- conversion values. The selectivity control was ascribed to preferential blockage of the sites responsible for ammonium generation. The results showed the potential of the interaction between the AOT and the NPs as a tool to control catalytic selectivity.

In *Chapter V* size-controlled Pd NPs synthesized by AOT-based w/o ME method were supported on activated carbon (AC) and used in NO_2^- reduction. The blocking effect of AOT was attenuated by the immobilization of the support,

which led to catalysts with an activity only slightly lower than that of Pd/C catalysts prepared by incipient wetness impregnation (IWI). However, the interaction between Pd NPs and AOT still allowed blocking of active centres responsible for ammonium generation and the catalysts yielded negligible selectivity towards ammonium. To gain insight into the role of AOT, some thermal treatments were applied to the catalysts to remove AOT and increase the activity, although a higher production of ammonium was also observed.

Chapter VI explores the applicability to the reduction of NO_3^- of the unique features of the supported Pd-AOT NPs, i.e. the negligible selectivity to ammonium in the reduction of intermediate species NO_2^-. Bimetallic Pd:Cu catalysts and monometallic Pd and Cu catalysts, all of them supported on AC, were prepared by different methods. The catalysts containing a Pd phase subjected to exposure to AOT at some stage of the preparation of the catalysts showed lower activity in the reduction of nitrate than the catalysts prepared by IWI. However, the catalysts showed still high activity in the reduction of NO_3^-. The strong interaction between Pd and AOT prevents the interaction between Pd and Cu. Therefore, the redox reaction needed to maintain Cu in metallic state is also prevented and the activity in NO_3^- reaction is low.

In *Chapter VII* immobilized Pd NPs synthesized via w/o ME using the water/AOT/isooctane system were used as catalysts in the BrO_3^- reduction reaction. In order to minimize the influence of AOT the Pd NPs were immobilised on different supports, namely AC, multi-walled carbon nanotubes (CNT) and titanium dioxide (TiO_2); and ddifferent thermal treatments in air and nitrogen were carried out. The immobilization of Pd NPs on TiO_2 led to higher activity than the immobilization on the carbon-based supports. Thermal treatment of the catalysts at 673 K in air removed successfully AOT and decomposition fragments, leading to a significant increase in activity. The activity of the catalysts was also affected by a thermal treatment of the TiO_2 support leading to different proportions of rutile and

anatase phases. The experiments with catalysts prepared with Pd NPs of different size did not evidence structure sensitiveness.

Conclusion Chapter summarizes the main conclusions generated during the development of the thesis.

CHAPTER I

Introduction

CHAPTER I

Introduction

Water is one of the most abundant components of nature, which has been present on Earth for more than 3000 million years, occupying three quarters of the surface of the planet [1]. It is the majority constituent of living things, the human body is made of 70 % of water. Water is vital for life and constitutes a precious natural resource. It is essential to most life processes and living organisms, to societal advancement and, equally, it is fundamental to innumerable economic, cultural, commercial and productive activities. Thus, there are continuing and changing demands from citizens, society, industry and agriculture for this basic resource. Global consumption of water is doubling every 20 years, which is more than twice the rate of human population growth [2].

The Earth is known as the "Blue Planet", however, according to the World Health Organization (WHO), more than thousand million people do not currently have access to drinking waterways. This contradiction is due to the freshwater shortage and its poor distribution in space and time [3]. The total volume of water on Earth is about $1{,}360 \cdot 10^6$ km^3, distributed as shown in **Figure 1.1**. As can be

seen, most of the water present on the planet is salty and is found in the oceans, constituting 97.5 % of the total water present on Earth. The remaining 2.5 % is freshwater, of which 68.9 % is in the form of ice in the polar ice caps and glaciers, while, 29.9 % is located in the ground as groundwater. The 0.3 % is found as continental water in lakes and rivers, only this water is removable. Finally, the rest (0.9 %) is presented in like Earth as other (i.e. atmosphere).

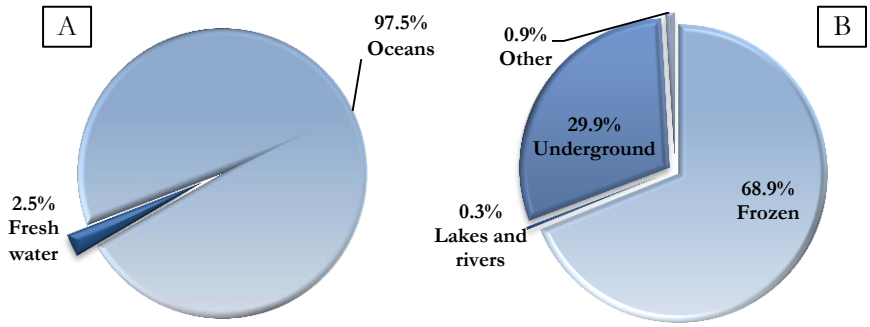

Figure 1.1. **A)** Water present on the planet and **B)** fresh water distribution.

Most of our demand for water is fulfilled by rain water, which gets deposited in surface and ground water resources. The quantity of this utilizable water is very much limited on the Earth. However, water is continuously purified by evaporation and precipitation, though the pollution of waster has emerged as one of the most significant environmental problems of the recent times. Nowadays, there is an increasing concern about the rapidly deteriorating supply of water and the fast decreasing of utilizable water. The causes of this situation are due to the urbanization, industrialization, agriculture and increase in human population.

The uses of water at a global level are reflected in **Figure 1.2**. Worldwide, agriculture accounts for 70 % of all water consumption, compared to 20 % for industry and 10 % for domestic use. In industrialized nations, however, industries consume more than half of the water available for human use. Spain, for example, uses 77 % of the water available for agriculture and the remaining 20 % is divided

between applications in the industrial sector (7 %) and domestic consumption (16 %).

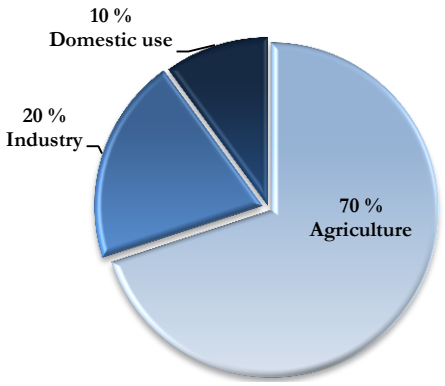

Figure 1.2. Distribution of water consumption in the world [4].

1.1. Water framework directive

Water is a vital resource for natural ecosystems and human life, and therefore, as stated by the European Union (EU) Water Framework Directive (WFD), a "heritage which must be protected, defended and treated as such"[5].

Water is both a right and a responsibility with economic, environmental and social value. The problem of water scarcity and its importance for the development of life have forced the necessity of establishing legal actions and developing efficient treatments to remove water pollutants or, alternatively, to convert them into friendly products for the environment.

At European level, in 2000, building on the achievements of existing EU water legislation, the WFD introduced new and ambitious objectives to protect aquatic ecosystems in a more holistic way, while considering the use of water for life and human development. "Directive 2000/60/EC" of the European Parliament and of the Council of 23 October 2000 establishing a framework for Community action in the field of water policy [6], and later supplemented and amended in Directive 2006/11/EC to force the members of the EU to achieve good qualitative

and quantitative status of all its water bodies by 2015. The WFD (2000/60/EC) has been transposed into Spanish law through the modification of Law 46/1999 and the revised text of the Water Law 1/2001 of 20 July by Article 129 of Law 62/2003 of 30 December regarding fiscal, administrative and social measures (Spanish Official Gazette (BOE) No. 313 of 31 December 2003)[7]. In this way, it is necessary to include the requirements on the observed list as defined in the Commission Implementing Decision (EU) 2015/495 of 20 March 2015 establishing a list of substances to be observed for the purpose of Monitoring in the field of water policy, in accordance with Directive 2008/105/EC of the European Parliament and of the Council.

Especially freshwater is limited in quantity and in quality, and currently under a variety of increasing pressures; for example, climate change, overexploitation and contamination from point and diffuse sources, including agriculture, industry and households. Ensuring a high quality of water and a high level of protection from chemical contamination is fully in line with the major societal goals presented by the 7th Environmental Action Plan of the EU "Living well within the limits of our planet" [8].

The trend of both Europe and Spain, especially after the enactment of Law 16/2002 (BOE, 2002) on Integrated Prevention and Control Pollution is to reduce the discharge of some specific pollutants and use advanced wastewater treatment systems "in situ". This Law is characterized by its horizontality, due to the diversity of industrial sectors that include the surface treatment as part of their productive process and/or subcontract to other job-shops (i.e. specialist surface treatment companies operating as subcontractors in the engineering industries). That is the reason why it is worth differentiating inside this activity from those industrial ones dedicated exclusively to this job and those that in spite of not being their main activity have auxiliary facilities with this intention.

In addition, the Law regulating the discharge of environmental quality standards for priority substances and other pollutants in Spain, BOE 817 / 2015, establishes the need to identify and define discharges pollution parameters.

1.2. Water pollution

Water pollution could be defined as a physical, chemical or biological factor causing aesthetic or detrimental effects on aquatic life and on those who consume the water [9].

In order to evaluate changes in quality, the so-called quality indicators are used, which can be physical, chemical or biological parameters. The physical indicators are color, turbidity, conductivity, temperature, taste and smell. The chemical indicators are pH, hardness, alkalinity and dry residue. Other indicators, apart from the previous ones, can be indicators of organic contamination (total organic carbon (TOC), biological oxygen demand (BOD), chemical oxygen demand (COD), N_2, nitrogen total Kjeldhal (NTK)) or the radioactivity indicator [9].

The main phenomena that cause water pollution are related to the growth of population centers by increasing the amount of wastewater; i) with the soils contamination; ii) with intensive cultivation of the land, due to excess nutrients carried rainwater or irrigation that reaches the aquifers; iii) with livestock, which generates important quantities of slurry; iv) with the generation of polluting of industrial wastes [10] and, v) with the contamination of aquifers by marine intrusion [11,12].

Water pollutants can be classified according to their nature or origin. According to their nature, water pollutants can be classified into three groups:

- *Physical pollutants* these can be also categorized as follows: solids type, turbidity, color, taste, temperature, etc. Each of these categories can have chemical or

biological sources. Physical pollutants recommended parameters are shown in **Table 1.1** and

- **Table 1.2** summarizes the typical composition of domestic wastewater with no industrial waste.

Table 1.1. Physical pollutant [13].

Pollutant	Public water supplies	
	Permissible	**Desirable**
Colour (units)	75	<10
Odour	Narrative	Virtually absent
Temperature	Narrative	Narrative
Turbidity	Narrative	Virtually absent

Table 1.2. Typical domestic wastewater composition [13].

Pollutant	Concentration (mg/L)		
	Weak	**Average**	**Strong**
Total solids	350	800	1200
Total suspended solids	100	240	350
Total dissolved solids	250	500	850
Settleable solids (mL/L)	5	10	20
Volatile suspended solids	80	180	280
Volatile dissolved solids	100	260	300
NH_3-N	10	20	35
Total N_2	20	35	80
Phosphorous	5	10	15
Alkalinity as $CaCO_3$	50	100	250
Oil , grease	50	100	150
5-day biochemical oxygen demand	120	225	400
COD	175	325	575

- *Biological pollutants,* all organisms that use oxygen for energy and cause disease, as can be bacteria, viruses, protozoa and helminths. The test can involve the measurement of either carbon content or oxygen demand, or an actual bacterial count.
- *Chemical pollutants* can be organic or inorganic. There are thousands of organic pollutants consisting of various combinations of carbon, H_2, and perhaps oxygen and/or many other inorganic or organic molecules. In general, organic

pollutants are more biodegradable with fewer carbon and/or other molecules attached. On the other hand, inorganic chemical pollutant can be categorized in metallic ions, predominantly Ca and Mg, cations such as Mn and Sr, anions such as nitrate (NO_3^-) and bromate (BrO_3^-), etc. The NO_3^- is from agricultural activity, particularly the breakdown of plant material in the soil when there is no plant growth to take up the released NO_3^-. BrO_3^- is very stable in water, and its presence is mainly due to the ozonation of Br^- containing water during the respective treatment for human consumption. Br^- has various natural and anthropogenic sources, such as seawater intrusion, pesticide run-off, industrial wastes and impurities from road deicing salts.

According to a classification based on their sources, the pollutants can be divided into:

- *Contaminants of agricultural origin*, agriculture is only one among various causes of non-point sources of pollution. However it is generally regarded as the largest contributor of pollutants of all the categories. Pollutants, irrespective of source, are transported overland and through the soil by rainwater and melting snow. Ultimately, these pollutants find their way into groundwater, wetlands, rivers and lakes and, finally, to oceans in the form of sediment and chemical loads carried by river.
- *Pollutants from urban areas*, these are basically urban wastewaters, which are characterized as complex aqueous solutions containing a large variety of organic and inorganic components, both dissolved and suspended. Some pollutants, such as insecticides, road salts and fertilizers are intentionally placed in the urban environment. Other pollutants, including lead from automobile exhaust and oil drippings from trucks and cars, are the indirect result of urban activities.
- *Pollutants of industrial origin*, industrial sources of pollution can vary greatly depending on the size, type and location of the industry. In developed countries, the industrial pollutants are strictly controlled, while in many developing countries such discharges are sometimes carried out without any control. The

sources of pollution due to the industry are, for the most part, of a specific type, that is to say, they are located in a generally reduced area.

- *Pollutants from municipal sources*, from non-industrial municipal sources are all biological and as such can be readily biodegraded. The main pollutants are: solid waste, urine, paper, food waste, laundry wastewater, etc.

The main pollutants that can appear in the water are [9,13]:

- *Biodegradable organic compounds*, these are organic matter, which can be decomposed by bacteria. This fact leads to a decrease in the concentration of dissolved oxygen in the water, which produces harmful effects on aquatic life and the appearance of bad odors. Biodegradable organic compounds can come in large part from agro-food industries and human activity. Notice that due to the activities of these bacteria, if there is much organic matter in the water, the concentration of dissolved oxygen may fall to a level at which even the aerobic bacteria may not survive (fish and other aquatic organisms may not survive also). This is why solid wastes and refuse are disallowed from being emptied into the rivers or lagoons or any mass of water. The decomposition process may then be taken over by anaerobic bacteria, which produce gases such as CH_4, H_2S and NH_3.
- *Non-biodegradable organic compounds*, these are organic compounds which are in a very small concentration. These are stable to be degraded by microorganisms and nature. Generally, these compounds come from the plastics, fuels, solvents, paints, pesticides, detergents, food additives, pharmacists, etc. This group also includes hydrocarbons and other petroleum derivatives that may appear in the aquatic environment through uncontrolled accidents or spills.
- *Heavy metals*, the most important are Hg salts and Pb. Other polluting metals are V, As, Ni, Zn, Co, Cu, Cd, Mg, Se, Be and Cr. Some of these metallic elements are micronutrients, i.e., these are necessary for many animals and plants, but from certain concentrations are toxic. A particular feature of metal contamination is its persistence in the environment and its accumulation in the food chain.

- *Sediments*, the largest amount of water pollutants are sediments or suspended materials. Mainly, these are produced by natural processes of erosion of the earth and by the domestic or industrial spills. Sediments cloud water and reduce photosynthesis. Sediments destroy food and fish spawning areas.
- *Salinity*, the amount of dissolved salts limits the applications of water. Usually, the most important problems appear in aquifers near the coast that can suffer this type of pollution by phenomena of marine intrusion.
- *Pathogenic elements*, these are organisms capable of producing diseases. Examples of pathogens associated with water are some types of viruses such as hepatitis, bacteria such as legionella, protozoans, etc.
- *Thermal contamination*, this type of pollution is due to the use of water as a refrigerant in many industrial processes, so it returns heated to its origin with some degrees of temperature. The increase in temperature leads to a decrease the solubility of oxygen in water and increases the speed of metabolic reaction.
- *Nutrients,* these are the essential chemical elements for the growth of living beings. In addition to C, N and P are fundamentally needed. N is the nutrient applied in the largest quantities for lawn and garden care and crop production. In addition to fertilizer, N occurs naturally in the soil in organic forms from decaying plant and animal residues. In the soil, bacteria convert various forms of N to NO_3^-, a N/O ion. This is desirable as the majority of the N used by plants is absorbed in the NO_3^- form. However, NO_3^- is highly leachable and readily moves with water through the soil profile. If there is excessive rainfall or over-irrigation, NO_3^- will be leached below the plant's root zone and may eventually reach groundwater. Nutrients are polluting when their concentrations are so high that cause excessive growth of aquatic plants. This process is called eutrophication and is mainly due to the increased concentration of phosphates and NO_3^- in the water. In general, stream eutrophication can have a number of deleterious effects on a stream or river. First, the profuse growth of plants decreases water clarity and some species from unsightly scums. Second, certain species of algae cause taste and odor problems in drinking water. Third, certain

blue-green algae can be toxic when consumed by animals. Fourth, eutrophication can alter the species composition of a river ecosystem. Native biota may be displaced as the environment becomes more productive. Finally, the nutrients can indirectly affect other aspects of stream chemistry.

1.3. Contamination of water by nitrates, nitrites and bromates

Surface and ground waters are increasingly contaminated with NO_3^- due to anthropogenic activities such as overuse of fertilizers in the agriculture intensification, disposal of massive amounts of human and animal sewage and discharge of poorly treated industrial wastewater [14,15]. NO_3^- anion is found in natural water as the result of the bacteriological oxidation of nitrogenous materials in soil. That is due to the concentration of these anions, which rapidly increases in summer when the process of the nitrification takes place very intensively. Another important source for dressing of the surface water with NO_3^- anion is precipitations, which absorb NO_x and convert them into HNO_3.

Studies on groundwater contamination suggest that NO_3^- pollution will persist and be increased for the next decades, therefore it is attracting considerable research attention [15–17]. In recent years, intensive agriculture has been promoted based on the availability of synthetic fertilizers of high yield and the cultivation of plant species of fast growth and increasing profitability for the farmer. This rapid and intense agricultural development has generated a series of adverse effects with negative environmental implications. Also in terms of livestock, the volume and number of activities has increased considerably, constituting a potential source of contamination of surface and groundwater [18]. In addition, the presence of NH_4^+ in groundwater is usually below 0.2 mg/L. However, in surface water the NH_4^+ concentration may achieve 12 mg/L. This pollutant may be present in drinking-water as a result of disinfection with chloramines.

Water contamination by BrO_3^- occurs in the treatment processes of ozonation or chlorination of drinking water. The treatment with O_3 is a water purification method that takes advantage of the high oxidizing power of O_3 to disinfect, reduce the odor, color and total organic carbon of the water. During disinfection by ozonation (or also by chlorination) of water originally containing Br^-, BrO_3^- (oxyhalides) are produced.

1.3.1. Effect of nitrates and bromates on health

NO_3^- anion is potentially harmful in drinking water because it can be transformed into NO_2^- and possible endogenous formation of nitro compounds in human body may occur [15,18], which can cause blue baby syndrome, and it is also a precursor of the carcinogenic nitrosamines [14, 19]. NO_3^-, as a naturally occurring substance, is found as a component of food in meat, dairy, vegetables, cereals and fruits, with the exception of certain types of vegetables (beet, celery, lettuce and spinach among others) concentrations in which they are presented are very low. Studies on groundwater contamination suggest that NO_3^- pollution will persist and be increased for the next decades, therefore it is attracting considerable research attention [20].

At present the FAO / WHO recommendation is that the maximum amount of NO_3^- and NO_2^- to be ingested is 0-3.7 mg NO_3^- / kg body weight and 0-0.06 mg NO_2^- / kg body weight, respectively [3]. In addition, this guideline proposed a value for $NO_2^-$of 3 mg/L. As a final point, the WHO suggested a relative potency for NO_3^- and NO_2^- with respect to methaemoglobin formation of 1:10 (on a molar basis)[3].

On the other hand, BrO_3^- is a potential carcinogen to humans, the WHO and the United States Environmental Protection Agency (USEPA) have strictly regulated the BrO_3^- level in drinking water (provisional guideline value: 0.01 mg/L).

Also, the International Agency for Research on Cancer (IARC) classified BrO_3^- as a Group 2B substance (i.e. possibly carcinogenic to humans) [21]. Thus, it is highly desirable to develop effective treatment methods to remove BrO_3^- from drinking water [3].

1.3.2. Legal Regulations

The Nitrates Directive (91/676/EEC) aims to control N_2 pollution and requires Member States to identify groundwaters that contain more than 50 mg/L NO_3^- or could contain more than 50 mg/L NO_3^- if preventative measures are not taken. In addition, the Drinking Water Directive (98/ 83/ECC) sets a maximum allowable concentration for NO_3^- of 50 mg/L. It has been shown that consuming drinking water in excess of the NO_3^- limit can result in adverse health effects, especially in infants less than two months of age. Groundwater is a very important source of drinking water in many countries and it is often used untreated particularly from private wells [22]. The Directive pursues the application of a series of measures and actions that are summarized in: i) the determination of waters affected by pollution or likely to be affected by no action taken, ii) the designation of vulnerable zones, which would correspond to those areas of the territory whose runoff causes or can cause NO_3^- pollution of the waters referred to in the previous section, iii) The development of one or more codes of good agricultural practice.

NO_2^- and NH_4^+ are substances which could have a harmful effect on groundwater and according to Directive 98/83 /ECC sets maximum admissible in drinking water 0.5 mg/L for NH_4^+ and 0.1 mg/L for NO_2^-.

The presence of BrO_3^- in drinking water is a concern for public health since it is considered a genotoxic carcinogen [23]. A maximum allowed contaminant level of 10 μg/L was imposed for BrO_3^- by the EU [1] and USEPA [24], while the WHO set a provisional guideline value of 25 μg/L [3].

In Spain, the sanitary judgment for the quality of water human consumption is regulated by R.D. 1798/2010 which indicates that the limits of NO_3^-, NO_2^- and BrO_3^- are 50 mg/L, 0.5 mg/L and 3μg/L, respectively.

1.3.3. Anthropogenic sources of nitrogen compounds in natural waters

Given their origin and spatial distribution, the anthropogenic sources of N_2 compounds are grouped into two types: the punctual ones, associated to industrial and urban activities, and the diffuse ones, associated to the activities of agricultural origin.

Specifically, the contributions of N_2 compounds to groundwater may come from [16,25]: i) N_2 compounds of atmospheric origin, especially important in industrial areas; ii) inadequate dumping of industrial activities or storage of raw materials without proper control; iii) discharges to surface streams, or directly to the soil, of urban effluents with or without pre-treatment; iv) the inadequate management of leachates from municipal solid waste dumps; v) excess N_2 from fertilizers, not assimilated by crops and leached to aquifers through the unsaturated zone; vi) the effluents originated in the intensive livestock farms, by accumulation and incorrect elimination of the same.

The scientific literature generally considers that agricultural practices are mainly responsible for NO_3^- pollution in groundwater. This is supported, among other arguments, by the relationship between the increase in NO_3^- content in waters and the increase in agricultural land area, the increase in fertilizer consumption and the emergence of intensive livestock farms [26,27].

Another variable to consider is the chemical form in which the N_2 compound is in the fertilizer. Those fertilizers that contain n NO_3^-, molecules of high mobility, are easily carried away by infiltration water, while ammoniacal

compounds take longer because these molecules have less mobility. However, the passage of urea and ammoniacal compounds to NO_3^- occurs rapidly, provided adequate temperature and humidity conditions exist, which will increase the risk of contamination.

Finally, another important factor related to NO_3^- pollution is the production of manure. In Spain, manure generated by animals found in stables is 110 million tonnes per year in the last 8 years. The large volume of liquid manure, particularly from pigs, generated in intensive livestock areas is giving rise to significant NO_3^- contamination in groundwater, either because of its inadequate use for agriculture or because of its incorrect treatment or purification [17].**Figure 1.3** summarizes the N_2 cycle.

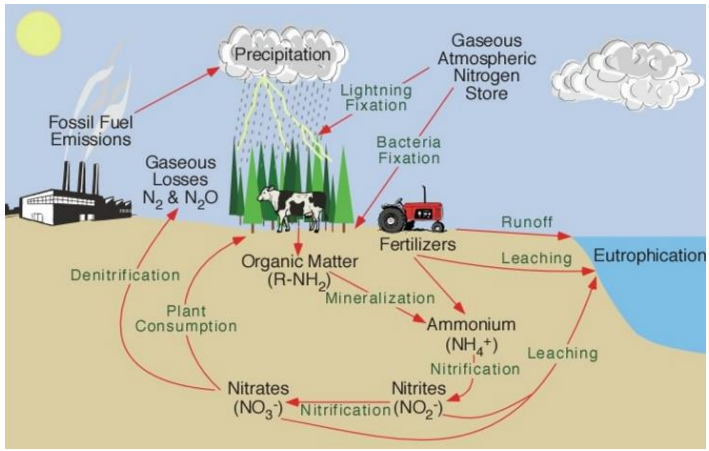

Figure 1.3. Nitrogen cycle[28].

1.3.4. Major sources of bromates

In literature there are a lot of authors that establish the mechanisms for the formation of BrO_3^- in ozonated water [29-32].

In natural waters, it is generally accepted that O_3 reacts with Br^- in three ways, as shown in **Figure 1.4**. The formation of BrO_3^- can occur by three ways: i) the first one is a "direct" pathway. This theory suggests that during ozonation, Br^- is first oxidized by dissolved O_3 to OBr^-, which is then further oxidized to BrO_3^-. The reaction is pH-dependent because OBr^- is in equilibrium with HOBr. OBr^- rapidly builds up during ozonation and becomes the main reservoir for BrO_3^-. OBr^- reacts further with O_3 to form Br^- and BrO_3^- in pure water solutions; ii) the second pathway, referred to as a "direct/indirect" pathway, O_3 and Br^- react to form $HOBr/OBr^-$[30]. Additional the oxidation of oxidation $HOBr/OBr^-$ to OBr is dominated by hydroxyl radicals ($OH^•$) formed from O_3 decomposition. The intermediate OBr^-, required for the formation of BrO_3^-, is more reactive towards O_3 than HOBr [33]; iii) the third pathway, referred to as an "indirect/direct" pathway, Br^- is oxidized by hydroxyl radicals to form $Br^•$, additional oxidation by O_3 ultimately forms BrO_3^-.

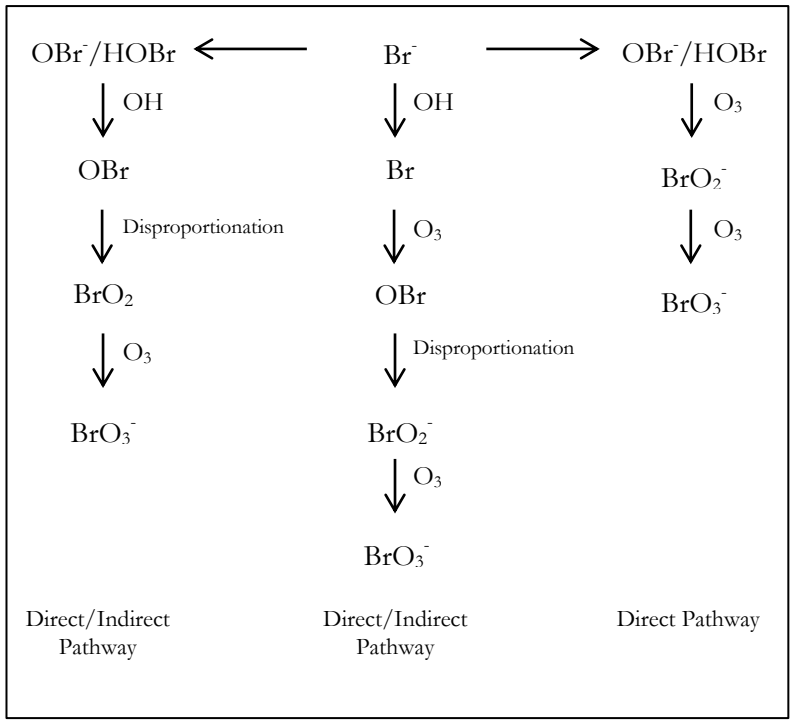

Figure 1.4. Bromate formation during ozonation.

On the other hand, more recently it has been reported that BrO_3^- is present drinking waters as a result of treatment using hypochlorite solutions worldwide [34]. Hypochlorite solutions are produced by electrolyzing sodium or calcium chloride brines. Br^- naturally co-exists with chloride in the brines and is oxidized to BrO_3^- during the manufacturing or on-site generation process. The amount of BrO_3^- contamination will depend on the sources of the salt used to produce brines for electrolysis for both commercially produced bulk hypochlorite and on-site generated hypochlorite.

1.4. Hydrotreatments for the removal of pollutants in water

The hydrotreatment is a reduction process, which requires the presence of a reducing agent that can be developed at room temperature and atmospheric pressure with the adequate selection of the catalyst system. The hydrotreatments

techniques include process as hydrodehalogenation (HDH)[35,36], which reduces the ecotoxicity of pollutants which are include in the lists of priority pollutants of the EU or the USEPA such as dioxins, biocides such as chlorophenols or halogenated pesticides. The hydrotreatments have been also used in processes of removal of pollutants such as NO_3^- or NO_2^-.

The catalytic hydrodechloration (HDC) process is presented as a promising alternative for the treatment of aqueous effluents contaminated with chlorinated organic compounds [37]. Liquid phase catalytic HDC has been reported by many different researchers [38-41]. The reported studies have mainly focused on the catalytic activity, which is affected by the active phase, the support, the source of H_2 and the reaction media [42-45]. Though HDC does not provide the complete destruction of the pollutants, it can lead to convenient transformation of them into substantially less harmful species [46]. This treatment has advantages such as possibility of treating the contaminated water in a large range of concentrations. Others advantages versus incineration or wet oxidation process are that HDC can operate at mild conditions (not require high temperatures and/or pressures). Besides, large amounts of reagents, such as in Fenton oxidation, are not needed and can be applied within a wide range of concentrations of chlorinated compounds, which is not the case of biological methods [47]. These features are of interest in cases as the treatment of supply water contaminated with chlorinated herbicides such as clopyralid (3,6-dichloro-2-pyridinecarboxylic acid), 2-(4-chloro-2-methylphenoxy) propionic acid (MCPP) and acid (4-chloro-2-methylphenoxy) acetic acid (MCPA).

The aqueous phase HDC has successfully been developed using catalysts based on noble metals, being Pd the most active [38, 48-50]. Pd is the metal used in most of the cases because it combines high catalytic ability with some resistance to HCl produced, making it less sensitive to poisoning. In most of the studies on liquid-phase HDC, it has been found that Pd catalysts containing both species, Pd metal and electrodeficient Pd, are the most active. The relationship between species

that confers maximum activity is unclear [51] . However, some author like Baeza et al. [52] reported that a Pd^{n+}/Pd^0 ratio close to one improve the catalytic activity.

One of the treatments for removing NO_3^- that has more projection can be hydrodenitrification (HDN). The catalytic reduction of NO_3^- is a reaction with series and parallel routes, in which the species is reduced to NO_2^- by the action of H_2, and then through an intermediate product, nitric oxide, N_2 or NH_4^+ ion is produced. One of the major limitations of the catalytic reduction of NO_3^- is the production of NO_2^- as an intermediate (level allowed in drinking water 0.1 mg/L) and end product NH_4^+ (level allowed in drinking water 0.5 mg/L). The metal phases that show greater activity for the removal of NO_3^- in water are essentially combinations of Pd with Cu [53-58]. A variety of supports has also been reported, including mainly alumina (Al_2O_3) [54, 59], silica (SiO_2) [60], zeolites [61], titanium dioxide (TiO_2) [62,63] and activated carbon (AC) [64-67].

Recent studies indicate that catalytic hydrogenation can be used as a potential treatment technique for the removal of BrO_3^- in drinking water. Catalytic hydrogenation of BrO_3^- is a promising approach to remove BrO_3^- from water considering that this approach not only removes BrO_3^- but also converts it into Br^-. The first research in this topic used noble metal (Pd, Pt) catalysts with different supports of SiO_2, Al_2O_3 and AC. This reaction is influenced by metal load in the reactor and by pH. In this sense, increasing metal loading amount resulted in enhanced BrO_3^- reduction. Besides, BrO_3^- reduction is strongly pH-dependent and enhanced reduction rate could be achieved at low pH. In the presence of coexisting anions (Cl^-, Br^- and SO_4^{2-}) the BrO_3^- reduction is suppressed, wherein SO_4^{2-} exhibited the most marked inhibition effect, attributed to competitive adsorption for active surface sites [68].

The optimization of catalytic systems to be applied in water treatment is now an urgent need due to the increasing presence of hazardous contaminants and

increasingly restrictive discharge limits. Thus, the catalytic systems containing nanoparticles (NPs) show excellent characteristics for the development of water hydrotreatment reactions.

In addition, the presence of significant quantities of NO_3^- in the water prevents its use for public supply networks. In the present work, the removal of NO_3^- in natural waters will be treated. For this reason the effects of these pollutants are further developed in the following point. On the other hand, the removal of BrO_3^- is studied in this work, too. This group includes a large group of pollutants of a very diverse nature, which may appear at very low concentrations in water, nevertheless they must be removed due to their toxicity.

1.5. Nitrate removal treatments

Water contaminated with NO_3^- must be treated before use. There are several techniques, which are commonly divided into separation techniques and transformation techniques [69,70]. The techniques of NO_3^- in a second waste that should be treated or stored in a deposit, in this group are electrodialysis, reverse osmosis and anionic resins. On the other hand, the transformation techniques, which transform NO_3^- into other compounds chemical are the biological elimination and the catalytic reduction [67].

The most common treatments for NO_3^- and NO_2^- removal from water involve physicochemical (ion exchange, reverse osmosis and electrodialysis) or biological methods [71]. An overview of the comparative characteristics of these technologies for water remediation after NO_3^- contamination is reported in **Table 1.3** The main disadvantage of the physicochemical methods is associated to the generation of additional sludge and unwanted by products, at high operational cost. Among the disadvantages of biological treatments, the needed of adding substrate and nutrients to water and the significant post-treatment requirements can be

highlighted [20]. **Table 1.4** summarizes the principal advantages and disadvantages of the different techniques of NO_3^- removal.

Table 1.3. Different technologies for water remediation after nitrate contamination [17].

Method/ Characteristics of technologies	**Ion exchange**	**Reverse osmosis**	**Electrodialysis**	**Biological denitrification**	**Catalytic reduction**
Full-scale systems	Yes	Yes	Yes	Yes	no
Pre-treatment needs	Pre-filter, address hardness	Pre-filter, address hardness	Pre-filter, address hardness	pH adjustment, nutrient and substrate addition, need for anoxic conditions	pH adjustment
Post-treatment needs	pH adjustment	pH adjustment Remineralization	pH adjustment Remineralization	Filtration, disinfection, possible substrate adsorption	pH adjustment, potential ammonia control
Fate of NO_3^-	Adsorbed and concentrated	Concentrated in a waste stream	Concentrated in a waste stream	Transformed to N_2	Transformed to N_2
Waste	Waste brine	Waste brine	Concentrate	Bacteria sludge	None
Percentage of efficiency in water purification (%)	85-98	75-80	> 95	98	98-100
Space requirements	Limited	Limited	Limited	High	Low
Odors	No	No	No	Yes	No
Selectivity of the process	Low	Low	Low	High	High
Sensitivity of costs to scale-down	Medium	High	High	High	Low

Table 1.4. Main advantages and disadvantages of the different techniques for nitrate removal [72].

Method	Advantages	Disadvantages
Ion exchange	Multiple contaminant removal. Selective NO_3^- removal. Financial feasibility. Use in small and large systems. The ability to automate.	The potential for NO_3^- dumping specifically for non-selective resin use for high sulfate waters. The need to address resin susceptibility to hardness, iron, manganese, suspended solids, organic matter, and chlorine. The possible role of resin residuals in DBP formation.
Reverse osmosis	High quality product water. Multiple contaminant removal. Desalination (TDS removal). Feasible automation. Small footprint.	The need to address membrane susceptibility to hardness, iron, manganese, suspended solids, SiO_2, organic matter, and chlorine. High energy demands. The lack of control over target constituents (complete demineralization).
Electrodialysis	Limited to no chemical usage. Long lasting membranes. Selective removal of target species. Flexibility in removal rate through voltage control. Better water recovery (lower waster volume). Feasible automation. Multiple contaminant removal.	The need to address membrane susceptibility to hardness, iron, manganese, and suspended solids. High maintenance demands. The need to vent gaseous byproduct. The potential for precipitation with high recovery. High system complexity. Dependence on conductivity.

Table 1.4. Main advantages and disadvantages of the different techniques for nitrate removal [72].(Cont.).

Method	Advantages	Disadvantages
Biological denitrification	High water recovery. No brine or concentrate waste stream. Low sludge waste. Less expensive operation. Limited chemical input. Increased sustainability. Multiple contaminant removal.	The need for substrate and nutrient addition. High monitoring needs. The possibility of partial denitrification. Permitting and piloting requirements. Slower initial start-up, which could cause challenges for wells with intermittent run time.
Catalytic reduction	Conversion of NO_3^- to other N_2 species. The potential for more sustainable treatment. High water recovery. Multiple contaminant removal.	The potential reduction of NO_3^- beyond N_2 to NH_4^+. The possibility of partial denitrification. The possible dependence of performance on pH and temperature. The lack of full-scale chemical denitrification systems resulting in: o unknown reliability, o unknown costs, and o unknown

The catalytic reduction with H_2 has been suggested in the literature as a promising method, which was reported for the first time by Vorlop et al. in 1989 [73]. Catalytic hydrogenation with Pd-based bimetallic catalysts has emerged as a promising new technology for treating NO_3^- and other oxyanions (eg., NO_2^-, BrO_3^-, ClO_4^-) in drinking water or concentrate waste streams that is capable of converting NO_3^- to harmless N_2 [74,75].

The catalytic reduction consists on the reduction of NO_3^- by H_2 transforming it into N_2 and water by means of a solid catalyst. However, during the reaction, NO_2^- can also be produced as an intermediate product and NH_4^+ as a by-product [56,67,76].

Typically, NO_3^- is hydrogenated by Pd-based bimetallic catalysts, while NO_2^- and further intermediates can be reduced with Pd catalyst. With H_2 as the reducing agent, NO_3^- is converted to N_2 as a desired product and NH_4^+ as by-product. In this typical reaction scheme, the role of NO reduction on N_2 and NH_4^+ formation was previously unclear due to lack of direct experimental evidence. The findings of different researchers confirmed the involvement of NO in the NO_3^- /NO_2^- reduction pathways and its key role in affecting the end product distribution of N_2 and NH_4^+. Rapid NO_3^- reduction has been reported for supported Pd:Cu, Pd:In, and Pd:Sn catalysts using exogenous H_2 as the reducing agent [54,75,77,78]. A possible and most accepted mechanism but heretofore unproven for the NO_3^- reduction is shown in the next equations:

$$2NO_3^- + 5H_2 \rightarrow N_2 + 4H_2O + 2OH^- \quad [1.1]$$

$$NO_3^- + H_2 \rightarrow NO_2^- + H_2O \quad [1.2]$$

$$2NO_2^- + 3H_2 \rightarrow N_2 + 2H_2O + 2OH^- \quad [1.3]$$

$$NO_2^- + 3H_2 \rightarrow NH_4^+ + 2OH^- \quad [1.4]$$

$$NO_3^- + 4H_2 \rightarrow NH_4^+ + H_2O + 2OH^- \quad [1.5]$$

The above equations can be summarized in the following two, which represent the general reactions of catalytic reduction of NO_3^- using H_2 as the reducing agent.

$$2NO_3^- + 5H_2 \rightarrow N_2 + 2OH^- + 4H_2O \quad [1.6]$$

$$2\,NO_3^- + 8H_2 \rightarrow 2NH_4^+ + 4OH^- + 2H_2O \quad [1.7]$$

Figure 1.5 shows the most accepted reaction mechanism for the catalytic reduction of NO_3^- in water studied by Epron et al. [79] in presence of bimetallic Pt:Cu catalysts and additional step for NO_2^- reduction was proposed by Barrabés et al. [80]. Epron et al. [79] obtained that monometallic Pt catalysts are inactive for NO_3^- reduction, while metallic state Cu is able to reduce NO_3^- according to a redox reaction, although it is rapidly deactivated. In addition, they deduced that the first step in the NO_3^- reduction is probably a redox reaction between Cu^0 and NO_3^- leading to NO_2^- intermediates or directly to N_2 or NH_4^+ and to an oxidized form of Cu. Hence, the role of the precious metal is to activate H_2, allowing the reduction of Cu.

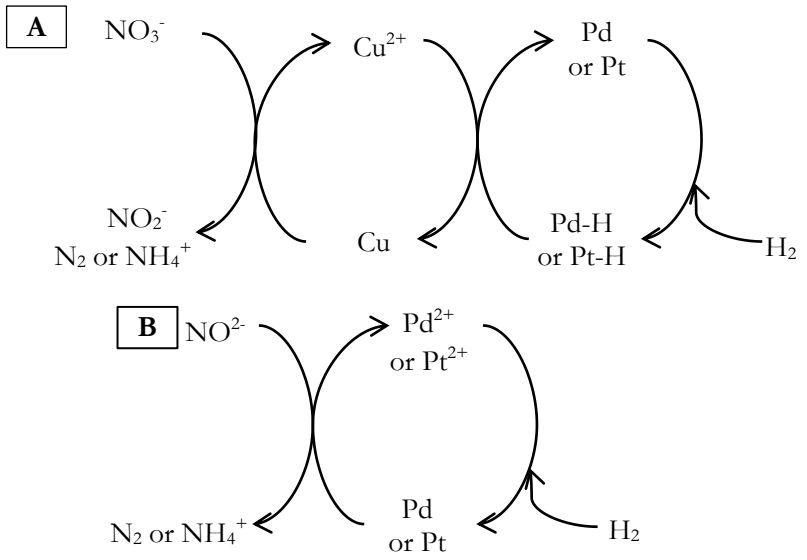

Figure 1.5. Reaction mechanism for **A)** nitrate [79, 80]and **B)** nitrite reduction[80].

Yoshinaga et al. [53] studied the catalytic removal of NO_3^- in water by hydrogenation using supported Pd:Cu. They concluded that using AC as supports was excellent for Pd:Cu, since not only showed the high activity and selectivity to N_2 but also the insolubility of the metallic components. In addition, Yoshinaga et al. [53] pointed out that edge and corners sites of Pd in Pd microcrystallites possess high abilities for hydrogenation, these sites are probably favorable for deep hydrogenation of NO_2^-, that is, formation of NH_4^+. On the other hand, N_2 would be favorably formed on the terrace sites of the Pd crystallites, because these sites have mild hydrogenation abilities.

Many variables can affect the mechanism of the reaction, as can be the pH, the temperature, the N:H molar ratios or the catalytic system, Pd nanocluster size and shape and catalyst support [65,78,81,82]. A fundamental issue that affects the impact of all such factors on selectivity is the NO_3^- reduction pathway on the type of catalyst to the reaction conditions. The catalysts used in this reaction being mainly bimetallic catalysts constituted by a combination of a noble metal and a non-noble metal [66,83–85].

There are many studies that demonstrate that monometallic catalysts are less efficient in comparison to bimetallic ones [67,86,87]. The bimetallic catalysts on which the research has been focused are consisted of a noble metal and a promoting transition metal [88]. The transition metal reduces the NO_3^- to NO_2^- according to a redox process leading to its oxidation. On contrary, the noble metal is used to stabilize the transition metal in its lower oxidation states by H_2 spillover. In literature the metals most used as transition metal are Cu, Sn, Ag or Ir, and the typical metals used as noble metal are Pd, Pt, Rh or Ir [66,67,71,89].

The type of the support, catalysts composition and structure play an important role in NO_3^- reduction. Many supports have been studied, such as Al_2O_3 [90-92], AC [53,58,66,86], SnO_2 [93] CeO_2 [94], resin[95], zeolites [61,96], Nb_2O_5 [91], pumice [97], pillared clays [56], SiO_2 [92], or AC prepared by chemical activation of grape seed with phosphoric acid [67].

Gavagnin et al. [93] proposed the use of SnO_2 as an active support for NO_3^- reduction in the absence of an added promoter. In this way, they observed that the good results are associated to the semiconductor property of SnO_2. This property favors the effect of H_2 spill-over from Pd metal, it is conceivable that some oxygen vacancies may create on SnO_2, even at room temperature, especially at the interface between the Pd particles and the support. This would result in the presence of electron rich Sn centers that may change the electron density on Pd through a sort of ligand effect.

The activity of monometallic Pd/CeO_2 catalyst was reported for first time by Epron et al. [98]. They established that CeO_2 support has an important promoting effect on the activity of monometallic Pd catalyst for NO_2^- reduction, and it allows NO_3^- reduction without adding a second metal. Despite the high activity shown for NO_3^- reduction, the CeO_2 support is not suitable for water denitrification due to the high selectivity towards NH_4^+.

Guo et al. [99] found that monometallic catalysts $Pd/TiO_2–SnO_2$ and Pd/SnO_2 showed high catalytic activity for the NO_3^- reduction. As it was shown in **Figure 1.5** the main mechanism accepted in NO_3^- reduction is when the reaction occurs over bimetallic catalysts, where the role of the noble metal is to activate hydrogen, which reduces the promoter metal completing the catalytic cycle. In this way, when monometallic catalyst is active, the mechanism involves partially reduced species of the support. They proposed that the first step in NO_3^- reduction occurs by the interaction of oxygen vacancies created at the surface catalyst. This fact led to conclude that NO_3^- may be reduced to NO_2^- on vacancies located at metal support interface. Besides, they concluded that $Pd/TiO_2–SnO_2$ showed better catalytic properties than Pd/SnO_2. This fact may be attributed to an increase in the amount of oxygen vacancies related to the TiO_2 doping over SnO_2. Nevertheless, the best catalyst synthesized by this method showed a high value of NH_4^+ concentration, 2.4 mg/L.

Other support less used in NO_3^- reduction is magnetite, thus, Sun et al.[100] explored the activity of a monometallic Pd/Fe_3O_4 catalyst. This catalyst showed a fast NO_3^- reduction, especially when the solution pH was controlled at values below 5.8. Nevertheless, the NH_4^+concentration in the reaction is high. This support had been studied for various water treatments (dehalogenation, removal of heavy metal ion, etc.) because of its easy separation from aqueous solution.

Zhao et al. [101] studied the catalytic NO_3^- reduction with Pd, Ni and Cu supported on elemental Al. These monometallic catalysts showed a greater NO_3^- reduction, though all NO_3^- was converted practically into NH_4^+.

Pillared clays (PILCs) have been recently used as catalytic supports for hydrotreatments using precious metals as active phase. In this way, Pizarro et al. [56] evaluated the NO_3^- reduction using monometallic (Ir, Pd, Pt and Rh) catalysts supported on Al-PILCs. In these experiments, the Pd/Al-PILCs achieved the best

NO_3^- conversion (65 %) while the other ones showed a lower catalytic activity. The production of NH_4^+ was high for all the catalysts except for Pt/Al-PILCs, which is also in concordance with its lower activity. The activity observed in these catalysts may be attributed to iron present in the clay. The Fe^{3+} and the Fe^{2+} oxidation states are very easily interchangeable. Fe^{3+} present in the PILCs is reduced to Fe^{2+} when it is in contact with H_2. Iron in its Fe^{2+} oxidation state acts as a reducing agent and can promote the NO_3^- reduction.

Despite all the studies done so far, it can be concluded that monometallic catalysts deposited on reducible supports are not sufficiently selective to the formation of N_2 due to the strong tendency to hydrogenation of these supports that promotes the generation of NH_4^+.

Since Vorlop and Tracke's [73] proposal, the use of bimetallic catalysts for NO_3^- reduction in water has been the focus of many researchers. According to literature, the bimetallic catalysts most studied in NO_3^- reduction are Pd:Cu, Pt:Cu, Rh:Cu and Pd:Sn. They have been considered as the most actives for NO_3^- reduction, but they are still inadequate on terms of selectivity towards N_2. On the other hand, it is also of importance the molar ratio between both metals. In the results reported by Pintar et al. using Pd:Cu promoted catalysts were more active and more selective to N_2 than corresponding Pd:Sn catalyst when both were supported on Al_2O_3 spheres [102]. However, when NO_3^- reduction with Pd:Sn and Pd:Cu catalyst supported on Al_2O_3 was investigated by Jacinto Sá et al. [103], better results were obtained with the Pd:Sn couple because this catalyst was less affected by the water hardness and conductivity. Besides, NH_4^+ formation was more pronounced with catalyst containing Cu [54,89]. Activity of the catalysts for NO_3^- reduction is strongly dependent on the ratio of the two metals. In this sense, Pd:Sn catalysts show a greater selectivity for N_2 than Pd:Cu where the latter exhibits both high NH_4^+ and NO_2^- formation rates.

On the contrary, the most employed system for NO_3^- reduction is Pd:Cu. Some authors are in accordance that the molar ratio Pd:Cu equal to 2 is the best for this bimetallic catalyst system. In this sense, the NO_3^- conversion was complete with a selectivity to NH_4^+ around 39 % [67,75]. Other studies employed molar ratios Pd:Cu between 0.6 and 1 on AC achieving 80 % of NO_3^- conversion and 50 % of selectivity to NH_4^+ [67,80].

Yoshinaga et al. [53] investigated the influence of the support in the reduction of NO_3^- in water with H_2 over supported Pd:Cu. They observed that AC was superior in conversion, selectivity and mechanical stability to the other supports (Al_2O_3, SiO_2 and ZrO_2). Of all the supports studied so far, the AC have been shown to be very active and selective towards N_2 in NO_3^- reduction, which has been attributed to high surface area allowing higher metals dispersion. Soares et al. [76] carried out an exhaustive research using different materials as support (AC, CNT, CeO_2, TiO_2, MnO_2, Al_2O_3 and SiO_2), showing the remarkable effect they had on the performance of Pd:Cu catalysts. In this work, they concluded that the support of the Pd:Cu catalysts plays an important role in NO_3^- reduction. The 100 % NO_3^- conversion was achieved for the catalysts supported on TiO_2 or CNT-TiO_2. In the same experimental conditions for the amount of metal on the support, the N_2 selectivity for the catalysts supported on TiO_2 was 17 %. Nevertheless, a significantly increase was obtained when the composite CNT-TiO_2 is used as support, in this case the N_2 selectivity was 66 %.

In this way, Jowarski et al. [104] reported a very complete study in which they developed bimetallic Pd:Cu catalysts supported on Al_2O_3, ZrO_2 and ZrO_2-Al_2O_3 mixed to evaluate their activity and selectivity in NO_3^- reduction. They found that the advantage of ZrO_2-Al_2O_3 as support was its high surface area. This property led to generate a high dispersion of Pd, facilitating their interaction with Cu. The catalyst Pd:Cu/ZrO_2-Al_2O_3 reached a complete NO_3^- conversion and the highest concentration of NH_4^+ detected was 0.5 mg/L, which is within the acceptable limits for this compound.

Bahri et al. [67] carried out NO_3^- reduction experiments using a commercial AC and one prepared by chemical activation of grape seeds with H_3PO_4 (GS). These supports were used for the preparation of bimetallic catalysts (Pd:Cu, Pd:Sn and Pd:In). They observed that the nature and the concentration of promoting metal seem to affect significantly the catalytic performances, concluding that Cu was the most adequate promoting metal when selectivity towards NH_4^+ was considered. The Pd–based bimetallic catalysts containing Sn and In as promoting metal showed a lower catalytic activity and significantly higher selectivity towards NH_4^+. However, Pd:Cu catalyst supported on GS showed the highest NO_3^- removal activity and NO_2^- was not found as by-product. Moreover, the selectivity towards NH_4^+ was also lower. In this case, the support plays an important role in the catalytic performances for NO_3^- removal. The acidity of the reaction medium is associated with this behavior, attributing this effect to the chemical composition of the catalyst support.

An original eco-friendly support material used in NO_3^- reduction was the maghemite (γ-$Fe^{III}_2O_3$). Jung et al. [55] developed a Pd:Cu/ maghemite (0.25 %-0.5 %, wt.%) catalyst which achieved 99.5 % NO_3^- conversion in 90 min. However, this catalyst showed 47 % selectivity towards N_2. Jung et al. [105] also investigated the use of hematite (α-$Fe^{III}_2O_3$) as support.. They obtained relatively high NO_3^- removal (94 %) with N_2 selectivity to 72.4 % when 2.8 % Pd-2.2 % Cu (wt.%) were fixed to synthesized the bimetallic catalyst.

Recently, Pizarro et al. [56] have used PILCs as support for the catalytic NO_3^- reduction. They synthetized bimetallic catalysts based on Pd with inclusion of a second metal (Cu, Sn or In). Their results were better compared to monometallic catalysts. Although all the catalysts achieved a complete NO_3^- conversion, Pd:Cu (5 %-2.5 %, wt.%) catalyst showed a higher activity. Nevertheless, the NH_4^+ selectivity for this catalyst was 25 % after 6 h reaction time.

Another key parameter is pH, since the reduction of NO_3^- leads to the formation of $OH^•$, increasing the pH of the reaction medium up to 10. This value is unacceptable for drinking water and induces a decrease of both the activity and the selectivity towards N_2 [58]. In particular, Sakamoto et al. [106] observed that an increase of pH in NO_3^- reduction lead to an increase of $OH^•$ in the medium of reaction, which will poison the catalyst by joining the active phase of the same reducing the selectivity and activity of the reaction. Calvo et al. [58] observed that a pH above to 8, a decrease in NO_3^- conversion was obtained, besides when the NO_3^- reaction was carried out at pH below 5, this effect was more pronounced. In this sense, most of the authors work under buffer systems to control pH. In this way, different inorganic and organic buffers have been widely tested like PO_4^{3-} and HCO_3^- buffers at pH values of 6 and 10, respectively. However, CO_2 [56,107], formic acid [54,97,99,103] or HCl [92,108] have been the most used compounds to control the pH.

1.6. Bromates removal systems

BrO_3^- removal methods have been studied since the early 1990s [109], with the vast majority of research into remediation focusing on developing postozonation methodologies for potable water supplies. A variety of treatment techniques have been explored to eliminate BrO_3^- pollution in drinking water. Biological technique is effective to reduce BrO_3^- to Br^- using glucose, pyruvate, formate or starch as electron donors. However, the continuous release of biomass and excessive organic compounds during the treatment process limits the practical use of the technique [110]. Alternatively, chemical reduction provides more efficient and cost effective approaches to reduce BrO_3^-.

Overviews of the comparative characteristics of these technologies for water remediation after BrO_3^- contamination are:

- ✓ *Physical and electrical techniques,* the BrO_3^- can be reduced to Br^- with the addition of reducing agents. This reduction may be chemical or catalytic [21,68]. The chemical reduction follows a redox mechanism, using Fe^{2+}/Fe^0 [111] or sulfurous compounds [72] as reducing agents.
- ✓ *Catalytic reduction techniques,* this hydrogenation is not yet recognized as an effective industrial scale treatment technique to remove pollutants in wastewater. As indicated in NO_3^- removal system, Vorlop et al. [73] developed for the first time the method of catalytic hydrogenation using bimetallic catalysts to selectively and efficiently reduce NO_3^- to N_2 in aqueous medium. The main disadvantage of the process is that NO_2^- is formed as intermediate and NH_4^+ as by-product. This technique could be also applied for the reduction of BrO_3^- in water. Nevertheless, scarce information is available regarding the catalytic removal of BrO_3^- from aqueous solutions.
- ✓ *Biological techniques,* methods are used to degrade many organic compounds [112], and some inorganic species, including Mn, NO_3^- and ClO_4^-.
- ✓ *Activated carbon adsorption,* is commonly used in potable water treatment plants. AC has some activity for the elimination of BrO_3^-. The efficiency of processes using AC depends on several parameters, including the nature of the AC, the contact time, the initial concentration of BrO_3^-, the presence of organic matter, etc.

  In the reduction of BrO_3^- with AC the mechanism has two stages, the first one involves the adsorption of the BrO_3^- on the AC reducing the BrO_3^- to hypobromite (OBr^-) and, on the other hand, the AC is oxidized in the presence of CO_2 that is adsorbed on the AC surface. In the second stage, the OBr^- is reduced to bromide (Br^-), oxidizing another center of AC surface to CO_2, that is adsorbed on the surface of the AC [113].

Considering the oxidative nature of BrO_3^- it is reasonable to hypothesize that the catalytic hydrogenation is also an effective method for the reductive removal of aqueous BrO_3^-, as it has been shown recently by Chen et al. [68]. They

found that Al_2O_3 was the best support and Pd/Al_2O_3 outperformed Pt/Al_2O_3. The influence of various parameters was also considered. The results of these studies highlighted the influence of solution pH, structural properties of Pd on the Al_2O_3 surface and competitive adsorption of coexisting anions.

Thakur et al. [21] studied the catalytic reduction of BrO_3^- in water. They observed a high catalytic activity for carbon nanofiber supported Ru catalyst layers integrated in silicon based microreactors.

Restivo et al. [114] used different supports for exploring the catalytic reduction of BrO_3^-. The different supports selected were AC, multiwalled carbon and TiO_2, since they had shown promising results as catalyst supports in the reduction of NO_3^- in water under H_2 [76]. Restivo et al. [114] concluded that the activity of the support and the interaction of the support with the metallic catalyst were postulated to be responsible for the differences in activity, founding that the TiO_2 is the most active.

1.7. Current topic status in catalysts

The development of efficient catalysts for the treatment of contaminated water has been a demand for years in the field of Environmental Technology. Catalytic systems containing noble and transition metal NPs are excellent candidates for the development of water hydrotreatments reactions, regarding the good results obtained in hydrogenations oriented towards synthesis processes. The hydrotreatments of water have been oriented to a great extent towards the removal of heteroatoms and aromatic rings hydrogenation with a view to the reduction of toxicity and the increase of biodegradability. Another important field of application is the reduction of NO_3^- in water supply.

The use of noble metal-based NPs in catalytic applications has focused on reactions involving the formation of carbon-carbon bonds, such as the conversion of aryl halides to carboxylic acids, esters or amides in a carbonylation step, the Heck

reaction [115,116], the Suzuki reaction [117] or the Sonogashira process [116]. Also, catalysts with controlled size have gained interest in catalytic systems, such as hydrotreatments: semi-hydrogenation of phenylacetylene[118], benzene hydrogenation [119], or hydrodechloration of aromatic compounds [120].

The use of catalysts based in supported metallic NP has gained important attention in catalytic applications due mainly to the high surface area per unit volume. There are indications that the structure of the metallic NPs confers additional activity versus high size of NP. In the literature, there is no consensus about the effect of NP size on activity, selectivity and reaction mechanism. The most employed supports for the immobilization of metal NPs are SiO_2 substrates [121-123], Al_2O_3 [124,125], zeolites [126] and AC [127–129].

Most of the metal-based catalysts prepared at industrial scale are commonly synthesized through few conventional steps [130]. These steps involve the impregnation/precipitation of a precursor of the active phase on a support, a calcination treatment and, finally, a reduction stage, e.g. in H_2. Catalysts with high activity, selectivity or stability can be achieved following this procedure, but no precise control of size and structure of the active phase can be achieved. The preparation of rationally-designed catalysts with high performance is still one of the classical challenges in catalysis [131]

Since the performance of metallic catalysts is closely linked to the structure of the metal phase, the methods of control of NP size have gained important attention in the last years as a strategy to facilitate rational design [131-133], particularly in the case of structure sensitive reactions. Chemical methods have been proved to be especially interesting due to their effectiveness and simplicity [134]. These methods have in common the use of a reducing agent, which reduces the metal precursor to metal NPs, in the presence of a stabilizing agent (SA) limiting the NPs growth and preventing their aggregation. SAs are also named as capping agents, surfactants or ligands in the literature. Many different organic compounds have been successfully used as SA, such as polyvinylpyrrolidone (PVP),

polyvinyl alcohol (PVA), sodium bis[2-ethylhexyl] sulfosuccinate (AOT), cetyltrimethylammonium bromide (CTAB), ascorbic acid (AA) and polyethylene glycol (PEG), among others [135]. The SA remaining in the synthesis medium or on the NPs surface after the catalysts synthesis has been considered as a drawback, since they usually interact strongly with the metallic phase/support and can have an impact in the catalyst performance [136]. Thus, the metal surface can be hindered making them less accessible to the reactants, or the active centers can be blocked by the groups of the SA attached to metal surface. Different approaches have been used to remove SAs and promote activity. The most common procedure is washing NPs after synthesis with solvents of different polarity, which is quite efficient in the removal of the excess of SA, but does not remove it completely [134]. Decomposition of SA through thermal or oxidizing treatments achieves removal of SAs, but some side problems such as sintering, deposition of coke on the metal surface or partial oxidation of the NPs can occur. The weakening of bonds between the SA and the metal surface through competition with chemicals exhibiting higher affinity for the SA or metal surface has also been described. Although the removal of SA after washing NPs is an important concern, some authors have reported that the lower catalytic activity provoked by the presence of the SA was accompanied by changes in selectivity [137,138]. The role of the SA in the promotion of selectivity has especial interest in those cases where the interaction between SA and metal surface is strong enough to result in stable performance of the catalyst. Thus SAs can become a tool for rational design of high-performance catalysts. Further research is still needed in this promising field to address questions such as how the SA is attached to the NPs surface, what is the surface coverage, what is the interaction between reactant and the SA or how is the charge transfer between SA and metal surface, among others.

One of these methods to control of NPs characteristics is the reverse microemulsion (ME) (water in oil, w/o) technique, which requires the use of water, a non-polar solvent, a reducing agent and SA (surfactant). The NPs size can be controlled using different water-to-surfactant (w_0) and/or reducing agent-to-metal

molar ratios. The novelty of the strategy lays on the control of the physical operations during the synthesis, providing with knowledge about the influence of the purification of the NPs, the reaction (reduction) time and the temperature during the concentration of the Pd NPs. In order to obtain a homogeneous distribution of NPs on the support, it is frequent to use tetrahydrofuran for destabilizing the ME and deposit metal particles on the substrate [139]. Another option less used for the preparation of these catalysts is in situ generation of metal NPs on the support [121], which has certain advantages since it could be controlled adjusting accurately the concentration of the precursor salt and the reducing agent and the water-surfactant synthesis if used by MEs. This will provide more control over the size and distribution of metal NPs anchored on the support.

1.8. Microemulsion method for the synthesis of catalysts

Synthesis of NPs by ME method is recently an ideal technique for the preparation of inorganic NPs. One of the best definitions of MEs is from Danielsson and Lindman [140] "a ME is a system of water, oil and an amphiphilic which is a single optically isotropic and thermodynamically stable liquid solution". Some authors assumed that MEs can be considered as small-scale versions of emulsions, i.e., droplet type dispersions either of oil-in-water (o/w) or of water-in-oil (w/o), with a size range in the order of 0.1- 50 micron in drop radius [141].

Structurally, ME consist of microdroplets of oil- or water-entrapped pockets, which is the dispersed phase, stabilized by a layer of surfactant (or a mixture or surfactant and cosurfactant) on the surface, similar to conventional emulsions. ME domains are usually characterized by constructing ternary-phase diagrams. Basically, the main components of MEs system are: two immiscible liquids and a surfactant. Sometimes a co-surfactant is used, in this case, it can be represented at a fixed ratio to surfactant as a single component, and treated as a single "pseudocomponent". The relative amounts of these three components are represented in the ternary phase diagram. Pseudoternary phase diagram of oil, water, and cosurfactant/surfactant mixture are constructed at fixed co-

surfactant/surfactant weight ratios. Gibbs phase diagrams can be used to show the influence of change in the volume fractions of the different phases on the phase behavior of the system. At constant temperature and pressure, the ternary phase diagram of a simple three-component ME is divided into two or four regions as shown in **Figure 1.6.**

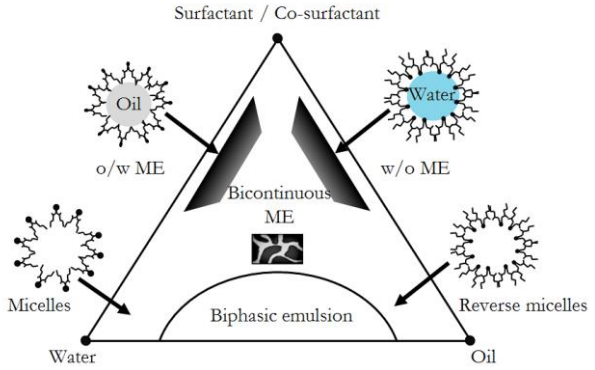

Figure 1.6. Phase diagram of ME.

The type of the structure and phase depends upon the proportions of the components. In this regard, flexibility of the surfactant film plays an important role.

Depending on structure and composition of components, ME can be any of the following types [142]:

- ✓ *Oil-in-water ME (o/w),* droplets of oil dispersed in the continuous aqueous phase.
- ✓ *Water-in-oil ME (w/o),* droplets of water are dispersed in the continuous oil phase.
- ✓ *Bicontinuous ME,* microdomains of oil and water are interdispersed within the system. A bicontinuous ME is formed in case where the amounts of water and oil are more or less similar.

A well-known classification of MEs is that of Winsor [143] who identified four general types of phase equilibria:

- ✓ *Type I,* the surfactant is preferentially soluble in water and o/w MEs form (Winsor I). The surfactant-rich water phase coexists with the oil phase where surfactant is only present as monomers at small concentration.
- ✓ *Type II*, the surfactant is mainly in the oil phase and w/o MEs form. The surfactant-rich oil phase coexists with the surfactant-poor aqueous phase (Winsor II).
- ✓ *Type III*, a three-phase system where a surfactant-rich middle-phase coexists with both excess water and oil surfactant-poor phases (Winsor III or middle-phase ME).
- ✓ *Type IV*, a single-phase (isotropic) micellar solution, which forms upon addition of a sufficient quantity of amphiphile (surfactant plus alcohol).

In aqueous solution, surfactants aggregate into structures called micelles. Micelles are closed shape structures where the hydrophilic portions of the molecule are exposed to the surrounding water while the hydrophobic portions are protected from contact with water. When dissolved in non-polar organic solvents (hereafter referred simply as oils), surfactants form reversed micelles where the hydrophilic portions are shielded from contact with the surrounding solvent in the interior of the micelles, as seen in **Figure 1.7**. Depending on the particular molecular architecture of the surfactant molecule, a variety of microstructures may be formed. Possible aggregate structures are spherical, cylindrical and worm-like micelles, spherical vesicles, lamellar sheets, or a variety of other topologies. The surfactant aggregates form in order to minimize the free energy of the solution, so as a result, they are dynamic structures, but equilibrium.

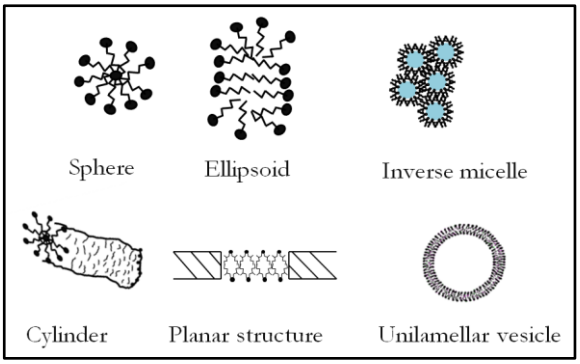

Figure 1.7. Different shape of micelles.

The surfactant is an amphiphilic molecule containing a water-loving (hydrophilic) part and another oil-loving (lipophilic) one [141]. The hydrophobic part usually is a hydrocarbon chain. Owing to this characteristic, they tend to adsorb at the water-oil interface. Hence, it is a chemical species with a nature or polar-nonpolar structure, it tends to be located between the organic and aqueous phases, forming a monolayer adsorbed at the interface. In **Figure 1.8** can be seen the schematic structure of surfactant.

Figure 1.8 . Structure of surfactant.

Depending on the nature of the hydrophilic group, surfactants are further classified [144,145] as following (**Figure 1.9**):

- ✓ *Anionic*, the surface-active part bears negative charge. This type of surfactant is formed in it head by sulfonate group, sulfate group, carboxylate group, etc. These surfactants are the most employed in the industry due to the relatively low cost in manufacture. Sodium dodecylsulfate (SDS) is a well-known example with the molecular formula $CH_3(CH_2)_{11}SO_4^-$ Na^+. Other examples are

$RCOO^-Na^+$ (soap) and $RSO_3^-Na^+$ (sulfonates) like the sodium bis[2-ethylhexyl] sulfosuccinate (AOT).

- ✓ *Cationic*, in which the head groups are positively charged. They are not biodegradable and are used as bactericides. Due to the tendency to be adsorbed at negatively charged surfaces, they are anticorrosive and antistatic agents. These type of surfactants are generally molecules derived from substituted NH_4^+ compounds. Examples: $RNH_3^+Cl^-$ (salt of long-chain amine), $RN(CH_3)_3^+Cl^-$ (quaternary ammonium chloride), CTAB.
- ✓ *Zwitterionic*, these surfactants contain both cationic and anionic groups. In general, their properties highly depend on the pH of the solution. Example: $RH^+H_2CH_2COO^-$ (long-chain amino acid), $RN^+(CH_3)_2CH_2CH_2SO_3^-$ (sulfobetaine).
- ✓ *Non-ionic*, apparently bears no ionic charge but are polar. Two important classes of non-ionic surfactants are the ones based on ethylene oxide, referred to as ethoxylated surfactants and the multihydroxy products such as glycerols and sucrose esters. The former category has a general form $H(CH_2)_i(OCH_2CH_2)_jOH$ (abbreviated as C_iE_j). Octyl triethylene glycol ether (C_8E_3) is an example of an ethoxylated surfactant.

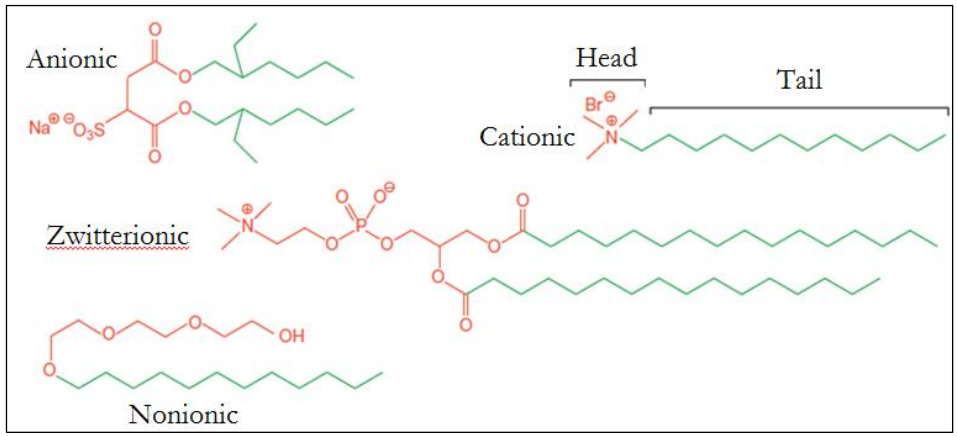

Figure 1.9. Surfactant classification according to the nature of the hydrophilic. The red colored part represents the hydrophilic head and the green colored part represents the hydrophobic chains of the surfactant [146].

1.8.1 Nanoparticle synthesis by microemulsion

The basic methodology for the synthesis of NPs by ME consists of the preparation of two MEs in the same conditions, in which the metal precursor or the reducing agent is in the organic phase. The mixing of the MEs leads to an exchange of matter during collisions of droplets in the ME. The NPs synthesis can be summarized in different steps: i) the ME start to aggregate to form the nuclei; ii) nucleation, in which the nuclei are formed; and ii) growth of the nuclei, processes take place within the droplets and are responsible for controlling the size of the particles. Depending on the ratio of organic compound and water and the hydrophilic-lipophilic balance of the surfactant, MEs can be organic micelles dispersed in water (o/w) or reverse micelles dispersed in aqueous organic phase (w/o). Controlling the size of the drops of water is very important because it determines the final size of metal NPs [139,147–149]. The surfactant type and surfactant concentration also affects the size of the metal particles [150,151].

The NPs obtained through the use of MEs have important advantages, among control over particle size and narrower size distribution are remarkable [139]. The most frequent NPs in ME structures consist of droplets, either of water or of oil, surrounded by a surfactant layer and dispersed in oil or in water, respectively.

Boutonnet et al. (1982) [152] used this procedure for the first time to obtain NPs of Pt, Pd, Rh and Ir from type w/o MEs. As in classical methods of preparation of catalysts based on noble metals, reduction requires the participation of a reducing agent. Most work has focused on the preparation of ME type w/o [139,152,153] formed by aqueous cores are surrounded by molecules of surfactant and have their apolar part directed toward the organic phase. The metal precursor phases are located in the aqueous core and form the metal NPs through the use of a reducing agent or a suitable precipitating agent. The preparation of NPs from o/w MEs is being considered in recent years as to require a smaller amount of solvent, which would be advantageous from an environmental perspective [154].

Several systems based in w/o ME have been used to synthesize Pd NPs, being the systems based on the anionic surfactant AOT among the most used for the synthesis of inorganic NPs in w/o ME. AOT provides good control of droplet size and the large ME regions found in the water/AOT/alkane systems give important flexibility for the modification of the conditions for NPs synthesis. It has also been found that the size of the inverse ME droplets formed by this type of systems increases linearly with the amount of water. Thus, Kosydar et al. [155] reported on the use of two ME systems, one based on AOT/isooctane/water of Pd^{2+}, and another based on the non-ionic surfactant polyoxyethylene(7-8)octylphenyl ether (Triton-X 114)-cyclohexane- aqueous solution of Pd^{2+}. Pd NPs with sizes between 9.4 and 8.0 nm were obtained, respectively, with N_2H_4 as reducing agent at equivalent conditions. It has also been found that at the same water to surfactant ratio (w_0), the ME droplets for the non-ionic surfactants are slightly larger than those based on anionic surfactants, thus giving larger NPs [122,156]. The application of the ME system based on water/AOT/isooctane for the synthesis of Pd NPs has also been reported by Semagina et al. [157], Heshmatpour et al. [158] and Noh et al.[129,159], who reported different NP size and size distributions obtained depending on the reducing agent or precursor salt. Regarding the reducing agent, larger NPs and a wider size range were obtained with N_2H_4 (6-13 nm), compared to the results with $NaBH_4$ (3.9-5 nm). NPs with smaller size (around 4.5 nm) and narrower size distribution were also reported when NaH_2PO_2 was used as reducing agent [155]. Though all these results clearly demonstrate that the type of reducing agent plays a crucial role on the size of the metal particles formed, some works [160] showed that Pd NPs with similar mean size and size distribution were obtained when N_2H_4 or $NaBH_4$ were used as a reducing agent, thus indicating the contribution of other factors.

Another more complex system using octadecyl amine polyoxyethylene ether (OAPE-5)/hydrogenated tallow amine (HTA)/n-butylalcohhol/toluene has been reported [128] for the synthesis of Pd NPs with an average size of 10 nm. A

drawback associated to the stability was observed for these NPs, undergoing aggregation after 30-50 min and loss of their catalytic properties.

A variety of surfactants have been using, mainly as a consequence of the metal studied: AOT, octadecyl amine polyoxyethylene ether (BEPA-5), polyethylene glycol ether docecil (NP-5), cetyltrimethylammonium chloride (CTAC), polyoxyethylene cetyl ether (C15), polyoxyethylene octylphenol (TX-100) [161,162]. The metal precursor used depends mainly on the metal, being usually chlorides, acetates and NO_3^- for Pd, Rh and Cu. The selection of the organic phase also plays an important role in the average size of NPs obtained. The literature contains a wide variety of organic compounds used for this purpose: cyclohexane, 1-butanol, 1-hexanol, 1-octanol, n-octane 1-decanol, toluene, isooctane, etc. Salabat et al. [163] studied the influence of solvent (n-hexane, cyclohexane and n-nonane) employed during the NPs synthesis in ME. They observed that for the synthesis of Pt NPs in w/o using AOT as surfactant, the organic phase affected the NPs size. The NPs size increased as a function of the solvent used as follows: n-hexane < cyclohexane < n-nonane. In this sense, Wojcieszak et al. [164] evaluated the Pd NPs size supported on TiO_2 by w/o system and AOT as surfactant using different organic solvents (cyclohexane, 1-butanol, 1-octanol, and n-octane). Their experiments concluded that the smallest NPs were obtained when n-octane, 1-octanol or cyclohexane were used as organic solvent. In this work, Pd NPs size was controlled with the solvent, increasing the NP size from 1 to 8 nm when shorter chain alcohols (1-octanol and 1-butanol respectively) were used.

The most common reducing agents are N_2H_4 [165-167], $NaBH_4$ [129,165,167,168] and H_2 [128,139]. The choice of the two first mentioned versus H_2 is primarily motivated by the high rate of reduction that is achieved with the use of them. In general, a faster nucleation process leads to the production of smaller particles [139].

The most studied case is the preparation of NPs consisting of a single metal, although there are some studies that refer to the synthesis of bimetallic NPs

such as Pd-Ni [166] and Pd-Au [127]. However, the potential of NPs composed of two different metals is very large. In addition to optical, electronic and magnetic properties this kind of particles can lead to an intensification of catalytic activity. This enhancement is caused mainly by two factors: the structure and size of bimetallic NPs, thus bimetallic NPs can be arranged in a structure core-shell or nanoalloy.

1.10. References

[1] European Environment Agency, – water, www.eea.europa.eu/themes/water, (accessed April, 2017).

[2] S. Anandan, G.-J. Lee, P.-K. Chen, C. Fan, J.J. Wu, Removal of Orange II Dye in Water by Visible Light Assisted Photocatalytic Ozonation Using Bi_2O_3 and Au/Bi_2O_3 Nanorods, Ind. Eng. Chem. Res. 49 (2010) 9729–9737.

[3] Http://www.euro.who.int/en/home, World Health Organitation, (accessed April, 2017).

[4] UNESCO, Programa Mundial de Evaluación de los Recursos Hídricos de las Naciones Unidas, (2016).

[5] European Union, Directive 2000/60/EC of the European Parliament and of the Council of 23 October 2000 Establishing a Framework for Community Action in the Field of Water Policy, 2000, http://eur-lex.europa.eu, (accessed May, 2017).

[6] EUR-Lex, Acess to European Union law, (n.d.). http://eur-lex.europa.eu/homepage.html, (accessed May, 2017).

[7] W. Brack, V. Dulio, M. Ågerstrand, I. Allan, R. Altenburger, M. Brinkmann, et al., Towards the review of the European Union Water Framework Directive: Recommendations for more efficient assessment and management of chemical contamination in European surface water resources, Sci. Total Environ. 576 (2017) 720–737.

[8] E. Union, Decision No 1386/2013/EU of the European Parliament and the Council of 20 November 2013 on a General Union Environment Action Programme to 2020 "Living Well, Within the Limits of Our Planet".OJ L345. 28.12.2013, 2013.

[9] Agarwal S. K., Water Pollution, APH Publishing, 2005.

[10] A. Koolivand, H. Mazandaranizadeh, M. Binavapoor, A. Mohammadtaheri, R. Saeedi, Hazardous and industrial waste composition and associated management activities in Caspian industrial park, Iran, Environ. Nanotechnology, Monit. Manag. 7 (2017) 9–14.

[11] E. Custodio, Coastal aquifers of Europe: an overview, (n.d.).

[12] P. Pulido-Leboeuf, Seawater intrusion and associated processes in a small coastal complex aquifer (Castell de Ferro, Spain), Appl. Geochemistry. 19 (2004) 1517–1527.

[13] E. Alley, Water Quality control Handbook. McGraw - Hill, New York., 2000.

[14] M.E. Stuart, P.J. Chilton, D.G. Kinniburgh, D.M. Cooper, Screening for long-term trends in groundwater nitrate monitoring data, Q. J. Eng. Geol. Hydrogeol. 40 (2007) 361–376.

[15] F.T. Wakida, D.N. Lerner, Non-agricultural sources of groundwater nitrate: a review and case study, Water Res. 39 (2005) 3–16.

[16] B.P. Chaplin, E. Roundy, K.A. Guy, J.R. Shapley and C.J. Werth, Effects of Natural Water Ions and Humic Acid on Catalytic Nitrate Reduction Kinetics Using an Alumina Supported Pd-Cu Catalyst, Environ. Sci. Technol. 40 (2006) 3075–3081.

[17] G. Centi, S. Perathoner, Remediation of water contamination using catalytic technologies, Appl. Catal. B Environ. 41 (2003) 15–29.

[18] Ministerio de Medio Ambiente, Caracterización de las Fuentes Agrarias de Contaminación de las Aguas por Nitratos, (1996).

[19] Z. Zhao, G. Tong, X. Tan, Nitrite removal from water by catalytic hydrogenation in a Pd-CNTs/Al 2 O 3 hollow fiber membrane reactor, J. Chem. Technol. Biotechnol. 91 (2015) 2298–2304.

[20] T. Harter, J.R. Lund, Addressing Nitrate in California's Drinking Water, Calif. State Water Resour. Control Board. (2012). http://groundwaternitrate.ucdavis.edu/files/138956.pdf, (accessed May, 2017).

[21] D.B. Thakur, R.M. Tiggelaar, Y. Weber, J.G.E. Gardeniers, L. Lefferts, K. Seshan, Applied Catalysis B : Environmental Ruthenium catalyst on carbon nanofiber support layers for use in silicon-based structured microreactors . Part II : Catalytic reduction of bromate contaminants in aqueous phase, "Applied Catal. B, Environ. 102 (2011) 243–250.

[22] Nitrate in groudwater, European Environment Agency, http://www.eea.europa.eu/data-and-maps/indicators/nitrate-in-groundwater, (accessed May, 2017).

[23] T.F. Marhaba, K. Bengrane, Review of strategies for minimizing bromate formation resulting from drinking water ozonation, Clean Technol. Environ. Policy. 5 (2003) 101–122.

[24] S.D.W.A. SDWA, U. S. EPA National primary drinking water standards, https://www.epa.gov/dwstandardsregulations#listmcl, (accessed April, 2017).

[25] D. Bamba, M. Coulibaly, D. Robert, Nitrogen-containing organic compounds: Origins, toxicity and conditions of their photocatalytic mineralization over TiO_2, Sci. Total Environ. 580 (2016) 1489–1504.

[26] N. Wehbe, K. Fiaty, S. Miachon, Hydrogenation of nitrates in water using mesoporous membranes operated in a flow-through catalytic contactor, Catal. Today. 156 (2010) 208–215.

[27] Z. Zhang, Y. Xu, W. Shi, W. Wang, R. Zhang, X. Bao, et al., Electrochemical-catalytic reduction of nitrate over Pd–Cu/γAl_2O_3 catalyst in cathode chamber: Enhanced removal efficiency and N_2 selectivity, Chem. Eng. J. 290 (2016) 201–208.

[28] M. Pidwirny, Fundamentals of Physical Geography: The Nitrogen Cycle, 1 (2006). http://www.physicalgeography.net/fundamentals/9s.html, (accessed April, 2017).

[29] M.S. Elovitz, U. von Gunten, H.-P. Kaiser, Hydroxyl Radical/Ozone Ratios During Ozonation Processes. II. The Effect of Temperature, pH, Alkalinity, and DOM Properties, Ozone Sci. Eng. 22 (2000) 123–150.

[30] M.B. Heeb, J. Criquet, S.G. Zimmermann-Steffens, U. Von Gunten, Oxidative treatment of bromide-containing waters: Formation of bromine and its reactions with inorganic and organic compounds - A critical review, Water Res. 48 (2014) 15–42.

[31] M. Siddiqui, W. Zhai, A. Gary, C. Mysore, Bromate ion removal by activated carbon, Water Res. 30 (1996) 1651–1660.

[32] J. Restivo, O.S.G.P. Soares, J.J.M. Órfão, M.F.R. Pereira, Bimetallic activated carbon supported catalysts for the hydrogen reduction of bromate in water, Catal. Today. 249 (2015) 213–219.

[33] U. Von Gunten, Ozonation of drinking water: Part II. Disinfection and by-product formation in presence of bromide, iodide or chlorine, Water Res. 37 (2003) 1469–1487.

[34] R.J. Garcia-Villanova, M.V. Oliveira Dantas Leite, J.M. Hernández Hierro, S. de Castro Alfageme, C. García Hernández, Occurrence of bromate, chlorite and chlorate in drinking waters disinfected with hypochlorite reagents. Tracing their origins, Sci. Total Environ. 408 (2010) 2616–2620.

[35] X. Ma, S. Liu, Y. Liu, G. Gu, C. Xia, Comparative study on catalytic hydrodehalogenation of halogenated aromatic compounds over Pd/C and Raney Ni catalysts, Sci. Rep. 6 (2016) 25068.

[36] A. Pyo, S. Kim, M.R. Kumar, A. Byeun, M.S. Eom, M.S. Han, et al., Palladium-catalyzed hydrodehalogenation of aryl halides using paraformaldehyde as the hydride source: high-throughput screening by paper-based colorimetric iodide sensor, 2013.

[37] F. Murena, F. Gioia, Catalytic hydrotreatment of water contaminated by chlorinated aromatics, Catal. Today. 75 (2002) 57–61.

[38] E. Diaz, A.F. Mohedano, J.A. Casas, L. Calvo, M.A. Gilarranz, J.J. Rodriguez, Comparison of activated carbon-supported Pd and Rh catalysts for aqueous-phase hydrodechlorination, Applied Catal. B, Environ. 106 (2011) 469–475.

[39] C. Amorim, M.A. Keane, Catalytic hydrodechlorination of chloroaromatic gas streams promoted by Pd and Ni: The role of hydrogen spillover, J. Hazard. Mater. 211 (2012) 208–217.

[40] L. Calvo, M.A. Gilarranz, J.A. Casas, A.F. Mohedano, J.J. Rodriguez, Hydrodechlorination of diuron in aqueous solution with Pd, Cu and Ni on activated carbon catalysts, Chem. Eng. J. 163 (2010) 212–218.

[41] M. Al Bahri, L. Calvo, A.M. Polo, M.A. Gilarranz, A.F. Mohedano, J.J. Rodriguez, Identification of by-products and toxicity assessment in aqueous-phase hydrodechlorination of diuron with palladium on activated carbon catalysts, Chemosphere. 91 (2013) 1317–1323.

[42] J.A. Baeza, L. Calvo, J.J. Rodriguez, E. Carbó-Argibay, J. Rivas, M.A. Gilarranz, et al., Activity enhancement and selectivity tuneability in aqueous phase hydrodechlorination by use of controlled growth Pd-Rh nanoparticles, Appl. Catal. B Environ. 168–169 (2015) 283–292.

[43] J.A. Baeza, N. Alonso-Morales, L. Calvo, F. Heras, J.J. Rodriguez, M.A. Gilarranz, Hydrodechlorination activity of catalysts based on nitrogen-doped carbons from low-density polyethylene, Carbon N. Y. 87 (2015) 444–452.

[44] S. Ordóñez, E. Díaz, R.F. Bueres, E. Asedegbega-Nieto, H. Sastre, Carbon nanofibre-supported palladium catalysts as model hydrodechlorination catalysts, J. Catal. 272 (2010) 158–168.

[45] F.-D. Kopinke, K. Mackenzie, R. Koehler, A. Georgi, Alternative sources of hydrogen for hydrodechlorination of chlorinated organic compounds in water on Pd catalysts, Appl. Catal. A Gen. 271 (2004) 119–128.

[46] L. Calvo, M.A. Gilarranz, J.A. Casas, A.F. Mohedano, J.J. Rodríguez, Hydrodechlorination of 4-chlorophenol in water with formic acid using a Pd/activated carbon catalyst, J. Hazard. Mater. 161 (2009) 842–847.

[47] L. Calvo, M.A. Gilarranz, J.A. Casas, A.F. Mohedano, J.J. Rodríguez, Hydrodechlorination of 4-chlorophenol in aqueous phase using Pd/AC catalysts prepared with modified active carbon supports, Appl. Catal. B Environ. 67 (2006) 68–76.

[48] F. Ukisu, T. Miyadera, Hydrogen-transfer hydrodehalogenation of aromatic halides with alcohols in tiae presence of noble metal catalysts, J. Mol. Catal. A Chem. 125 (1997) 135–142.

[49] V. Felis, C. De Bellefon, P. Fouilloux, D. Schweich, Hydrodechlorination and hydrodearomatisation of monoaromatic chlorophenols into cyclohexanol on Ru/C catalysts applied to water depollution: in¯uence of the basic solvent and kinetics of the reactions, Appl. Catal. B Environ. 20 (1999) 91–100.

[50] L. Calvo, M.A. Gilarranz, J.A. Casas, A.F. Mohedano, J.J. Rodríguez, Hydrodechlorination of alachlor in water using Pd, Ni and Cu catalysts supported on activated carbon, 78 (2008) 259–266.

[51] G. Yuan, M.A. Keane, Liquid phase catalytic hydrodechlorination of chlorophenols at 273 K, Catal. Commun. 4 (2003) 195–201.

[52] J.A. Baeza, L. Calvo, M.A. Gilarranz, A.F. Mohedano, J.A. Casas, J.J. Rodriguez, Catalytic behavior of size-controlled palladium nanoparticles in the hydrodechlorination of 4-chlorophenol in aqueous phase, J. Catal. 293 (2012) 85–93.

[53] Y. Yoshinaga, T. Akita, I. Mikami, T. Okuhara, Hydrogenation of Nitrate in Water to Nitrogen over Pd–Cu Supported on Active Carbon, J. Catal. 207 (2002) 37–45.

[54] A.E. Palomares, C. Franch, A. Corma, Nitrates removal from polluted aquifers using (Sn or Cu)/Pd catalysts in a continuous reactor, Catal. Today. 149 (2010) 348–351.

[55] J. Jung, S. Bae, W. Lee, Nitrate reduction by maghemite supported Cu-Pd bimetallic catalyst, Appl. Catal. B Environ. 127 (2012) 148–158.

[56] A.H. Pizarro, C.B. Molina, J.J. Rodriguez, F. Epron, Catalytic reduction of nitrate and nitrite with mono- and bimetallic catalysts supported on pillared clays, J. Environ. Chem. Eng. 3 (2015) 2777–2785.

[57] S. Jung, S. Bae, W. Lee, Development of Pd−Cu/Hematite Catalyst for Selective Nitrate Reduction, Environ. Sci. Technol. 48 (2014) 9651–9658.

[58] L. Calvo, M.A. Gilarranz, J.A. Casas, A.F. Mohedano, J.J. Rodriguez, Denitrification of Water with Activated Carbon-Supported Metallic Catalysts, Ind. Eng. Chem. Res. 49 (2010) 5603–5609.

[59] V.K. Tzitzios, V. Georgakilas, Catalytic reduction of N_2O over Ag-Pd/Al_2O_3 bimetallic catalysts., Ag-Pd/Al_2O_3 Chemosph. Bimetallic. 59 (2005) 887–91.

[60] A. Garron, K. Lázár, F. Epron, Effect of the support on tin distribution in Pd–Sn/Al_2O_3 and Pd–Sn/SiO_2 catalysts for application in water denitration, Appl. Catal. B Environ. 59 (2005) 57–69.

[61] K. Nakamura, Y. Yoshida, I. Mikami, T. Okuhara, Cu-Pd/b-Zeolites as Highly Selective Catalysts for the Hydrogenation of Nitrate with Hydrogen to Harmless Products, Chem. Lett. 34 (2005) 678–679.

[62] O.S.G.P. Soares, M.F.R. Pereira, J.J.M. Órfao, J.L. Faria, C.G. Silva, Photocatalytic nitrate reduction over Pd-Cu/TiO_2, Chem. Eng. J. 251 (2014) 123–130.

[63] Y. Guo, J. Cheng, Y. Hu, D. Li, The effect of TiO_2 doping on the catalytic properties of nano-Pd/SnO_2 catalysts during the reduction of nitrate, Appl. Catal. B Environ. 125 (2012) 21–27.

[64] H. Demiral, G. Gündüzoğlu, Removal of nitrate from aqueous solutions by activated carbon prepared from sugar beet bagasse, Bioresour. Technol. 101 (2010) 1675–1680.

[65] L. Lemaignen, C. Tong, V. Begon, R. Burch, D. Chadwick, Catalytic denitrification of water with palladium-based catalysts supported on activated carbons, Catal. Today. 75 (2002) 43–48.

[66] O.S.G.P. Soares, J.J.M. Órfão, M.F.R. Pereira, Nitrate reduction with hydrogen in the presence of physical mixtures with mono and bimetallic catalysts and ions in solution, Appl. Catal. B Environ. 102 (2011) 424–432.

[67] M. Al Bahri, L. Calvo, M.A. Gilarranz, J.J. Rodriguez, F. Epron, Activated carbon supported metal catalysts for reduction of nitrate in water with high selectivity towards N_2, Appl. Catal. B Environ. 138–139 (2013) 141–148.

[68] H. Chen, Z. Xu, H. Wan, J. Zheng, D. Yin, S. Zheng, Aqueous bromate reduction by catalytic hydrogenation over Pd/Al_2O_3 catalysts, Appl. Catal. B Environ. 96 (2010) 307–313.

[69] P.Y. Yang, S. Nitisoravut, J.S. Wu, Nitrate removal using a mixed-culture entrapped microbial cell immobilization process under high salt conditions, Water Res. 29 (1995).

[70] J. Kim, M.M. Benjamin, Modeling a novel ion exchange process for arsenic and nitrate removal, Water Res. 38 (2004) 2053–2062.

[71] N. Barrabés, J. Sá, Catalytic nitrate removal from water, past, present and future perspectives, Appl. Catal. B Environ. 104 (2011) 1–5.

[72] K. Watson, M.J. Farré, N. Knight, Strategies for the removal of halides from drinking water sources, and their applicability in disinfection by-product minimisation: A critical review, J. Environ. Manage. 110 (2012) 276–298.

[73] T. Vorlop, KD and Tacke, 1st steps towards noble-metal catalyzed removal of nitrate and nitrite from drinking-water, Chemie Ing. Tech. 61 (1989) 836--837.

[74] I. Mikami, R. Kitayama, T. Okuhara, Hydrogenations of nitrate and nitrite in water over Pt–promoted Ni catalysts, Appl. Catal. A Gen. 297 (2006) 24–30.

[75] O.S.G.P. Soares, J.J.M. Órfão, J. Ruiz-Martínez, J. Silvestre-Albero, A. Sepúlveda-Escribano, M.F.R. Pereira, Pd-Cu/AC and Pt-Cu/AC catalysts for nitrate reduction with hydrogen: Influence of calcination and reduction temperatures, Chem. Eng. J. 165 (2010) 78–88.

[76] O.S.G.P. Soares, J.J.M. Órfão, M.F.R. Pereira, Nitrate reduction in water catalysed by Pd–Cu on different supports, Desalination. 279 (2011) 367–374.

[77] S.D. Ebbesen, B.L. Mojet, L. Lefferts, In situ ATR-IR study of nitrite hydrogenation over Pd/Al_2O_3, J. Catal. 256 (2008) 15–23.

[78] J.K. Chinthaginjala, L. Lefferts, Support effect on selectivity of nitrite reduction in water, Appl. Catal. B Environ. 101 (2010) 144–149.

[79] F. Epron, F. Gauthard, C. Pi, J. Barbier, Catalytic Reduction of Nitrate and Nitrite on $Pt–Cu/Al_2O_3$ Catalysts in Aqueous Solution: Role of the Interaction between Copper and Platinum in the Reaction, J. Catal. 198 (2001) 309–318.

[80] N. Barrabés, J. Just, A. Dafinov, F. Medina, J.L.G. Fierro, J.E. Sueiras, et al., Catalytic reduction of nitrate on Pt-Cu and Pd-Cu on active carbon using continuous reactor: The effect of copper nanoparticles, Appl. Catal. B Environ. 62 (2006) 77–85.

[81] F. Zhang, S. Miao, Y. Yang, X. Zhang, J. Chen, N. Guan, Size-Dependent Hydrogenation Selectivity of Nitrate on Pd - Cu/TiO_2 Catalysts, J. Phys. Chem. C. 112 (2008) 7665–7671.

[82] S. Hörold, T. Tacke, K. Vorlop, Catalytical removal of nitrate and nitrite from drinking water: 1. Screening for hydrogenation catalysts and influence of reaction conditions on activity and selectivity, Environ. Technol. 14 (1993) 931–939.

[83] K. Wada, T. Hirata, S. Hosokawa, S. Iwamoto, M. Inoue, Effect of supports on Pd-Cu bimetallic catalysts for nitrate and nitrite reduction in water, Catal. Today. 185 (2012) 81–87.

[84] K.A. Guy, H. Xu, J.C. Yang, C.J. Werth, J.R. Shapley, Catalytic nitrate and nitrite reduction with Pd-Cu/PVP colloids in water: Composition, structure, and reactivity correlations, J. Phys. Chem. C. 113 (2009) 8177–8185.

[85] Z. Xu, L. Chen, Y. Shao, D. Yin, S. Zheng, Catalytic Hydrogenation of Aqueous Nitrate over Pd - Cu/ZrO_2 Catalysts, Ind. Eng. Chem. Res. 48 (2009) 8356–8363.

[86] O.S.G.P. Soares, J.J.M. Órfão, M.F.R. Pereira, Bimetallic catalysts supported on activated carbon for the nitrate reduction in water: Optimization of catalysts composition, Appl. Catal. B Environ. 91 (2009) 441–448.

[87] J. Trawczyński, P. Gheek, J. Okal, M. Zawadzki, M.J.I. Gomez, Reduction of nitrate on active carbon supported Pd-Cu catalysts, Appl. Catal. A Gen. 409 (2011) 39–47.

[88] S. Hörold, K.D. Vorlop, T. Tacke, M. Sell, Development of catalysts for a selective nitrate and nitrite removal from drinking water, Catal. Today. 17 (1993) 21–30.

[89] C. Franch, E. Rodríguez-Castellón, Á. Reyes-Carmona, A.E. Palomares, Characterization of (Sn and Cu)/Pd catalysts for the nitrate reduction in natural water, Appl. Catal. A Gen. 425–426 (2012) 145–152.

[90] J. Sá, H. Vinek, Catalytic hydrogenation of nitrates in water over a bimetallic catalyst, Appl. Catal. B Environ. 57 (2005) 247–256.

[91] M.P. Maia, M.A.M.A. Rodrigues, F.B. Passos, Nitrate catalytic reduction in water using niobia supported palladium-copper catalysts, Catal. Today. 123 (2007) 171–176.

[92] F.A. Marchesini, L.B. Gutierrez, C.A. Querini, E.E. Miró, Pt,In and Pd,In catalysts for the hydrogenation of nitrates and nitrites in water. FTIR characterization and reaction studies, Chem. Eng. J. 159 (2010) 203–211.

[93] R. Gavagnin, L. Biasetto, F. Pinna, G. Strukul, Nitrate removal in drinking waters: the effect of tin oxides in the catalytic hydrogenation of nitrate by Pd/SnO_2 catalysts, Appl. Catal. B Environ. 38 (2002) 91–99.

[94] A. Devadas, S. Vasudevan, F. Epron, Nitrate reduction in water: Influence of the addition of a second metal on the performances of the Pd/CeO_2 catalyst, J. Hazard. Mater. 185 (2011) 1412–1417.

[95] C. Neyertz, F.A. Marchesini, A. Boix, E. Miró, C.A. Querini, Catalytic reduction of nitrate in water: Promoted palladium catalysts supported in resin, Appl. Catal. A Gen. 372 (2010) 40–47.

[96] O.S.G.P. Soares, L. Marques, C.M.A.S. Freitas, A.M. Fonseca, P. Parpot, J.J.M. Órfão, et al., Mono and bimetallic NaY catalysts with high performance in nitrate reduction in water, Chem. Eng. J. 281 (2015) 411–417.

[97] F. Deganello, L.F. Liotta, A. Macaluso, A.M. Venezia, G. Deganello, Catalytic reduction of nitrates and nitrites in water solution on pumice-supported Pd-Cu catalysts, Appl. Catal. B Environ. 24 (2000) 265–273.

[98] F. Epron, F. Gauthard, J. Barbier, Catalytic Reduction of Nitrate in Water on a Monometallic Pd/CeO_2 Catalyst, J. Catal. 206 (2002) 363–367.

[99] Y.-N. Guo, J.-H. Cheng, Y.-Y. Hu, D.-H. Li, The effect of TiO 2 doping on the catalytic properties of nano-Pd/SnO_2 catalysts during the reduction of nitrate, Applied Catal. B, Environ. 125 (2012) 21–27.

[100] W. Sun, Q. Li, S. Gao, J.K. Shang, Monometallic Pd/Fe_3O_4 catalyst for denitrification of water, Applied Catal. B, Environ. 125 (2012) 1–9.

[101] W. Zhao, X. Zhu, Y. Wang, Z. Ai, D. Zhao, Catalytic reduction of aqueous nitrates by metal supported catalysts on Al particles, Chem. Eng. J. 254 (2014) 410–417.

[102] A. Pintar, J. Batista, I. Musevic, Palladium-copper and palladium-tin catalysts in the liquid phase nitrate hydrogenation in a batch-recycle reactor, Appl. Catal. B Environ. 52 (2004) 49–60.

[103] J. Sá, D. Gasparovicova, K. Hayek, E. Halwax, J.A. Anderson, H. Vinek, Water denitration over a Pd-Sn/Al2O3 catalyst, Catal. Letters. 105 (2005) 209–217.

[104] M.A. Jaworski, I.D. Lick, G.J. Siri, M.L. Casella, ZrO_2-modified Al_2O_3-supported PdCu catalysts for the water denitrification reaction, Appl. Catal. B Environ. 156–157 (2014) 53–61.

[105] S. Jung, S. Bae, W. Lee, Development of Pd-Cu/hematite catalyst for selective nitrate reduction, Environ. Sci. Technol. 48 (2014) 9651–9658.

[106] Y. Sakamoto, Y. Kamiya, T. Okuhara, Selective hydrogenation of nitrate to

nitrite in water over Cu-Pd bimetallic clusters supported on active carbon, J. Mol. Catal. A Chem. 250 (2006) 80–86.

[107] M. D'Arino, F. Pinna, G. Strukul, Nitrate and nitrite hydrogenation with Pd and Pt/SnO_2 catalysts: the effect of the support porosity and the role of carbon dioxide in the control of selectivity, Appl. Catal. B Environ. 53 (2004) 161–168.

[108] U. Prüsse, M. Hähnlein, J. Daum, K.-D. Vorlop, Improving the catalytic nitrate reduction, Catal. Today. 55 (2000) 79–90.

[109] R. Meijers, J. Kruithof, Potential treatment options for restriction of bromate formation and bromate removal, Water Supply. (1995) 13:183.

[110] W.A.M. Hijnen, R. Jong, D. Van Der Kooij, Bromate removal in a denitrifying bioreactor used in water treatment, Water Res. 33 (1999) 1049–1053.

[111] L. Xie, C. Shang, Effects of copper and palladium on the reduction of bromate by Fe(0), Chemosphere. 64 (2006) 919–930.

[112] W. Ritter, R. Scarborough, A review of bioremediation of contaminated soils and groundwater., J. Environ. Sci. Health. A. Tox. Hazard. Subst. Environ. Eng. (1995) A30:333.

[113] M.P. WJ Huang, CY Chen, Adsorption / reduction of bromate from drinking water using GAC: effects on carbon characteristics and long-term pilot study, Water SA. 30 (2004) 369–375.

[114] J. Restivo, O.S.G.P. Soares, J.J.M. Órfão, M.F.R. Pereira, Catalytic reduction of bromate over monometallic catalysts on different powder and structured supports, Chem. Eng. J. 309 (2017) 197–205.

[115] J.Z. Jiang, C. Cai, In situ formation of dispersed palladium nanoparticles in microemulsion: Efficient reaction system for ligand-free Heck reaction, J. Colloid Interface Sci. 299 (2006) 938–943.

[116] Á. Molnár, Efficient, selective, and recyclable palladium catalysts in carbon-carbon coupling reactions, Chem. Rev. 111 (2011) 2251–2320.

[117] T. Moriya, A. Suzuki, N. Miyaura, A Stereoselective Preparation of T-Alkoxyailylboronates via Catalytic Isomerization of Pinacol [(E)-3-AIkoxy-1-propenyl]boronates, Tetrahedron Lett. 36 (1995) 1887–1888.

[118] S. A. NikolaevV. V. Smirnov, Selective hydrogenation of phenylacetylene on gold nanoparticles, Gold Bull. 42 (2009) 182–189.

[119] K.M. Bratlie, H. Lee, K. Komvopoulos, P. Yang, G.A. Somorjai, Platinum Nanoparticle Shape Effects on Benzene Hydrogenation Selectivity, Nano Letters. 7 (2007) 3097–3101.

[120] V.M. Mévellec, A. Roucoux, Nanoheterogeneous catalytic hydrogenation of N-, O- or S-heteroaromatic compounds by re-usable aqueous colloidal suspensions of rhodium(0), Inorganica Chim. Acta 357. 357 (2004) 3099–3103.

[121] A. Beck, A. Horvath, A. Szucs, Z. Schay, Z.E. Horvath, Z. Zsoldos, et al., Pd nanoparticles prepared by "controlled colloidal synthesis" in solid/liquid interfacial layer on silica. I. Particle size regulation by reduction time, Catal. Letters. 65 (2000) 33–42.

[122] T. Hanaoka, T. Hatsuta, T. Tago, M. Kishida, K. Wakabayashi, Control of the rhodium particle size of the silica-supported catalysts by using microemulsion, Appl. Catal. A Gen. 190 (2000) 291–296.

[123] H. Gustafsson, S. Isaksson, A. Altskär, K. Holmberg, Mesoporous silica nanoparticles with controllable morphology prepared from oil-in-water emulsions., J. Colloid Interface Sci. 467 (2016) 253–60.

[124] H.H. Ingelsten, J.-C. Béziat, K. Bergkvist, A. Palmqvist, M. Skoglundh, H. Qiuhong, et al., Deposition of Platinum Nanoparticles, Synthesized in Water-in-Oil Microemulsions, on Alumina Supports, (2002).

[125] M. Yashima, L.K.L. Falk, A.E.C. Palmqvist, K. Holmberg, Structure and catalytic properties of nanosized alumina supported platinum and palladium particles synthesized by reaction in microemulsion, J. Colloid Interface Sci. 268 (2003) 348–356.

[126] T. Hanaoka, T. Miyazawa, K. Shimura, S. Hirata, Effect of Pt particle density on the hydrocracking of Fischer–Tropsch products over Pt-loaded zeolite catalysts prepared using water-in-oil microemulsions, Chem. Eng. J. 274 (2015) 256–264.

[127] M. Bonarowska, Z. Karpinski, R. Kosydar, T. Szumelda, A. Drelinkiewicz, Hydrodechlorination of CCl4 over carbon-supported palladium-gold catalysts prepared by the reverse "water-in-oil" microemulsion method, Comptes Rendus Chim. 18 (2015) 1143–1151.

[128] C. Liang, J. Han, K. Shen, L. Wang, D. Zhao, H.S. Freeman, Palladium nanoparticle microemulsions: Formation and use in catalytic hydrogenation of o-chloronitrobenzene, Chem. Eng. J. 165 (2010) 709–713.

[129] J.H. Noh, R. Meijboom, Dendrimer-templated Pd nanoparticles and Pd nanoparticles synthesized by reverse microemulsions as efficient nanocatalysts for the Heck reaction: A comparative study, J. Colloid Interface Sci. 415 (2014) 57–69.

[130] J. Hagen, Homogeneously Catalyzed Industrial Processes, in: Ind. Catal., Wiley-VCH Verlag GmbH & Co. KGaA, Weinheim, FRG, 2006: pp. 59–82.

[131] J.J. Bravo-Suárez, R. V. Chaudhari, B. Subramaniam, Design of Heterogeneous Catalysts for Fuels and Chemicals Processing: An Overview, in: Nov. Mater. Catal. Fuels Process., Lawrence, Kansas 66047, USA, 2013: pp. 3–68.

[132] D.Y. Murzin, Nanokinetics for nanocatalysis, Catal. Sci. Technol. 1 (2011) 380.

[133] P. Mäki-Arvela, D.Y. Murzin, Effect of catalyst synthesis parameters on the metal particle size, Appl. Catal. A Gen. 451 (2013) 251–281.

[134] N. Toshima, H. Yan, Y. Shiraishi, Recent Progress in Bimetallic Nanoparticles: Their Preparation, Structures and Functions, in: Elsevier, 2008: pp. 49–75.

[135] J.P. Rao, K.E. Geckeler, Polymer nanoparticles: Preparation techniques and size-control parameters, Prog. Polym. Sci. 36 (2011) 887–913.

[136] S.H. Joo, J.Y. Cheon, J.Y. Oh, Current Trends of Surface Science and Catalysis, (2014) 93–119.

[137] I.M. Vilella, I. Borbáth, J.L. Margitfalvi, K. Lázár, S.R. de Miguel, O.A. Scelza, $PtSn/SiO_2$ catalysts prepared by controlled surface reactions for citral hydrogenation in liquid phase, Appl. Catal. A Gen. 326 (2007) 37–47.

[138] Y. Yuan, N. Yan, P.J. Dyson, Advances in the rational design of rhodium nanoparticle catalysts: Control via manipulation of the nanoparticle core and stabilizer, ACS Catal. 2 (2012) 1057–1069.

[139] S. Eriksson, Preparation of catalysts from microemulsions and their applications in heterogeneous catalysis, Appl. Catal. A Gen. 265 (2004) 207–219.

[140] I. Danielsson, B. Lindman, The definition of microemulsion, Colloids and Surfaces. 3 (1981) 391–392.

[141] K. Holmberg, Surfactant-templated nanomaterials synthesis, J. Colloid Interface Sci. 274 (2004) 355–364.

[142] M.K. Mishra, Handbook of encapsulation and controlled release, n.d.

[143] P.A. Winsor, Hydrotropy, solubilisation and related emulsification processes, Trans. Faraday Soc. 44 (1948) 376.

[144] Tharwat F. Tadros, (2005) Applied Surfactants: Principles and Applications. Verlag GmbH & Co. KGaA, Weinheim. Ed: WILEY-VCH.

[145] J.M. Corkill, J.F. Goodman, S.P. Harrold, Thermodynamics of micellization of non-ionic detergents, Trans. Faraday Soc. 60 (1964) 202.

[146] J. Eastoe, R.F. Tabor, Surfactants and Nanoscience, Elsevier B.V., 2014.

[147] K. Kimijima, T. Sugimoto, Effects of the water content on the growth rate of AgCl nanoparticles in a reversed micelle system, J. Colloid Interface Sci. 286 (2005) 520–525.

[148] M.N. Luwang, R.S. Ningthoujam, N.S. Singh, R. Tewari, S.K. Srivastava, R.K. Vatsa, Surface chemistry of surfactant AOT-stabilized SnO_2 nanoparticles and effect of temperature, J. Colloid Interface Sci. 349 (2010) 27–33.

[149] G. Granata, F. Pagnanelli, D. Nishio-Hamane, T. Sasaki, Effect of surfactant/water ratio and reagents' concentration on size distribution of manganese carbonate nanoparticles synthesized by microemulsion mediated route, Appl. Surf. Sci. 331 (2015) 463–471.

[150] N.N. Nassar, M.M. Husein, Study and modeling of iron hydroxide nanoparticle uptake by AOT (w/o) microemulsions, Langmuir. 23 (2007) 13093–13103.

[151] F. Debuigne, L. Jeunieau, M. Wiame, J.B. Nagy, Synthesis of organic nanoparticles in different W/O microemulsions, Langmuir. 16 (2000) 7605–7611.

[152] M. Boutonnet, J. Kizling, P. Stenius, G. Maire, The preparation of monodisperse colloidal metal particles from microemulsions, Colloids and Surfaces. 5 (1982) 209–225.

[153] I. Capek, Preparation of metal nanoparticles in water-in-oil (w/o) microemulsions, Adv. Colloid Interface Sci. 110 (2004) 49–74.

[154] M. Sanchez-Dominguez, K. Pemartin, M. Boutonnet, Preparation of inorganic nanoparticles in oil-in-water microemulsions: A soft and versatile approach, Curr. Opin. Colloid Interface Sci. 17 (2012) 297–305.

[155] R. Kosydar, M. Góral, J. Gurgul, A. Drelinkiewicz, The effect of support properties in the preparation of Pd size-controlled catalysts by "water-in-oil" microemulsion method, Catal. Commun. 22 (2012) 58–67.

[156] A. Martínez, G. Prieto, Breaking the dispersion-reducibility dependence in oxide-supported cobalt nanoparticles, J. Catal. 245 (2007) 470–476.

[157] N. Semagina, A. Renken, L. Kiwi-Minsker, Palladium nanoparticle size effect in 1-hexyne selective hydrogenation, J. Phys. Chem. C. 111 (2007) 13933–13937.

[158] F. Heshmatpour, R. Abazari, S. Balalaie, Preparation of monometallic (Pd, Ag) and bimetallic (Pd/Ag, Pd/Ni, Pd/Cu) nanoparticles via reversed micelles and their use in the Heck reaction, Tetrahedron. 68 (2012) 3001–3011.

[159] J.H. Noh, R. Meijboom, Synthesis and catalytic evaluation of dendrimer-templated and reverse microemulsion Pd and Pt nanoparticles in the reduction of 4-nitrophenol: The effect of size and synthetic methodologies, Appl. Catal. A Gen. 497 (2015) 107–120.

[160] M. Chen, Y. gang Feng, L. ying Wang, L. Zhang, J.Y. Zhang, Study of palladium nanoparticles prepared from water-in-oil microemulsion, Colloids Surfaces A Physicochem. Eng. Asp. 281 (2006) 119–124.

[161] M. Sanchez-Dominguez, M. Boutonnet, C. Solans, A novel approach to metal and metal oxide nanoparticle synthesis: The oil-in-water microemulsion reaction method, J. Nanoparticle Res. 11 (2009) 1823–1829.

[162] J.N. Solanki, R. Sengupta, Z.V.P. Murthy, Synthesis of copper sulphide and copper nanoparticles with microemulsion method, Solid State Sci. 12 (2010) 1560–1566.

[163] A. Salabat, M.R. Far, Solvent effect on the size of platinum nanoparticle synthesized in microemulsion systems, Russ. J. Phys. Chem. A. 86 (2012) 881–883.

[164] R. Wojcieszak, M.J. Genet, P. Eloy, E.M. Gaigneaux, P. Ruiz, Supported Pd nanoparticles prepared by a modified water-in-oil microemulsion method, Elsevier B.V., 2010.

[165] M. Boutonnet, S. Lögdberg, E. Elm Svensson, Recent developments in the application of nanoparticles prepared from w/o microemulsions in heterogeneous catalysis, Curr. Opin. Colloid Interface Sci. 13 (2008) 270–286.

[166] B.A. Cheney, J.A. Lauterbach, J.G. Chen, Reverse micelle synthesis and

characterization of supported Pt/Ni bimetallic catalysts on γ-Al2O3, Appl. Catal. A Gen. 394 (2011) 41–47.

[167] J. Bedia, L. Calvo, J. Lemus, A. Quintanilla, J.A. Casas, A.F. Mohedano, et al., Colloidal and microemulsion synthesis of rhenium nanoparticles in aqueous medium, Colloids Surfaces A Physicochem. Eng. Asp. 469 (2015) 202–210.

[168] J.N. Solanki, Z.V.P. Murthy, Highly monodisperse and sub-nano silver particles synthesis via microemulsion technique, Colloids Surfaces A Physicochem. Eng. Asp. 359 (2010) 31–38.

CHAPTER II

Experimental method

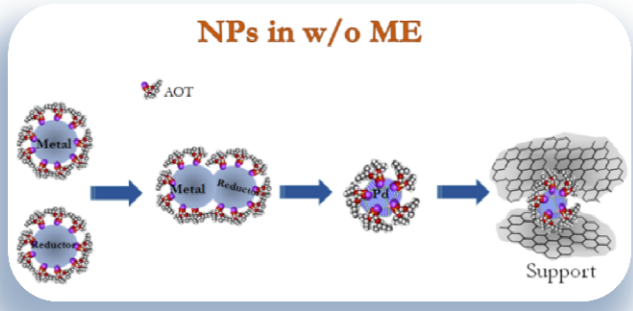

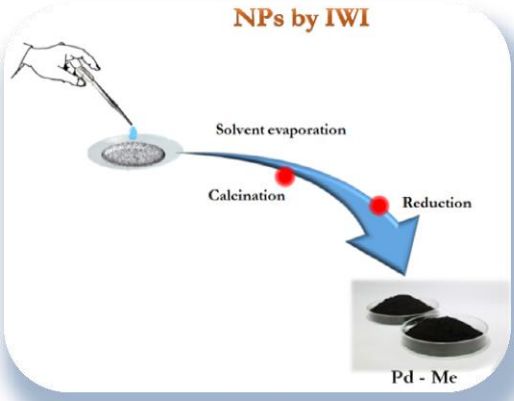

CHAPTER II

Experimental method

2.1. Materials

Tetraamminepalladium (II) chloride monohydrate (≥ 99 %, Sigma-Aldrich Co.), isooctane (99.8 %, Sigma-Aldrich Co.), hydrazine hydrate solution (50-60 %, Fluka) and sodium borohydride (≥ 99 %, Sigma-Aldrich Co.) were used as received. AOT (98 %, Sigma) was vacuum-dried for 24 h at 333 K directly before use. Methanol (> 99%), tri-fluoriethanol (≥ 99 %) and tetrahydrofuran anhydrous (≥99 %) were purchased from Sigma-Aldrich Co. A commercial activated carbon (Merck), commercial multi-walled carbon nanotubes (Nanocyl NC3100) and a commercial titanium dioxide (Degussa P25, 60 % anatase, 40 % rutile, particle size around 100 nm) were used as supports for the metal phase. Sodium nitrate (≥ 99 %, Panreac), sodium nitrite (≥ 99%, Panreac) and sodium bromate (≥99 %, Sigma-Aldrich Co.) were used to prepare nitrate, nitrite and bromate solutions for the catalytic reaction experiments, respectively. Hydrogen (>99 %) and dioxide of carbon (> 99 %) were purchased from PRAXAIR. Sodium hydrogen carbonate (≥ 99 % Merck), sodium carbonate anhydrous (≥99 %, Panreac), nitric acid (65 %, Panreac), 2,6-Pyridinedicarboxylic acid (≥99.5 %, Sigma-Aldrich Co.) and sodium bromide (≥99 %, Sigma-Aldrich Co.) were used to prepare solutions for ionic chromatography calibration. Demineralized bidistilled water was used throughout this work (Nihon Millipore Ltd., Tokyo).

2.2. Catalyst preparation

2.2.1. Supports

The purified NPs were immobilised on different supports such as activated carbon (AC), multi-walled carbon nanotubes (CNT) and titanium dioxide (TiO_2).

In some experiments the AC was subjected to an oxidative treatment with HNO_3, which is carried out by boiling 1 g of support in 10 mL a 6 N HNO_3 solution for 20 min. Afterwards the oxidized supports samples were washed with distilled water until neutral pH and dried overnight at 373 K [1].

The commercial CNT (CNT_M) were subjected to different functionalization in order to obtain supports with different textural and chemical properties. With that purpose, pristine CNTs were doped with N_2 using melamine (M) as N_2 precursor, for that pristine CNTs were ball milled with the N-precursor in a Retsch MM200 equipment using the milling conditions determined in a previous work (4 h at a constant vibration frequency of 15 vibrations/s) and then the resulting material was subjected to a thermal treatment under N_2 flow at 873 K (CNT_{M_873})[2]. Pristine CNTs were also oxidised with HNO_3 7 M during 3 h at boiling temperature to introduce oxygen-containing surface groups (CNT_{HNO3})[3].

Furthermore, in some experiments TiO_2 was calcined in air at 773 K for 5 h before its use as support (TiO_{2_773}). Whit this thermal treatment the contribution of the anatase crystalline phase decreased and rutile contribution increased.

2.2.2. Nanoparticles synthesis by microemulsion

Pd NPs were synthesized using the water/AOT/isooctane ME system [4]. In **Figure2.1** can be seen the mechanism for the formation of Pd NPs by ME. First, two separate MEs were prepared one with the metal precursor ($Pd(NH_3)_4Cl_2 \cdot H_2O$ and/or $CuCl_2 \cdot 2H_2O$) and the other one, with the reducing agent solution, these were stirred for 20 min to form the corresponding ME. The water core of these aggregates is surrounded by the surfactant molecules which have the apolar part of their molecules towards the oil phase. In the water core of these aggregates, electrolytes may be solubilized.

After, the MEs containing the metal precursor (Pd and/or Cu) and the reducing agent were mixed (pH = 9) and stirred to allow reduction, nucleation, growing and the formation of the Pd NPs. The water core of these aggregates is surrounded by the surfactant molecules which have the apolar part of their molecules towards the oil phase. In the water core of these aggregates, electrolytes may be solubilized.

After 10 - 60 min of reaction, the formed NPs were purified. Firstly the ME was subjected to evaporation in a rotary evaporator at 298-368 K and then the excess of surfactant was removed. The difficulty to be removed AOT from metal surface has been attributed to the presence of Na and S. Thus, AOT removal from NPs surface has been considered necessary to minimize the blocking of active centres. For this, it is necessary to purify the NPs from excess of surfactant by addition of solvent followed by centrifugation (this washing was carried out three times). The solvents considered for purification were methanol (MeOH), tetrahydrofuran (THF) and tri-fluoroethanol (TFE).

The NPs resulting from synthesis in AOT-based ME systems have high stability, small particle size, and good monodispersity. Due to its higher solubility in organic phase, AOT helps to extract metal cations from the aqueous to reverse micellar phase. In addition the NPs formed in AOT-based ME have relatively

strong electrostatic interactions with the negatively charged head polar group of AOT molecules, which provides with a protective effect against aggregation.

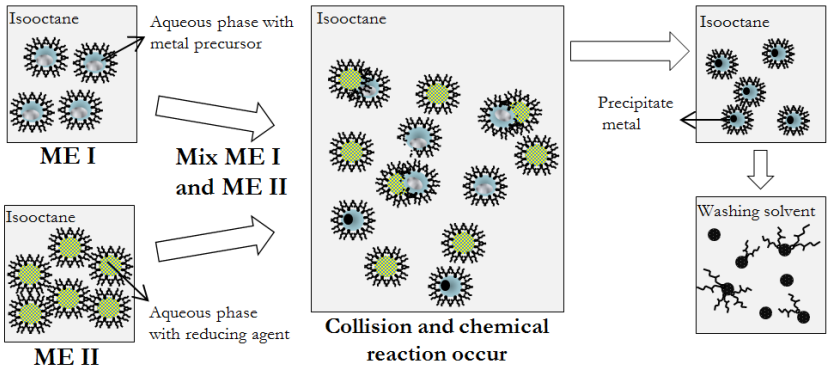

Figure2.1. Mechanism for the formation of NPs by ME.

Table 2.1 and **Table 2.2** summarize the experimental condition for the synthesis of Pd NPs by ME, and the chemical composition of each ME used in this work, respectively.

Table 2.1. Properties of solutions used to ME synthesis.

	Concentration
$[AOT]_{isooctane}$	0.35 M
$[Pd(NH_3)_4Cl_2 \cdot H_2O]_{water}$	0.05 M
$[N_2H_4]_{water}$	3 M

Table 2.2. Weight composition of ME system and ratio molar used to NPs synthesis.

	%wt. ME			Ratio molar		
	Water	AOT	Isooctane	N_2H_4/Pd	AOT/Pd	AOT/ N_2H_4
w_0=3	2.18	17.96	79.86	60	741	12.3
w_0=7	4.97	17.52	77.52		318	5.3
w_0=12	8.22	16.92	74.86		185	3.1

The **Figure2.2** shows the ternary phase diagram of a water/AOT/isooctane ME at constant temperature and pressure. In this phase diagram, L1 and L2 zones

for direct and reversed micellar solution, respectively. The **Figure2.2** also shows the region i) L+LC where liquid crystalline structures and micellar structures coexist in equilibrium; ii) LC region where lyotropic liquid crystal phase is present; and, iii) 2L region in which two separated phases are formed. Especially, this work is focused on the L2 zone, since the values of w_0 fixed for the NPs synthesis were 3, 7 and 12.

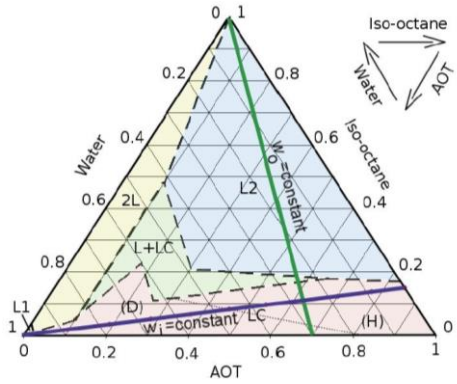

Figure2.2. Ternary phase diagram of water/AOT/isooctane at constant temperature (303 K) and pressure (1 atm) [5].

2.2.3. Immobilization of nanoparticles

In the first method, the Pd NPs purified were immobilized on different supports. The support was mixed with the Pd NPs ME in methanol suspension in a rotary evaporator (Büchi) at 368 K until complete removal of methanol. The nominal content of Pd of the catalysts was varied between 0.5 and 2.5 % (wt. %, dry support basis).

Some of the catalysts prepared were subjected to thermal treatment under 60 NmL·min^{-1} N_2 atmosphere (series N, 423-673 K, 2 h). Other ones were subjected to thermal treatment under N_2 (60 NmL·min^{-1}, 573 K, 2 h) or under air atmosphere (60 NmL·min^{-1}, 573 K, 2 h) and subsequently reduced with H_2 (60 NmL·min^{-1}. 673 K, 2 h). They were denoted as series NH and AirH respectively.

In the second method, the immobilization of the Pd NPs was carried out by incorporation of the support into the ME and destabilization with THF. In this case, Pd NPs were prepared using a w_0 value of 12 and TiO_2 as support. After 10 min of reduction time, the TiO_2 was added to the ME and the mixture was stirred for 1 h. Then 150 mL of THF was added dropwise (0.25 mL·min^{-1}) to destabilize the micellar medium, forcing the Pd NPs to deposit on the surface of the TiO_2. After NP deposition, the catalyst was recovered by filtration and subsequently washed with methanol and acetone. The catalyst was recovered after washing by centrifugation (30 min and 7,000 rpm) and the washing procedure was repeated three times.

In the third method, the NPs were synthesized using only one ME, which contained the metal precursor, using a w_0 of 12. Hydrazine (326 μL) was directly added dropwise to the ME until a reductor-to-metal molar ratio of 60 was reached. After 10 min of reaction, the ME was subjected to evaporation in a rotary evaporator, and then Pd NPs were washed three times with methanol followed by centrifugation (30 min and 7,000 rpm. Finally, the NPs were suspended in methanol and impregnated on TiO_2 (w12/TiO_2 only Pd ME).

2.2.4. Nanoparticles synthesis by incipient wetness impregnation

Incipient wetness impregnation (IWI) was also used a preparation method of supported catalysts. It is carried out as follows: the supported powder is impregnated by an aqueous solution of metal precursors in order to just fill the pores of the support. The volume of impregnating solution exceeded by 30 % the total pore volume of the support. After the impregnation, the catalysts were dried at room temperature for 2 h and overnight at 333 K. Finally, the catalysts were calcined at 473 K in air atmosphere and reduced under continuous H_2 flow (60 NmL·min^{-1}) [6]. The reduction temperature for this synthesis was 473 K for Pd catalysts and 573 K for Cu and Pd:Cu bimetallic catalysts.

The monometallic catalysts were prepared by the IWI method using an aqueous solution of $Pd(NH_3)_4Cl_2 \cdot H_2O$ and a nominal Pd content of 1 % (wt. %, dry AC basis).

When the monometallic catalysts were prepared through IWI using CNTs and TiO_2 like supports, $PdCl_2$ was used as metal precursor. Besides, prior to impregnation, the supports were degassed by ultrasonication in a low pressure system. After impregnation, the samples were dried at 373 K for 24 h, treated under 60 $NmL \cdot min^{-1}$ N_2 flow at 473 K for 1 h, and finally reduced at 373 K under 60 $NmL \cdot min^{-1}$ H_2 flow for 2 h.

The bimetallic catalysts were obtained by IWI and by co-impregnation using aqueous solution of corresponding metal salts ($Pd(NH_3)_4Cl_2 \cdot H_2O$ and $CuCl_2 \cdot 2H_2O$). The nominal metal load of the catalysts was 1% (wt. %, AC basis) with a Pd:Cu molar ratio of 2:1.

In some experiments, physical mixture of monometallic catalysts was used. In this case the monometallic catalysts were prepared fixing at 1.15 Pd wt. % and 0.7 Cu wt. % by IWI.

2.2.5. Nanoparticles synthesis by incipient wetness impregnation poisoned with AOT.

Additionally, some catalysts synthesized via IWI were exposed to a solution of AOT in isooctane using an AOT to Pd mass ratio of 159 (DEF. AOT) and 367 (EXC. AOT). After the poisoning, the catalysts were purified form the excess surfactant by addition of methanol followed by centrifugation (30 min and 7,000 rpm). This washing procedure was repeated three times.

2.3. Catalyst characterization

The Pd NPs synthesized were characterized by transmission electron microscopy (TEM) at 400 kV (JEOL, mod. JEM-4000 EX). Samples were prepared placing a drop of Pd NPs suspension onto a carbon-coated copper grid and letting it dry at room temperature. Software 'ImageJ 1.44i' was used for counting and measuring particles on digital TEM images (more than 200 NPs per sample were measured). Surface-area-weighted mean diameters ($d_s = \Sigma n_i d_i^3 / \Sigma n_i d_i^2$) and size distribution, characterized by the standard deviation ($\sigma_s = (\Sigma (d_i - d_s)^2/n)^{0.5}$), were calculated as described elsewhere[7].

Likewise, the catalysts were characterized by X-Ray Photoelectron Spectroscopy (XPS) (Physical Electronics, mod. K-Alpha equipped with a Al-Kα X-ray excitation source, 1486.68 eV). Samples for XPS analysis were evaporated on an aluminium grid under N_2 atmosphere at ambient temperature to avoid oxidation. Software "XPS Peak Fit" was used for deconvolution in order to determine both Pd electrodeficient and zerovalent species in the particle surface. Peak decomposition is performed using curves with an 80 % Gaussian type and a 15 % Lorentzian type, and a Shirley nonlinear sigmoid-type baseline. The following peaks were used for the quantitative analysis: C 1s, Pd 3d and S 2p. C 1 s peak (284.6 eV) was used as internal standard for binding energies. Deconvoluted peaks values were reported at NIST X- ray Photoelectron Spectroscopy Database [8]. C 1s peak (284.6 eV) was used as internal standard for binding energies [8]. Deconvoluted peaks showed binding energies in the range of 334.8 - 335.8 eV and 336.2 - 337.1

eV for Pd 3d5/2 which can be attributed to metallic Pd (Pd^0) and electron-deficient Pd (Pd^{n+}), respectively. A probing depth of several nanometres can be assumed.

Thermogravimetric analysis (TGA) was used as complementary technique in the study of AOT removal. The samples were heated from room temperature to 1173 K at a rate of 10 K·min^{-1} in N_2 or air. This measured weight loss curve gives information on: i) changes in sample composition, ii) thermal stability and iii) kinetic parameters for chemical reactions in the sample. The derivative weight loss curve can be used to tell the point at which weight loss is most apparent.

The porous structure of the AC supports and the catalysts was characterized by means of N_2 adsorption–desorption at 77 K using a Micromeritics apparatus (Tristar II 3020 model). The samples were previously outgassed at 423 K and a residual pressure lower than 10^{-3} Pa. The Brunauer, Emmett and Teller (BET) and Dubinin–Radushkevich equation are applied to obtain the BET surface area (S_{BET}) and the micropore volume. The external or non-microporous area (A_s) was obtained from the *t*-method.

The textural characterization of the catalysts prepared using CNTs and TiO_2 as support was based on the corresponding N_2 adsorption-desorption isotherms, obtained at 77 K with a Nova 4200e (Quantachrome Instruments) equipment. The samples were degassed at 423 K during 5 h. Surface areas of the CNT samples were determined according to the BET method (S_{BET}) and the total pore volume (V_p) determined from the N_2 uptake at $P/P_0 = 0.95$.

2.4. Nitrite reduction experiments

NO_2^- reduction experiments were carried out during 4 h in a jacketed glass batch reactor where H_2 was continuously fed at 50 NmL·min^{-1} flow rate under vigorous stirring (500-700 rpm) in order to facilitate H_2 distribution through the NO_2^-, solution (150 mL and 50 mg NO_2^-/L). Former works using this set-up showed that the system was not subjected to constrain due to H_2 transfer or

external diffusion [9,10]. The reaction temperature (303 K) was controlled by a thermostatic bath connected to the reactor jacket. In some experiments the pH of the reaction medium was buffered at a pH value around 6. Pure CO_2 was bubbled (50 NmL·min^{-1}) for 30 min through 140 mL of water containing the Pd NPs suspension under vigorous stirring. Then, 10 mL of a 750 mg/L NO_2^- solution was added and H_2 was fed (50 NmL·min^{-1}) together with carbon dioxide. A simple pseudo-first order kinetic equation was used to describe the rate of NO_2^- disappearance. Since H_2 is used in excess, its concentration was included into the pseudo-first-order rate constant ($k_{nitrite}$):

$$(-r) = \frac{-dC_{nitrite}}{dt} = k_{nitrite} \cdot [NO_2^-] \qquad [2.1]$$

The catalytic activity was calculated from the pseudo-first-order constant according to Eq.2.2,

$$a = k_{nitrite} \cdot \frac{[NO_2^-]_{t=0}}{[Pd]} \qquad [2.2]$$

The values of turnover frequency (TOF) were calculated in the case of reactions buffered with CO_2 [11]. This parameter provides the number of revolutions of the catalytic cycle per unit of time and per number of active sites, and it was calculated from the first-order rate constant as follows:

$$TOF\ (min^{-1}) = \frac{k_{nitrite} \cdot [NO_2^-] \cdot S_{Pd} \cdot N_A}{SSA_{Pd} \cdot M_{nitrite}} \qquad [2.3]$$

where S_{Pd} is the surface occupied by one Pd-atom (0.0787 nm^2), N_A is the constant of Avogadro, SSA_{Pd} is the specific surface area of Pd avalilabe and $M_{nitrite}$ is the molar mass of NO_2^-. TOF was calculated assuming a pseudo-spherical shape

of NPs and all surface sites were taken into account, thus ignoring any potential blocking of metal NPs by AOT.

The selectivity to NH_4^+ was defined as:

$$\text{ammonium selectivity (\%)} = \frac{\text{mole of ammonium formed}}{\text{mole of nitrite converted}} \cdot 100 \quad [2.4]$$

2.5. Nitrate reduction experiments

Catalytic NO_3^- reduction runs were carried out during 4 h in a three-necked jacketed glass reactor where CO_2 and H_2 were continuously fed at 50 N mL·min^{-1} flow each of them rate under vigorous stirring in order to facilitate CO_2 and H_2 distribution through the solution. Reduction reactions were performed with a reaction volume of 150 mL, consisting of a 100 mg NO_3/L solution prepared from $NaNO_3$, and at atmospheric pressure and 303 K. The concentration of metal in the reaction medium was 100 mg/L. In the experiments where a mixture of Pd/AC and Cu/AC monometallic catalysts was used, a Pd:Cu moral ratio was maintained. Initially, 1.5 g of catalyst was maintained under bubbling of CO_2 for 10 min with 140 mL of deionised water to generate the buffered medium (pH ≈ 6). After this period, 10 mL of stock NO_3^- solution were added to the reactor with the H_2. Then the reaction starts.

Conversion of NO_3^-, and selectivity to NH_4^+ and NO_2^- were defined as can be seen in Eq. 2.5, 2.6 and 2.7 respectively:

$$X_{NO_3^-}(\%) = \frac{n_{NO_{3,t=0}^-} - n_{NO_3^-\,t}}{n_{NO_{3,t=0}^-}} \cdot 100 \quad [2.5]$$

$$S_{NH_4^+}(\%) = \frac{n_{NH_4^+\,t}}{n_{NO_{3,t=0}^-} - n_{NO_3^-\,t}} \cdot 100 \quad [2.6]$$

$$S_{NO_2^-}(\%) = \frac{n_{NO_2^-\,t}}{n_{NO_{3,t=0}^-} - n_{NO_3^-\,t}} \cdot 100 \quad [2.7]$$

Where $n_{NO_{3,t=0}^-}$ and $n_{NO_{2,t=0}^-}$ is the initial amount of NO_3^- and NO_2^- (mmol) and $n_{NO_{3,t}^-}$, $n_{NO_2^-\,t}$ and $n_{NH_4^+\,t}$ are the amounts of the respective species (mmol) at time t (min). The selectivity towards N_2 was calculated by difference, considering that NO_2^- is the only reaction product in the reduction of NO_3^- and that NO_2^- can be reduced to NH_4^+ or N_2.

2.6. Bromate reduction experiments

Bromate reduction runs were carried out during 2 h in a semi-batch reactor, equipped with a magnetic stirrer working under vigorous stirring (700 rpm) at room temperature and atmospheric pressure. H_2 was used as reducing agent and it was continuously fed at 50 NmL·min^{-1} flow rate. The concentration of Pd in the reaction medium was 1.25·10-3 g/L. Initially, 790 mL of deionized water and 100 mg of catalyst were introduced into the reactor and H_2 was fed to the reactor during 15 min to remove oxygen. After this period, 10 mL of BrO_3^- solution, prepared from $NaBrO_3$, was added to the reactor, in order to obtain a concentration of 10 mg BrO_3^-/L in the reaction medium. Small samples were withdrawn from reactor after defined periods of time.

2.7. Analytical methods used for effluents

The samples of the reaction were analyzed by ion chromatography (Metrohm 790 Compact IC Plus) to know the concentration of ions in the medium of reaction. 1 mL samples were withdrawn from the reactor at different time intervals until the end of the reaction experiment. The samples were filtered over 0.22 μm pore size PTFE filters and analysed by ion chromatography using a Metrosep C4 column and a mixture of 1.7mM HNO_3 and 0.7 mM 2,6-pyridinedicarboxylic acid as mobile phase to analyze the NH_4^+ concentration. To

determine NO_3^-, NO_2^-, BrO_3^- and Br^- concentration, a MetrosepASupp 5 column and a mixture of 3.20 mM NaHCO and 1.00 mM Na_2CO_3 were used.

2.7. Reference

[1] L. Calvo, M.A. Gilarranz, J.A. Casas, A.F. Mohedano, J.J. Rodriguez, Hydrodechlorination of diuron in aqueous solution with Pd, Cu and Ni on activated carbon catalysts, Chem. Eng. J. 163 (2010) 212–218.

[2] O.S.G.P. Soares, R.P. Rocha, A.G. Gonçalves, J.L. Figueiredo, J.J.M. Órfão, M.F.R. Pereira, Easy method to prepare N-doped carbon nanotubes by ball milling, Carbon N. Y. 91 (2015) 114–121.

[3] G.P. Soares, M.F.R. Pereira, Pd - Cu and Pt - Cu Catalysts Supported on Carbon Nanotubes for Nitrate, Ind. Eng. Chem. Res. 49 (2010) 7183–7192.

[4] M. Chen, Y. gang Feng, L. ying Wang, L. Zhang, J.Y. Zhang, Study of palladium nanoparticles prepared from water-in-oil microemulsion, Colloids Surfaces A Physicochem. Eng. Asp. 281 (2006) 119–124.

[5] P. Coussot, J.S. Raynaud, F. Bertrand, P. Moucheront, J.P. Guilbaud, H.T. Huynh, et al., Coexistence of liquid and solid phases in flowing softglassy materials, Phys. Rev. Lett. 88 (2002) sp.

[6] M. Al Bahri, L. Calvo, A.M. Polo, M.A. Gilarranz, A.F. Mohedano, J.J. Rodriguez, Identification of by-products and toxicity assessment in aqueous-phase hydrodechlorination of diuron with palladium on activated carbon catalysts, Chemosphere. 91 (2013) 1317–1323.

[7] N. Krishnankutt., M.A. Vannice, The Effect of Pretreatment on Pd/C Catalysts, J. Catal. 155 (1995) 312–326.

[8] M. X- Ray Photoelectron Spectroscopy Database 20, Version 3.0, National Institute of Standards and Technology, Gaithersburg, http://srdata.nist.gov/XPS., (n.d.).

[9] J.A. Baeza, L. Calvo, M.A. Gilarranz, A.F. Mohedano, J.A. Casas, J.J. Rodriguez, Catalytic behavior of size-controlled palladium nanoparticles in the hydrodechlorination of 4-chlorophenol in aqueous phase, J. Catal. 293 (2012) 85–93.

[10] Y. Zhao, N. Koteswara Rao, L. Lefferts, Adsorbed species on Pd catalyst during nitrite hydrogenation approaching complete conversion, J. Catal. 337 (2016) 102–110.

[11] Y. Zhao, J.A. Baeza, N. Koteswara Rao, L. Calvo, M.A. Gilarranz, Y.D. Li, et al., Unsupported PVA- and PVP-stabilized Pd nanoparticles as catalyst for nitrite hydrogenation in aqueous phase, J. Catal. 318 (2014) 162–169.

CHAPTER III

This chapter is based on the published manuscript

A.M. Perez-Coronado, L. Calvo, N. Alonso-Morales, F. Heras, J.J. Rodriguez, M.A. Gilarranz. *Multiple approaches to control and assess the size of Pd nanoparticles synthesized via water-in-oil microemulsion*. Colloids and Surfaces A: Physicochem. Eng. Aspects 497 (2016) 28–3.

Sección de Ingeniería Química, Universidad Autónoma de Madrid, Av/Francisco Tomás y Valiente 7, 28049 Madrid, Spain

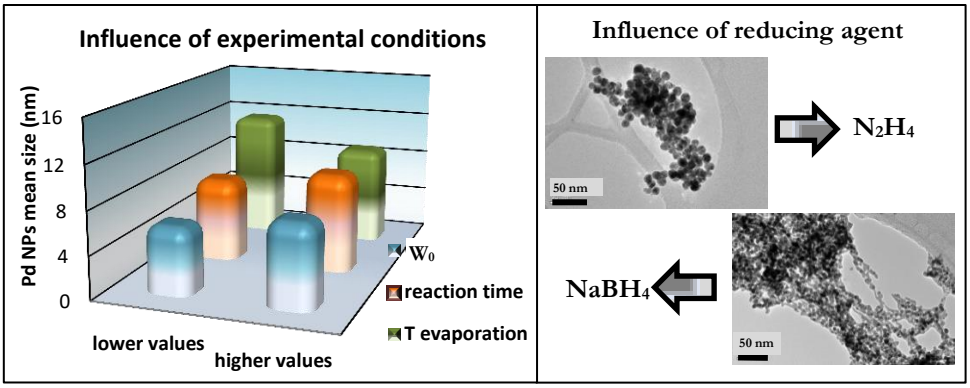

CHAPTER III

Multiple approaches to control and assess the size of Pd nanoparticles synthesized via water-in-oil microemulsion

3.1 Summary

Pd NPs were synthesized by a w/o ME method using the water/AOT/isooctane system. N_2H_4 and $NaBH_4$ were used as reducing agents and w_0 ratios between 3 and 7 were considered. Multiple approaches, considering the physical operations and the synthesis conditions, were followed to assess and control the size of Pd NPs. Thus, the effect of the reduction time, the evaporation temperature and the purification with solvents in the formation of NPs was studied. Smaller NPs and narrower size distributions were obtained by TEM when the NPs were washed with methanol, indicating that a purification stage is needed to assess the influence of the synthesis conditions. Likewise, lower agglomeration and higher hydrophilicity of NPs was observed after washing with methanol. After a reduction time of 10 min, the evaporation of the ME at 298 K led to larger NPs (7.1–9.7 nm) than at 368 K (6.2–7.7 nm). For a reduction time of 60 min, NPs with mean size between 9.1 and 11.7 nm were obtained, and the evaporation temperature only showed influence at high w_0 values. In general, smaller NPs and narrower size distributions were observed in the synthesis carried out with low w_0 values. The type of reducing agent also showed a relevant influence in Pd NPs size.

3.2. Results and discussion

Table 3.1 shows the different conditions considered for the synthesis of Pd NPs in w/o ME. In the water/AOT/isooctane system, the micelles consist of a hydrophilic core compartmentalized by the hydrophilic central head group of the AOT, forming a water-pool, and hydrophobic alkyl tails extending into the non-polar continuous phase solvent (isooctane).

Table 3.1. Experimental conditions for the synthesis of Pd NPs by ME method and results from TEM characterization.

Run	Sample	Reducing agent	w_0 (mol/mol)	Red./metal (mol/mol)	$[AOT]_{isooctane}$ (M)	Reaction time (min)	$T_{evaporation}$ (K)	Washing	d_s (nm)	σ_s (nm)
Pd1	1_Pd3_60_10_368N	N_2H_4	3	60	0.35	10	368	No	8.1	2.2
Pd2	2_Pd3_60_10_368Y		3	60	0.35	10	368	Yes	6.2	1.0
Pd3	3_Pd7_60_10_368N		7	60	0.35	10	368	No	11.7	2.9
Pd4	4_Pd7_60_10_368Y		7	60	0.35	10	368	Yes	7.7	2.5
Pd5	5_Pd3_60_60_368N		3	60	0.35	60	368	No	11.1	2.3
Pd6	6_Pd3_60_60_368Y		3	60	0.35	60	368	Yes	6.3	2.7
Pd7	7_Pd7_60_60_368N		7	60	0.35	60	368	No	11.8	2.9
Pd8	8_Pd7_60_60_368Y		7	60	0.35	60	368	Yes	9.1	2.0
Pd9	9_Pd3_60_10_298Y		3	60	0.35	10	298	Yes	7.1	1.3
Pd10	10_Pd7_60_10_298Y		7	60	0.35	10	298	Yes	9.7	2.0
Pd11	11_Pd3_20_10_298Y		3	20	0.35	10	298	Yes	13.7	1.7
Pd12	12_Pd7_60_60_298Y		7	60	0.35	60	298	Yes	11.7	2.9
Pd13	13_Pd3_60_10_298YB	$NaBH_4$	3	60	0.35	10	298	Yes	3.8	1.1
Pd14	14_Pd7_60_10_298YB		7	60	0.35	10	298	Yes	4.6	1.0
Pd15	15_Pd7_60_10_298YB0.1		7	60	0.1	10	298	Yes	3.5	0.6
Pd16	16_Pd7_60_10_298YB0.5		7	60	0.5	10	298	Yes	4.2	0.8

3.3.1 Approach via physical operations

The NPs size can be controlled via the physical operations and the conditions during the synthesis. The purification of the NPs is a common practice when a ME synthesis route is used, since the presence of surfactant can have a detrimental effect on the subsequent application of the NPs. However, the agglomeration of NPs and their hydrophilicity balance can be controlled during the purification stage. When the ME resulting from the reaction was subjected to evaporation, a sludge of NPs and AOT was obtained. This sludge was not dispersible in water or acetonitrile, but it was easily dispersible in THF, methanol and acetone. After two washes with methanol the NPs were easily recovered by centrifugation and had a high tendency to stick to plasticware. After three washes the hydrophilicity of the NPs increased substantially and they were dispersible in water, although separation by centrifugation became more difficult; thus, a fraction of the washed NPs could not be recovered after centrifugation at 14,000 rpm. Therefore, the AOT remaining on the NPs determines their hydrophobic character and promotes aggregation. TEM-EDX characterization (See appendix, **Figure A.1**) indicated that some AOT remained on the NPs after three washes with methanol, in spite of the important change in the hydrophilic balance. This is in good agreement with the literature, since Xiong and He [1] indicated that ionic surfactants, and particularly AOT, are difficult to remove, mainly due to the presence of Na and S[2].

The results from runs Pd1-Pd8 (**Table 3.1**) show that larger size and a broader size distribution for unwashed Pd NP samples, regardless the w_0 value used during the synthesis. It can be inferred that the unwashed NPs could not be totally dispersed during the preparation for TEM analysis and that aggregates of individual NPs were counted as larger particles. For instance, at $w_0 = 7$, larger size and a broader distribution was observed for the unwashed (d_s = 11.7 nm, σ_s = 2.9 nm) than for the washed NPs (d_s = 7.7 nm, σ_s = 2.5 nm). Therefore, the washing of the NPs is an interesting tool to adjust the hydrophilicity of the NPs and control the interactions among NPs and with supports. In addition, washing is needed in order

to assess the actual size of the individual NPs formed and evaluate the influence of the synthesis variables on size and size distribution. As can be seen from the TEM images in **Figure 3.1**, the Pd NPs exhibited pseudo-spherical shape, even in the case of unwashed samples. May and Ben-Shaul [3] reported that in the low surfactant concentration range, the surfactant molecules only form spherical micelles in solution, whereas in the high concentration range various types of molecule aggregation such as micelle, liquid crystal and vesicle can be formed and act as templates.

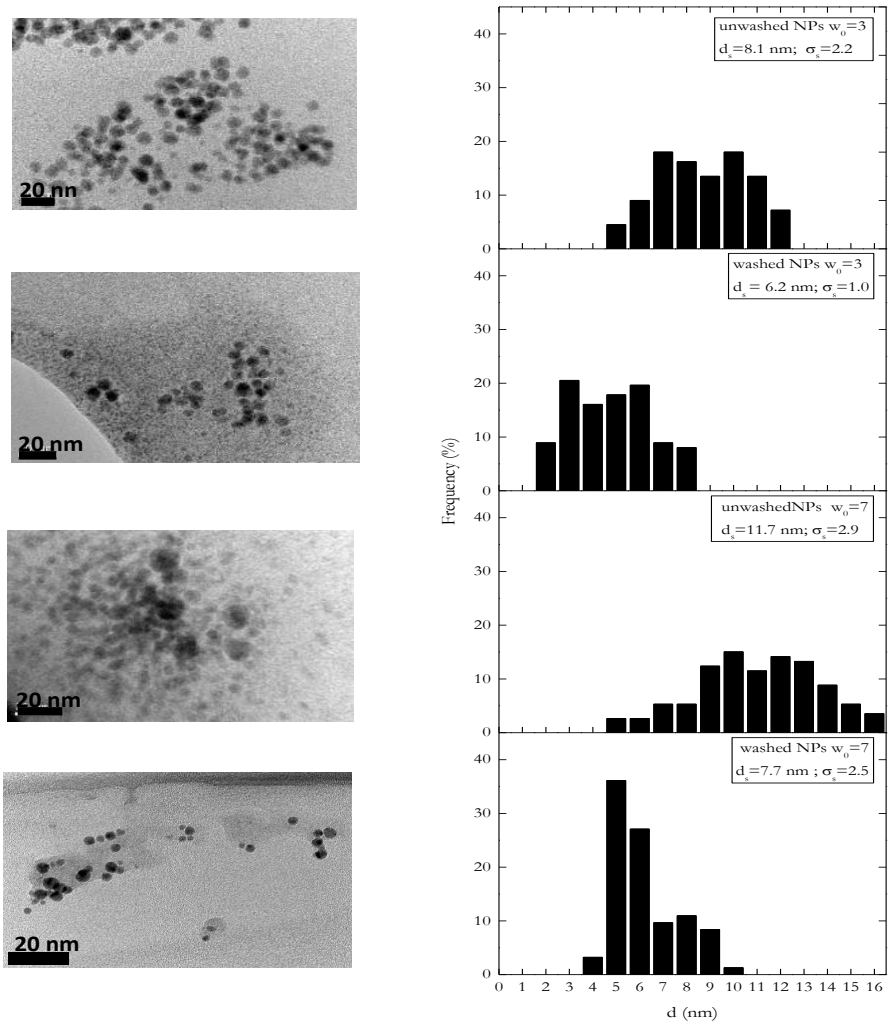

Figure 3.1. TEM images and particle size distributions of unwashed and washed Pd NPs synthesized with N_2H_4/Pd = 60 mol/mol, reaction time = 10 min and w_0 = 3–7.

Additional control of the size of the NPs can be achieved through the reaction time, since it affects the sequence of chemical reduction, nucleation and growth of particles during the formation of NPs. Many studies have reported on different growing, aging or ripening mechanisms in bulk involved in ME Ostwald ripening [4-6]. **Figure 3.2** compares runs carried out using different reaction times and identical evaporation temperature (368 K). It can be seen that when the reaction time was decreased from 60 to 10 min the NPs showed a narrower size distribution. Thus, experiments Pd6 and Pd8 (60 min) show a bimodal distribution

with evident queues on the right side of the histograms. These queues can correspond to growth of NPs after nucleation.

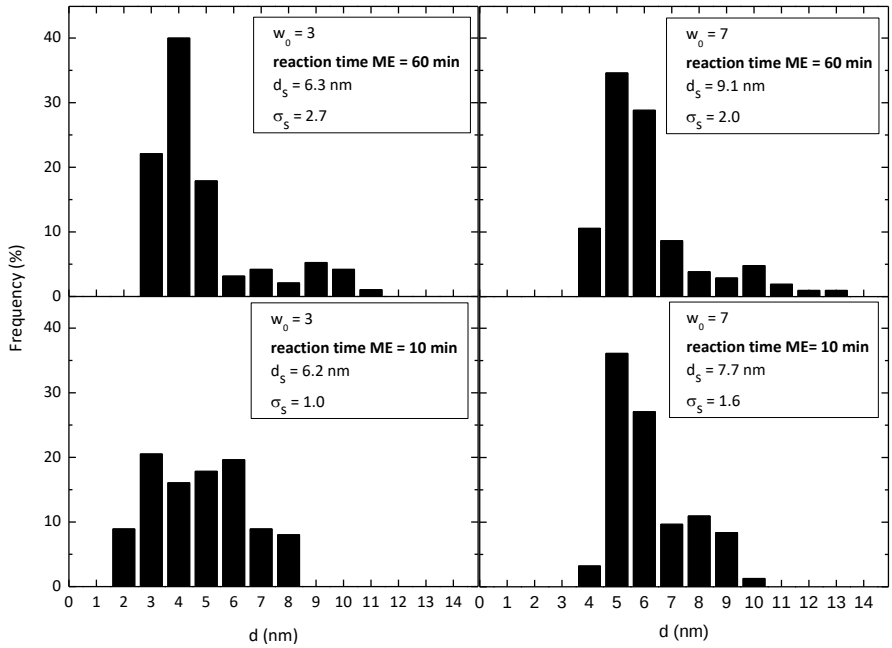

Figure 3.2. Particle size distribution of Pd NPs obtained at different reaction time.

The application of the NPs synthesized usually requires a partial removal/replacement of solvent to obtain a concentrated suspension. There is no available information about the possible changes in size, distribution or even morphology of the NPs during this process. Some evolution of the NPs takes place during the con- centration of the ME by evaporation. **Figure 3.3**, shows the results obtained when synthesis runs at $w_0 = 7$ where followed by evaporation at different temperatures (368 or 298 K). A higher evaporation temperature implies a shorter concentration period, which reduces NPs aggregation and nuclei growing. This effect is more evident in the case of the experiment where a reaction time of 10 min was used, since bell-shaped histograms without a queue on the right side indicate the absence of NPs larger than 10 nm. For a reaction time of 60 min the mean size also decreased with increasing evaporation temperature (from 11.7 to 9.1 nm), but an important contribution of large NPs can be observed. Likewise, a low

evaporation temperature yielded bell-shaped histograms with broader size distribution. When the synthesis of the NPs was carried out at w_0 = 3, the influence of the temperature during the concentration stage was not so evident, particularly for a reaction time of 10 min (decrease from 6.2 to 7.1 nm).

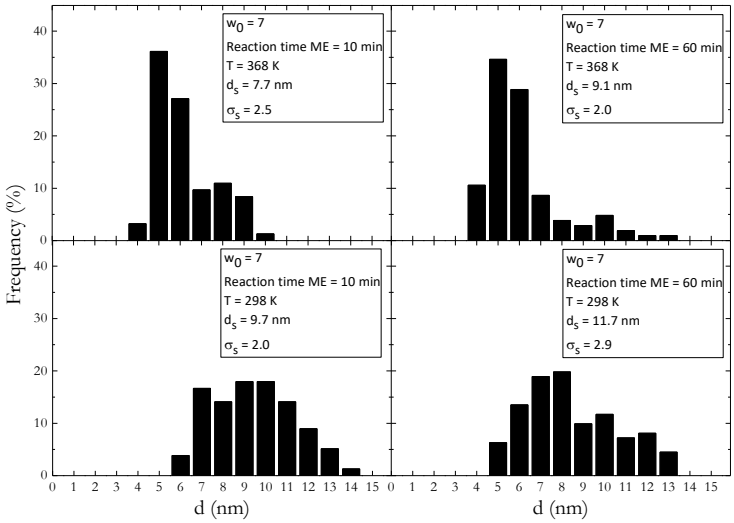

Figure 3.3. Particle size distribution of Pd NPs obtained at different reaction time (10 and 60 min) and evaporation temperature (368 and 298 K).

3.3.2 Approach via the chemical composition of the microemulsion system

Once, the control of the physical variables affecting the synthesis of NPs and the assessment of the size of NPs were studied, the effect of the water-to-surfactant molar ratio, reductor-to-metal molar ratio and type of reducing agent were analysed.

Table 3.1 shows the mean particle size and the standard deviation of the size distribution of the Pd NPs synthesized using w_0 values of 3 and 7, which correspond to water/AOT/isooctane weight percentages of 2.2/18/79.8 % and 5.1/18.1/76.8 %, respectively. Therefore, the total amount of AOT used remained constant, and a lower w_0 meant a lower amount of water in the ME. As a general trend, NPs with larger size and broader size distribution were obtained when w_0 increased. These results are in agreement with the values obtained by Chen et al. [7]. This phenomenon can be interpreted as the result of the larger droplet size achieved when the MEs are prepared with a higher water content. The results are in accordance with former studies, where it was shown that an increase in w_0 results in an increase in particle size [8]. Moreover, the growth is controlled by the presence of surfactants, which leads to the formation of particles with a homogeneous size distribution. Only in the case of samples Pd5 and Pd7 very small differences in particle size were observed when NPs synthesized at different w_0 values were compared. This can be mainly associated to the fact that the NPs were not washed and in both cases a large size (around 11 nm) was measured.

A ME with a low water content is characterized by small reverse micelles and consequently, smaller size of the Pd NPs synthesized [9–11]. Eastoe et al. [11] observed for the AOT/propane/water ME system that the relationship between the water core radius (R_w) and w_0 obeyed to the expression R_w (nm) = $0.18w_0 + 1.5$. Pileni et al. [12] found the linear relationship R_w(nm) = $0.15w_0$ for the water/AOT/isooctane/system. However, the application of these equations cannot be generalized. It is important to indicate that the amount of water in the system

can be increased not only by raising w_0, but also by increasing the concentration of AOT at constant w_0 level [13]. In the current *Chapter*, experiments Pd14 to Pd16 (**Table 3.1**) showed no clear influence of the concentration of AOT. Chen et al. [7] also observed that for a constant w_0 value, the increase in AOT concentration (0.1–1 M) did not affect significantly the size of reverse micelles.

Figure 3.4 shows representative histograms of the NPs obtained in experiments performed using N_2H_4 and $NaBH_4$ as reducing agents. A smaller size and narrower size distribution of the Pd NPs was achieved when $NaBH_4$ was used as reducing agent. Some differences were also observed in the reaction rate. Thus, the reaction medium turned dark brown in 3-5 min when N_2H_4 was used, whereas its color changed instantaneously in the case of $NaBH_4$. The chemical reaction rate affects directly to the time evolution of the number of nuclei and determines both nucleation and growth process. On one hand, if the chemical reaction is slow the NPs growth takes place for a longer period of time. This implies the continued production of seed nuclei and results in NP growth. On the contrary, when the chemical reaction is fast, the reactants are consumed at early stages of the process and smaller NPs are obtained. This fact explains the larger NPs size obtained when N_2H_4 was used as reducing agent [6].

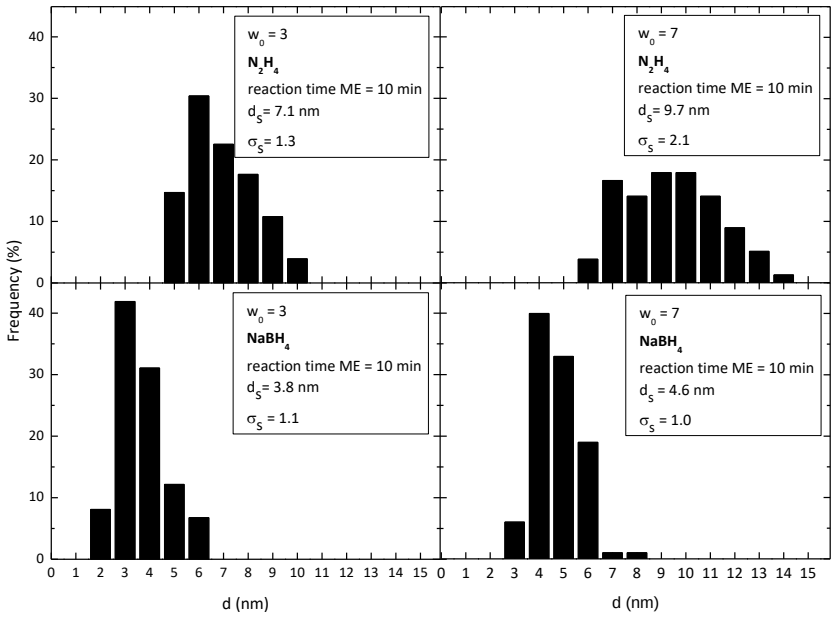

Figure 3.4. Particle size distributions of Pd NPs synthesized using N_2H_4 and $NaBH_4$ (reducing agent-to-metal ratio of 60, reaction time of 10 min, evaporation temperature of 298 K).

Small differences in mean size were observed for the synthesis at w_0 = 3 (3.8 nm) and 7 (4.6 nm) when $NaBH_4$ was used as reducing agent, in contrast to the broader range achieved when N_2H_4 was used (7.1–9.7 nm). These results are in agreement with those reported by Solanki and Murthy [14], who obtained Ag NPs with sizes of 11.3 nm and 12.9 nm, using of N_2H_4 and $NaBH_4$ as reducing agent, respectively, for the AOT/water/cyclohexane system. However, other works indicated no influence of the type of reducing agent used in the NPs size. Petit et al. [15] showed that the average size of Ag NPs remained unchanged, whereas the polydispersity increased when $NaBH_4$ was replaced by N_2H_4 in synthesis at a w_0 value of 7.5.

Additionally, the experiment number Pd11 was carried out to study the influence of reductor-to-metal ratio. **Figure 3.5** shows that an increase from 20 to 60 mol/mol resulted in an important decrease in the particle size from 13.7 to 7.1 nm and in some narrowing of the size distribution. Generally, an increase in the

number of NPs of large mean size is obtained when the N_2H_4 to Pd molar ratio is decreased [16].

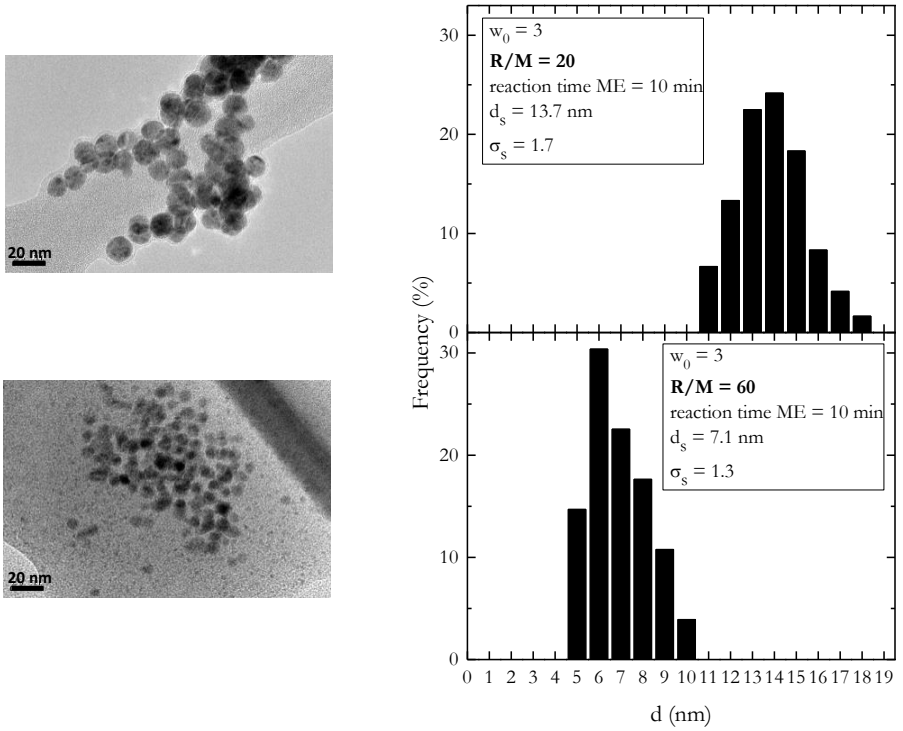

Figure 3.5. TEM images and particle size distribution of the Pd NPs obtained at different reducing agent-to-metal ratios (N_2H_4, w_0 = 3, reaction of 10 min, evaporation temperature of 298 K).

3.3. Conclusions

The control of the size and the size distribution of Pd NPs through multiple factors involved during the synthesis and purification stages have been assessed for the water/AOT/isooctane system. Like- wise, the conditions leading to obtain NPs with a wide diversity of characteristics have been identified. The purification with methanol showed a marked influence in both size and size distribution measured by TEM. Washing with methanol also resulted in changes in the hydrophilicity of NPs. Therefore, washing can be a tool to modify interactions among NPs and with supports. The control of the size of the NPs can be achieved through the reaction time and the temperature used for the concentration of NPs by evaporation. A low reaction time led to smaller NPs with a narrower size

distribution. A high evaporation temperature diminished NP aggregation and nuclei growing, which resulted in both a decrease in size and a narrower size distribution. This effect was more pronounced when a short reaction time was used. The Pd NPs shows a smaller size and a narrower size distribution when low water-to surfactant ratios are used. Additional control of NPs size is provided by the type of reducing agent ($NaBH_4$ and N_2H_4) and the reductor-to-metal ratio. Reduction with $NaBH_4$ results in smaller size and a narrower size distribution. For this reducing agent, an important decrease in particle size is also obtained when the reductor-to-metal ratio is increased.

3.4. References

[1] L. Xiong, T. He, Synthesis and characterization of ultrafine tungsten and tungsten oxide nanoparticles by a reverse microemulsion-mediated method, Chem. Mater. 18 (2006) 2211–2218.

[2] G. Hota, S. Jain, K.C. Khilar, Synthesis of CdS-Ag2S core-shell/composite nanoparticles using AOT/n-heptane/water microemulsions, Colloids Surfaces A Physicochem. Eng. Asp. 232 (2004) 119–127.

[3] S. May, A. Ben-Shaul, Molecular Theory of the Sphere-to-Rod Transition and the Second CMC in Aqueous Micellar Solutions, J. Phys. Chem. 105 (2001) 630–640.

[4] G. Hota, S. Jain, K.C. Khilar, Synthesis of CdS–Ag_2S core-shell/composite nanoparticles using AOT/n-heptane/water microemulsions, Colloids Surfaces A Physicochem. Eng. Asp. 232 (2004) 119–127.

[5] Y. De Smet, L. Deriemaeker, R. Finsy, A Simple Computer Simulation of Ostwald Ripening, Langmuir. 16 (1997) 6884–6888.

[6] M. de Dios, F. Barroso, C. Tojo, M.A. López-Quintela, Simulation of the kinetics of nanoparticle formation in microemulsions, J. Colloid Interface Sci. 333 (2009) 741–748.

[7] D. Chen, C. Wang, T. Huang, Preparation of Palladium Ultrafine Particles in Reverse Micelles., J. Colloid Interface Sci. 210 (1999) 123–129.

[8] M.P. Pileni, Reverser micelles as microreactors, J. Phys. Chem. 97 (1993) 6961–6973.

[9] M.M. Husein, E. Rodil, J.H. Vera, A novel method for the preparation of silver chloride nanoparticles starting from their solid powder using microemulsions, J. Colloid Interface Sci. 288 (2005) 457–467.

[10] F. Debuigne, L. Jeunieau, M. Wiame, J.B. Nagy, Synthesis of organic nanoparticles in different W/O microemulsions, Langmuir. 16 (2000) 7605–7611.

[11] Julian Eastoe, B.H. Robinson, A.J.W.G. Visser, D.C. Steytler, Rotational dynamics of AOT reversed micelles in near-critical and supercritical alkanes, J. Chem. Soc. Faraday Trans. 87 (1991) 1899–1903.

[12] M.P. Pileni, Z. Thomas, C. Petit, Solubilization by reverse micelles: Solute localization and structure perturbation, Chem. Phys. Lett. 118 (1985) 414–420.

[13] K. Kimijima, T. Sugimoto, Effects of the water content on the growth rate of AgCl nanoparticles in a reversed micelle system, J. Colloid Interface Sci. 286 (2005) 520–525.

[14] J.N. Solanki, Z.V.P. Murthy, Highly monodisperse and sub-nano silver particles synthesis via microemulsion technique, Colloids Surfaces A Physicochem. Eng. Asp. 359 (2010) 31–38.

[15] C. Petit, P. Lixon, M.-P. Pileni, In situ synthesis of silver nanocluster in AOT reverse micelle, J. Phys. Chem. 97 (1993).

[16] J. Eastoe, M.J. Hollamby, L. Hudson, Recent advances in nanoparticle synthesis with reversed micelles, Adv. Colloid Interface Sci. 128–130 (2006) 5–15.

CHAPTER IV

This chapter is based on the published manuscript

A.M. Perez-Coronado[a], L. Calvo[a], J.A. Baeza[a], J. Palomar[a], L. Lefferts[b], J.J. Rodriguez[a], M.A. Gilarranz[a]. *Metal-surfactant interaction as a tool to control the catalytic selectivity of Pd catalysts.* Applied Catalysis A: Geneneral 529 (2017) 32-39.

[a]Sección Departamental de Ingeniería Química, C/Francisco Tomás y Valiente 7, Universidad Autónoma de Madrid, 28049, Madrid, Spain.
[b]Catalytic Processes and Materials, MESA+ Institute for Nanotechnology, University of Twente, Enschede 7500AE, The Netherlands, The Netherland

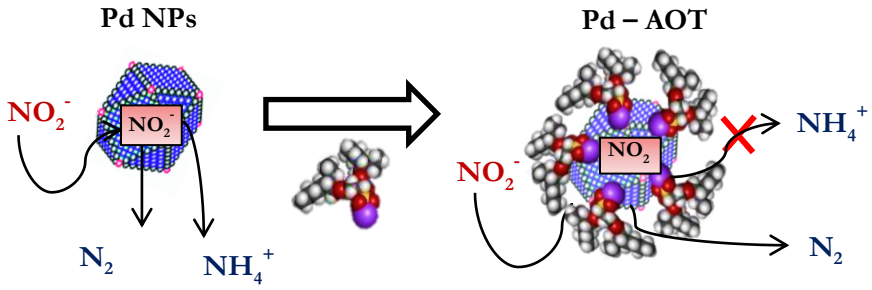

CHAPTER IV

Metal-surfactant interaction as a tool to control the catalytic selectivity of Pd catalysts

4.1. Summary

The catalytic activity of Palladium NPs synthesized via AOT/isooctane reverse ME was studied in NO_2^- reduction. The influence of reaction conditions and the synthesis and purification of the NPs was evaluated. In the NP size range studied (6.2–11.6 nm) a lower reaction rate and TOF were observed for small NPs. This apparent structure sensitiveness results from surface blockage due to interaction of AOT with the surface of NPs, as evidenced by purification with several solvents providing different removal of AOT. The activity loss was accompanied by negligible selectivity to NH_4^+. Large NPs in buffered medium produced insignificant amount of NH_4^+ for NO_2^- conversion values of ca. 80%. The selectivity control is ascribed to preferential blockage of the sites responsible for NH_4^+ generation. The results show the potential of the interaction between the AOT and the NPs as a tool to control catalytic selectivity.

4.2. Pd NPs size and size distribution

Pd NPs were prepared under different values of w_0 in order to obtain Pd NPs with different size and study the sensitiveness of the NO_2^- reduction reaction to structure of the NPs. **Figure 4.1** shows representative TEM images and the size distribution for the Pd NPs synthesized under the different conditions tested. The Pd NPs exhibited pseudo-spherical shape in the TEM images. **Table 4.1** shows the average mean diameter (d_s) and the size distribution (σ_s) calculated from the histograms shown in **Figure 4.1**. As a general trend, the mean NPs size increased with w_0, which was particularly evident for a w_0 value of 12. It has been reported that the role of AOT is to act as a protecting agent, allowing control of NPs growth during ME synthesis. An increase of this ratio for a constant concentration of surfactant will increase the average diameter of the droplets and consequently the size of the NPs [1]. According to σ_s no significant differences were found in size distribution, although a wider range of size was observed for the NP samples synthesized at lower w_0.

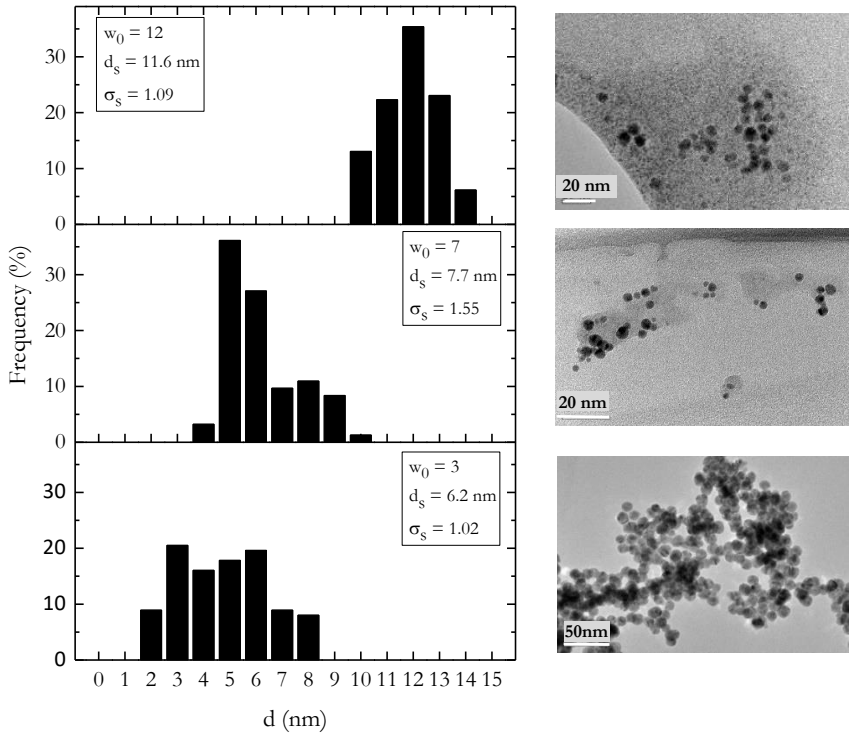

Figure 4.1. Particle size distribution and TEM images of the NPs samples obtained at different water-to-surfactant molar ratios.

Table 4.1. Characterization of Pd NPs and kinetic parameters for the reduction or NO_2^- (NPs purified with MeOH, buffered medium, 2.45 mgPd/L).

w_o	d_s (nm)	SSA Pd (m^2/g_{Pd})	$k_{NO_2^-}$ (min^{-1})	R^2	Pd^{n+}/Pd^0 ratio before reaction	Pd^{n+}/Pd^0 ratio after reaction	a ($mmol/g_{Pd}\cdot min$)	TOF (min^{-1})
3	6.2	80.5	$4\cdot10^{-3}$	0.99	0.55	0.15	1.39	0.82
7	7.7	65.2	$7\cdot10^{-3}$	0.99	n.m.	n.m	3.28	2.39
12	11.6	43.1	$15\cdot10^{-3}$	0.99	0.35	0.04	6.02	6.80

4.3. XPS characterization

XPS was used to establish the oxidation state of Pd. **Figure 4.2** shows the Pd 3d region deconvolved spectra for the NPs synthesized with w_0 = 3 and 12 before use in reaction (**Figure 4.2 A**) and after exposure in water to H_2 for 4 hours

at 303 K (**Figure 4.2 B**). As can be seen in **Table 4.1** and **Figure 4.2 A**, the smallest particles (6.2 nm) show initial Pd^{n+}/Pd^0 ratios of 0.55, whereas for the largest particles (11.6 nm) that initial ratio is 0.35. The presence of both Pd^{n+} and Pd^0 was observed in Pd NPs series synthesised with w_0 of 3 and 12. These results are in good agreement with previous ones reported in the literature, where larger Pd NPs synthetized via ME had a lower Pd^{n+}/Pd^0 ration than smaller ones [2]. Other authors also indicated that small particles are oxidized more easily thus leading to higher Pd^{n+}/Pd^0 ratios [3, 4]. After exposure to H_2 in conditions equivalent to those of NO_2^- reduction reaction both the small and large NPs were reduced, since Pd^{n+}/Pd^0 ratios decreased to 0.15 and 0.04 (**Figure 4.2 B**), respectively. Again higher Pd^{n+}/Pd^0 ratio was observed for the smallest NPs.

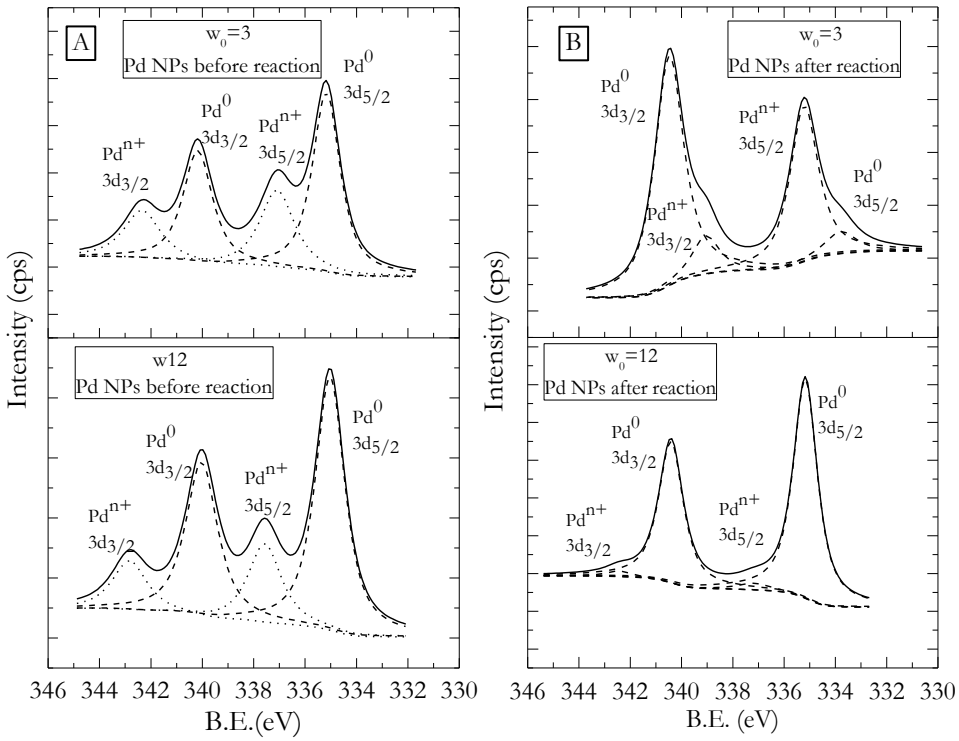

Figure 4.2. XPS spectra of Pd NPs synthesized with w_0 values of 3 and 12 for: **A)** Pd NPs before reaction and **B)** Pd NPs after exposure in water to H_2 for 4 h at 303 K.

4.4. Nitrite reduction with unsupported Pd NPs

Figure 4.3 shows the evolution of NO_2^- conversion upon reaction time with unsupported Pd NPs washed with methanol using a concentration of 2.45 mg Pd/L, for both buffered and non-buffered experiments. In these last experiments NO_2^- reduction was extremely slow and the final conversion varied between 5 % (6.2 nm NPs) and 22 % (11.6 nm NPs). The pH of the reaction medium varied between 8 and 9.3 due to the hydroxide ions from the NO_2^- reduction reaction. These results are in good agreement with other works, where low catalytic activity was ascribed to blockage of the palladium active sites by the OH^- ions generated during NO_2^- reduction [4 - 7]. Thus, the pH was found as a key parameter in NO_2^- conversion, since substantially higher values (50–80 %) were achieved when the reaction medium was buffered with CO_2.

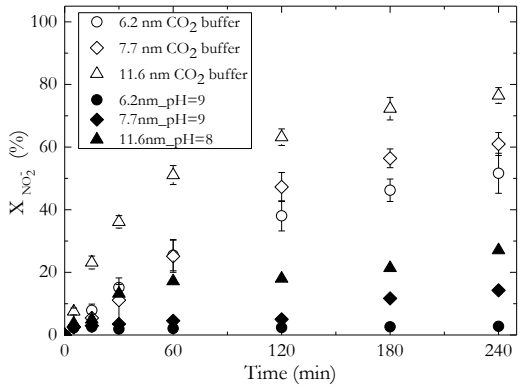

Figure 4.3. Influence of Pd NPs size and pH of the reaction medium on NO_2^- conversion (NPs purified with MeOH, 2.45 mg Pd/L).

As can also be seen in **Figure 4.3**, significant differences were found in NO_2^- conversion depending on the Pd NPs size. Larger sizes (higher w_0, less AOT) always led to higher NO_2^- conversion, regardless the pH of the reaction medium. These results show some discrepancies with most of the works in literature [8],

where the NO_2^- reduction is described as a size-independent reaction. Our results show that the synthesis method and/or the AOT remaining on the surface of the NPs after washing with methanol influence their catalytic behaviour. Thus, activity and TOF increased with Pd NPs size (**Table 4.1**, **Figure 4.4**), which was not expected from the common trend reported in other works and the much lower specific surface area of the larger NPs. Chinthaginjala et al. [9,10] reported that the TOF for Pd catalysts in NO_2^- reduction is independent of Pd NPs size in the range from 2.6 to 30 nm. Zhao et al. [8] observed that the TOF value for NO_2^- reduction using Pd-PVA colloids as catalyst is independent of particle size in the 2.2- 20 nm range.

The trend shown by **Figure 4.4** suggests that i) the number of exposed Pd sites increases with the NPs size, which does not follow the general assumptions in TOF calculation; ii) the active sites on large NPs are more active, and/or iii) an apparent structure sensitiveness results from the interaction between AOT and the NPs. Larger NPs are expected to retain on their surface a lower amount of AOT even after purification, due to the higher w_0 used in the synthesis. Likewise, small size NPs can be expected to interact more strongly with anionic AOT species due to higher prevalence of both low coordination sites and electron-deficient species. As a result, lower removal of AOT would take place in the purification stage.

In *Chapter III* [11], EDXS technique was employed to study the removal of AOT during the purification of the NPs. The EDXS spectra showed that after three washing steps with methanol the intensity of the S peak corresponding to the sulfonate group of AOT decreased dramatically. The very low signal observed indicated that the amount to AOT on the surface of the NPs was very low. TGA analysis of the purified NPs after deposition on an activated carbon support (5 % Pd/C, Norit SX PLUS, see **Figure A.2** in appendix) evidenced the low amount of AOT remaining in the NPs after purification.

In spite of the low amount of AOT on the purified NPs, important alteration of the catalytic behaviour was observed. Therefore, alternative

purification of the NPs was carried out with solvents of increasing acidity: TFE > MeOH > THF. The lower acidity of THF results in a lower capability for the removal of AOT from the surface of the NPs, due to the weak electrostatic interaction between the solvent and anionic AOT species. As can be seen in **Figure 4.5**, the NPs purified by washing with a THF + MeOH mixture are less active in the NO_2^- reduction for an identical particle size (7.7 nm). On the contrary, when NPs were purified with a solvent mixture with a higher acidity (TFE + MeOH), which results in higher AOT removal, a higher NO_2^- disappearance rate was obtained. After three washes with the TFE + MeOH mixture ca. 19% of the purified NPs could not be recovered by centrifugation and incorporated to the reaction medium. Interestingly, in this experiment much faster disappearance of NO_2^- was observed even though the metal concentration was slightly lower. These results are summarized in **Table 4.2** and support the hypothesis that the interaction between AOT and the Pd NPs reduces the accessible surface area.

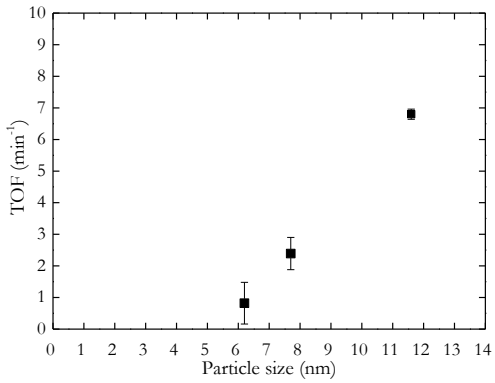

Figure 4.4. TOF as function of NP size (purification with MeOH; reaction: buffered medium, 2.45 mg Pd/L).

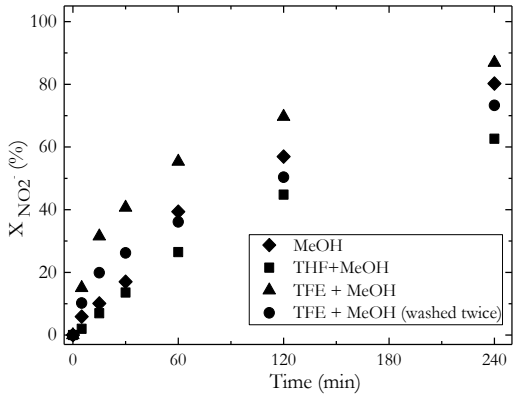

Figure 4.5. Conversion of NO_2^- in runs with Pd NPs purified with different solvents (synthesis: w_0 = 7; dp = 7.7 nm; reaction: buffered medium, 7.7 mg Pd/L).

Table 4.2. Kinetic constant ($k_{nitrite}$), (SSAPd), activity (a) and TOF calculated for NO_2^- reduction using different solvents for the purification of NPs (synthesis: w_0 = 7; dp = 7.7 nm; reaction: buffered medium, 7.7 mg Pd/L).

Solvent	$k_{NO_2^-}$ (min^{-1})	R^2	a (mmol/g Pd·min)	TOF (min^{-1})
MeOH	$7 \cdot 10^{-3}$	0.98	0.989	0.719
THF+MeOH	$4 \cdot 10^{-3}$	0.99	0.587	0.433
TFE+MeOH[b]	$8 \cdot 10^{-3}$	0.97	1.823	1.782
TFE+MeOH[a]	$5 \cdot 10^{-3}$	0.98	0.721	0.538

[a] Washed twice.

[b] 6.2 mgPd/L (19 % Pd NPs lost during 3rd wash).

Additional reaction experiments were carried out at different metal concentration in the reaction medium (2.45, 7.7, and 23 mg Pd/L). The NPs selected were those synthesized with a w_0 of 7 (7.7 nm) and purified with MeOH. **Figure 4.6** indicates a coherent increase in the conversion of NO_2^- at increasing concentration of Pd in the reaction medium, both for buffered and non-buffered reactions. Conversion values up to 92 % were achieved within the reaction time considered for the highest Pd concentration. In the low metal concentration range (< 10 mg Pd/L) the increase of the rate constant with catalyst concentration, and

therefore the increase of H_2 consumption, confirms that the reaction occurred under chemical control. The activity values normalized for Pd concentration and the TOF did not show significant changes when the metal load increased from 2.45 to 23 mg Pd/L (**Table 4.3**, **Figure 4.7**).

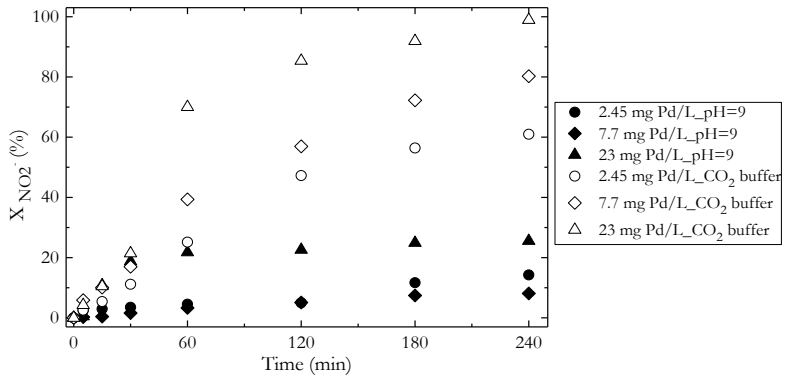

Figure 4.6. Influence of Pd concentration and pH of the reaction medium in NO_2^- conversion (synthesis: w_0 = 7, ds = 7.7 nm, NPs purified with MeOH).

Table 4.3. Kinetic parameters for NO_2^- reduction at different Pd concentration (synthesis: w_0=7, ds=7.7 nm, reaction: buffered; NPs purified with MeOH).

[Pd] mg Pd/L	$k_{NO_2^-}\cdot 10^{-3}$ (min^{-1})	R^2	a (mmol/g Pd·min)	TOF (min^{-1})
0.5	0.2	0.868	0.433	0.322
1.5	6	0.992	4.708	3.431
2.45	7	0.995	3.279	2.389
3.3	6	0.995	1.914	1.132
7.7	7	0.997	0.989	0.719
10	20	0.992	2.203	1.603
16.3	27	0.996	1.802	1.314
23	28	0.989	1.179	0.964

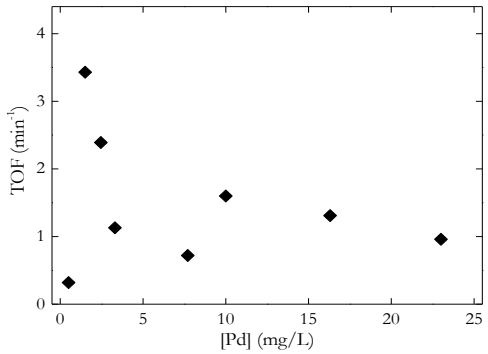

Figure 4.7. TOF versus Pd NPs concentration (synthesis: w_0 = 7, ds = 7.7 nm; NPs purified with MeOH; reaction: buffered).

Significant differences in selectivity were also observed depending on the NPs size and the pH of the reaction medium (**Figure 4.8**). The influence of NPs size was more evident at high pH, where selectivity to NH_4^+ was around 5 % for the largest NPs and well above 30 % for the smallest; on the contrary, very low selectivity towards NH_4^+ was observed in the case of the reaction carried out in buffered medium. Thus, NH_4^+ was in the detection limit for the largest NPs and at very low values below 0.08 mg/L for the smallest, with selectivity values below 1 % in all cases. At any NO_2^- conversion value, the selectivity to NH_4^+ was higher for smallest NPs, as can be seen in **Figure 4.8 B**. The selectivity to ammonium for the smallest NPs remained at low values up to 25% conversion a beyond that a substantial increase was observed. This increase in selectivity to ammonium with conversion was also observed for the 7.7 nm NPs, although in a lower extent. This change in behaviour could be related to the reduction of NPs in the reaction medium, as discussed from XPS characterization.

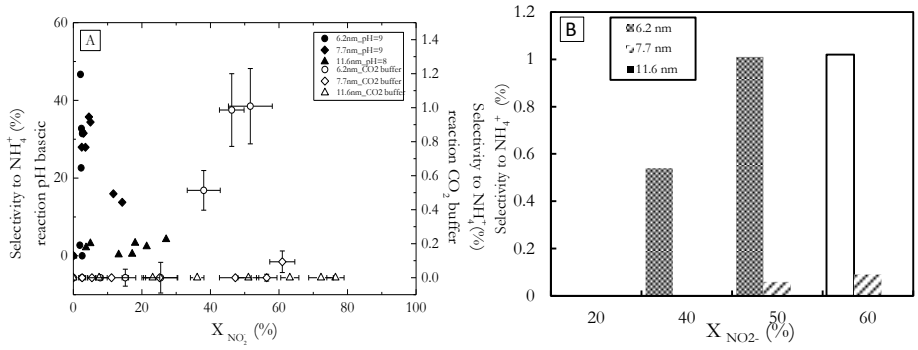

Figure 4.8. **A)** Influence of Pd NPs size and pH of the reaction medium on selectivity to NH_4^+. **B)** Selectivity to NH_4^+ for buffered medium at constant conversion. (reaction: 2.45 mgPd/L, NPs purified with MeOH).

Some works in literature described a lower generation of NH_4^+ in the reduction of NO_2^- by large Pd NPs due to the lower prevalence of low coordination sites such as edges, corners and defects, where the formation of NH_4^+ is supposed to take place [9]. In this sense, Danmeng Shuai et al. [12] observed an increase in the selectivity to NH_4^+ with decreasing size of Pd NPs supported on carbon nanofibers. The results in the current C*hapter* are in agreement with the literature, but extremely low selectivities to NH_4^+ were observed in our case. This behaviour is related to the interaction between Pd NPs and AOT, since the aforementioned works were carried out with clean surface NPs. To go deeper on this issue, the selectivity results for the NO_2^- reduction runs carried out with NPs purified with different solvents, i.e. different degree of removal of AOT, can be considered (**Figure 4.9**). Exceptional selectivity to N_2 can be observed for those samples purified with THF, which can be interpreted in terms of a lower removal of AOT and higher coverage of the Pd NPs, including low coordination sites. Thus NPs purified with THF are less active and exhibit lower selectivity to NH_4^+. On the contrary, for those NPs purified with a TFE+MeOH mixture a higher removal of AOT is achieved and higher selectivity to NH_4^+ is observed, which is particularly clear in the case of the NPs washed twice. Interestingly, the NPs washed three

times with TFE + MeOH exhibited a lower selectivity to NH_4^+ than these twice-washed ones. It should be noted that after the third wash with the TFE + MeOH mixture, 19 % of the Pd NPs were lost in the supernatant and were not available for the reaction. The fraction removed is expected to be integrated by the smallest and better purified NPs.

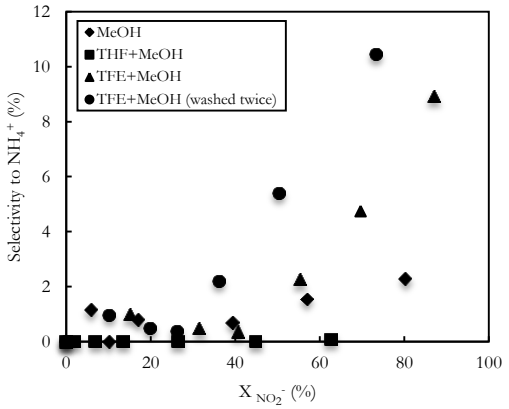

Figure 4.9. Selectivity to NH_4^+ in NO_2^- reduction runs for Pd NPs purified with different solvents (synthesis: w_0 = 7, 7.7 nm; reaction: buffered medium, 7.7 mg Pd/L).

Regarding selectivity for the reactions carried out at different metal concentrations (**Figure 4.10**), very high selectivity to NH_4^+ was obtained in non-buffered reactions. In buffered reactions NH_4^+ selectivity remained at very low values, but an increase was observed when the metal concentration was increased. At any NO_2^- conversion, the selectivity values were an order of magnitude higher for the runs carried out with a Pd NPs concentration of 7.7 mg/L. For instance, at 70 % NO_2^- conversion the interpolated values of ammoniums selectivity were 0.1 %, 1.6 % and 1.9 % for the runs carried out with metal concentrations of 2.45, 7.7 and 23 mg/L, respectively. This observation would be consistent with a higher presence of highly active low-coordination sites available for the reaction at higher metal concentration, but also indicate that influence of the control regime.

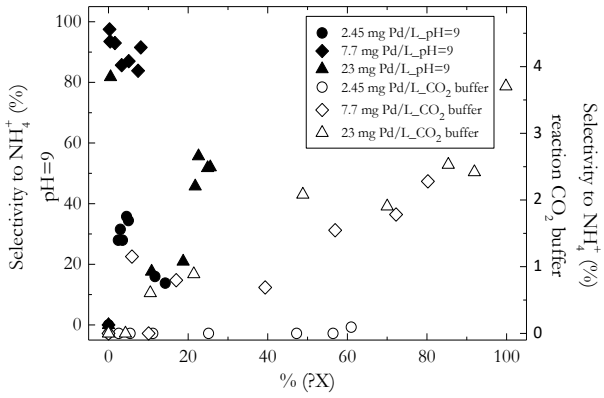

Figure 4.10. Influence of NH_4^+ selectivity using different Pd NPs concentration (synthesis: w_0 = 7, 7.7 nm; NPs purified with MeOH).

4.5. Conclusions

The catalytic reduction of NO_2^- with Pd NPs synthesized by ME using the water/AOT/isooctane system exhibits apparent structure sensitiveness. A lower reaction rate and TOF were observed for small NPs, which can be ascribed to surface blockage caused by strong AOT interaction with low-coordination sites and electron-deficient species on the surface of the Pd NPs. In addition to a decrease of activity, extremely low selectivity to NH_4^+ was achieved, probably due to preferential blockage of the sites responsible for NH_4^+ generation. The results show the feasibility of reaction control by means of selective blockage of active sites involved in non-desired side reactions.

4.6. References

[1] I. Mikami, Y. Sakamoto, Y. Yoshinaga, T. Okuhara, Kinetic and adsorption studies on the hydrogenation of nitrate and nitrite in water using Pd-Cu on active carbon support, Appl. Catal. B Environ. 44 (2003) 79–86.

[2] N. Semagina, A. Renken, D. Laub, L. Kiwi-Minsker, Synthesis of monodispersed palladium nanoparticles to study structure sensitivity of solvent-free selective hydrogenation of 2-methyl-3-butyn-2-ol, J. Catal. 246 (2007) 308–314.

[3] J.A. Baeza, L. Calvo, J.J. Rodriguez, E. Carbó-Argibay, J. Rivas, M.A. Gilarranz, Activity enhancement and selectivity tuneability in aqueous phase hydrodechlorination by use of controlled growth Pd-Rh nanoparticles, Appl. Catal. B Environ. 168 (2015) 283–292.

[4] F. Chen, Z. Zhong, X.J. Xu, J. Luo, Preparation of colloidal Pd nanoparticles by an ethanolamine-modified polyol process, J. Mater. Sci. 40 (2005) 1517–1519.

[5] H. Qian, Z. Zhao, J. Velazquez, L. Pretzer, Supporting palladium metal on gold nanoparticles improves its catalysis for nitrite reduction, Nanoscale. (2014) 358–364.

[6] U. Prüsse, K.D. Vorlop, Supported bimetallic palladium catalysts for water-phase nitrate reduction, J. Mol. Catal. A Chem. 173 (2001) 313–328.

[7] W. Lin, W.J. Rieter, K.M.L. Taylor, Modular synthesis of functional nanoscale coordination polymers, Angew. Chemie - Int. Ed. 48 (2009) 650–658.

[8] Y. Zhao, J.A. Baeza, N. Koteswara Rao, L. Calvo, M.A. Gilarranz, Y.D. Li, et al., Unsupported PVA- and PVP-stabilized Pd nanoparticles as catalyst for nitrite hydrogenation in aqueous phase, J. Catal. 318 (2014) 162–169.

[9] J.K. Chinthaginjala, A. Villa, D.S. Su, B.L. Mojet, L. Lefferts, Nitrite reduction over Pd supported CNFs: Metal particle size effect on selectivity, Catal. Today. 183 (2011) 119–123.

[10] J.K. Chinthaginjala, L. Lefferts, Support effect on selectivity of nitrite reduction in water, Appl. Catal. B Environ. 101 (2010) 144–149.

[11] A.M. Perez-Coronado, L. Calvo, N. Alonso-Morales, F. Heras, J.J. Rodriguez, M.A. Gilarranz, Multiple approaches to control and assess the size of Pd nanoparticles synthesized via water-in-oil microemulsion, Colloids Surfaces A Physicochem. Eng. Asp. 497 (2016) 28–34.

[12] D. Shuai, J.K. Choe, J.R. Shapley, C.J. Werth, Enhanced activity and selectivity of carbon nanofiber supported Pd catalysts for nitrite reduction., Environ. Sci. Technol. 46 (2012) 2847–55.

CHAPTER V

This chapter is based on the manuscript

A.M. Perez-Coronado[a], L. Calvo[a], J.A. Baeza[a], J. Palomar[a], L. Lefferts[b], J.J. Rodriguez[a], M.A. Gilarranz[a]. Selective reduction of nitrite to nitrogen carbon-supported with Pd-AOT nanoparticles.

[a]Sección Departamental de Ingeniería Química, C/Francisco Tomás y Valiente 7, Universidad Autónoma de Madrid, 28049, Madrid, Spain.
[b]Catalytic Processes and Materials, MESA+ Institute for Nanotechnology, University of Twente, Enschede 7500AE, The Netherlands, The Netherland

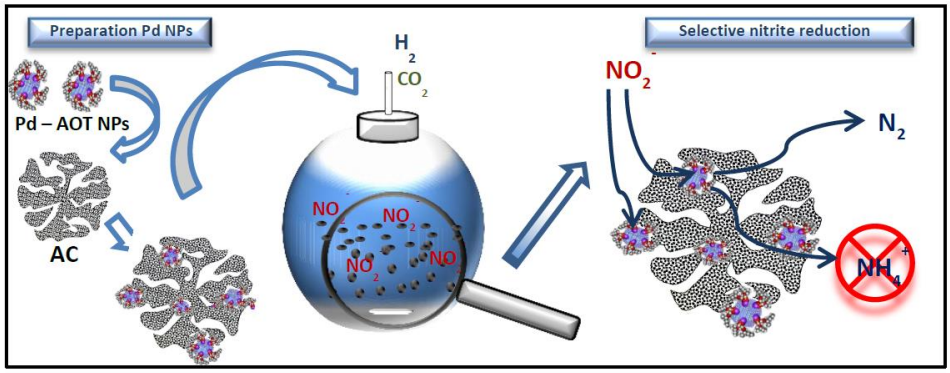

CHAPTER V

Selective reduction of nitrite to nitrogen carbon-supported with Pd-AOT nanoparticles

5.1 Summary

Size-controlled Pd-AOT NPs, synthesized via AOT/isooctane reverse ME, supported on activated carbon were used as catalysts in NO_2^- reduction. The effect of the preparation of the catalysts and the pH of the reaction medium were evaluated together with the role of AOT remaining on the surface of the Pd NPs after their synthesis.

Complete NO_2^- conversion was obtained for supported Pd-AOT NPs using CO_2 as buffer agent. The most remarkable feature was the negligible selectivity towards NH_4^+, which can be attributed to shielding effect of AOT due to its interaction with the Pd NPs. The shielding also led to slightly lower activity than that of Pd/C catalysts prepared by incipient wetness. Thermal treatment of the catalysts at mild temperature (473 K, N_2) increased the activity due to removal and rearrangement of AOT, although higher production of NH_4^+ was also observed. The interaction between AOT and the Pd metal NPs was proved as a tool to control the selectivity of catalysts.

5.2. Results and discussion

5.2.1. Pd NPs and catalysts characterization

Pd NPs were synthesized under different w_0 values in order to study the influence of Pd NP size on NO_2^- reduction. **Figure 5.1** shows representative TEM images and Pd NPs size distributions for catalysts prepared by impregnation of the activated carbon supported with Pd NPs obtained at w_0 = 3 and 7, and also after thermal treatment of the catalysts in N_2 and H_2 atmosphere. It can be observed that the mean NP size increase and the size distribution because narrower at increasing w_0. It has been reported that the role of AOT is to act as a protecting agent, allowing to control NPs growth in ME. Increasing w_0 at constant concentration of surfactant means a lower AOT content and consequently an increase in the average diameter of the droplets and the size of the NPs [1,2]. The thermal treatment of the catalysts increases the size of the NPs, which can be ascribed to sintering. The occurrence of oversized NPs (>10 nm) is particularly important in the case of the thermal treatment in H_2 atmosphere.

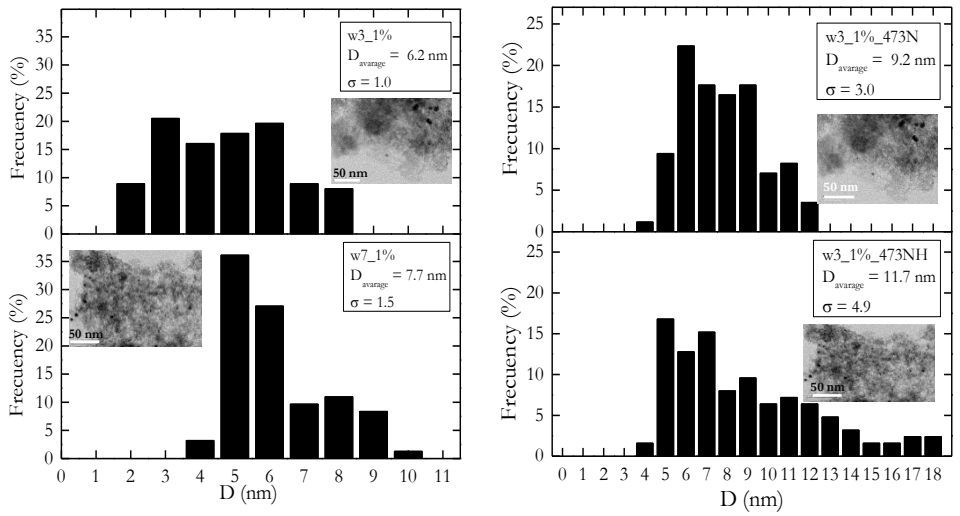

Figure 5.1. Particle size distribution and TEM images of selected catalysts prepared with NPs synthesized at w_0=7 and w_0=3.

Table 5.1 summarizes the working conditions used for the synthesis of the catalysts and the corresponding nomenclature.

Table 5.1. Experimental conditions for the synthesis of Pd catalysts.

Sample	% Pd (wt. %, AC d.b.)	Support	w_0 in NP synthesis	Thermal treatment T (K)		Purification
				N_2	H_2	
w3_1%	1	AC	3	-	-	MeOH washing of NPs
w3_1%_473N	1	AC	3	473	-	MeOH washing of NPs
w3_1%_473NH	1	AC	3	473	473	MeOH washing of NPs
w3_0.5%_473N	0.5	AC	3	473	-	MeOH washing of NPs
w3_0.5%_473NH	0.5	AC	3	473	473	MeOH washing of NPs
w3_2.5%_473N	2.5	AC	3	473	-	MeOH washing of NPs
w3_2.5%_473NH	2.5	AC	3	473	473	MeOH washing of NPs
w3_1%_423N	1	AC	3	423	-	MeOH washing of NPs
w3_1%_423NH	1	AC	3	423	473	MeOH washing of NPs
w3_1%_523N	1	AC	3	523	-	MeOH washing of NPs
w3_1%_523NH	1	AC	3	523	473	MeOH washing of NPs
w3_1%_623N	1	AC	3	623	-	MeOH washing of NPs
w3_1%_623NH	1	AC	3	623	473	MeOH washing of NPs
w3_1%_673N	1	AC	3	673	-	MeOH washing of NPs
w7_1%	1	AC	7	-	-	MeOH washing of NPs
w7_1%_473N	1	AC	7	473	-	MeOH washing of NPs
w7_1%_473NH	1	AC	7	473	473	MeOH washing of NPs

Table 5.1. Experimental conditions for the synthesis of Pd catalysts (cont.)

Sample	% Pd (wt. %, AC d.b.)	Support	w_0 in NP synthesis	Thermal treatment T (K)		Purification
				N_2	H_2	
w7THF_1%	1	AC	7	-	-	50/50 MeOH/THF (v/v) washing of NPs
w7_1% THF	1	AC	7	-	-	THF washing of impregnated NPs
IWI_1%	1	AC	-	573	473	-
IWI_1% AOT	1	AC	-	573	473	MeOH washing after AOT poisoning

The textural characterization of some selected Pd/C catalysts is summarized in **Table 5.2**. The activated carbon used as support showed high S_{BET} (980 m^2/g) and micro and mesoporous volumes (0.309 and 0.344 cm^3/g, respectively). In general, as the Pd load in the catalysts increased, the S_{BET} and the micropore and mesoporous volumes decreased, indicating partial pore blockage by the metal and the surfactant.

Table 5.2. Textural characteristics of selected catalysts.

Sample	S_{BET} (m^2/g)	A_s (m^2/g)	$V_{micropore}$ (cm^3/g)	$V_{mesopore}$ (cm^3/g)
SX PLUS commercial	977	329	0.309	0.344
w3_0.5%_473N	884	308	0.273	0.327
w3_0.5%_473NH	860	299	0.266	0.320
w3_1%_473N	621	260	0.169	0.277
w3_2.5%_473N	567	196	0.175	0.212
w3_2.5%_473NH	633	242	0.184	0.257

5.2.2 Nitrite reduction tests

5.2.2.1. Reaction at uncontrolled pH

As a first approach, NO_2^- reduction with the 1% Pd/C catalysts synthesized via ME, IWI and IWI followed by poisoning with AOT were tested at uncontrolled pH. The results are shown in **Figure 5.2 Figure 5.2 A** depicts the evolution of NO_2^- conversion upon reaction time and the selectivity to NH_4^+ versus NO_2^- conversion can be seen in **Figure 5.2 B**.

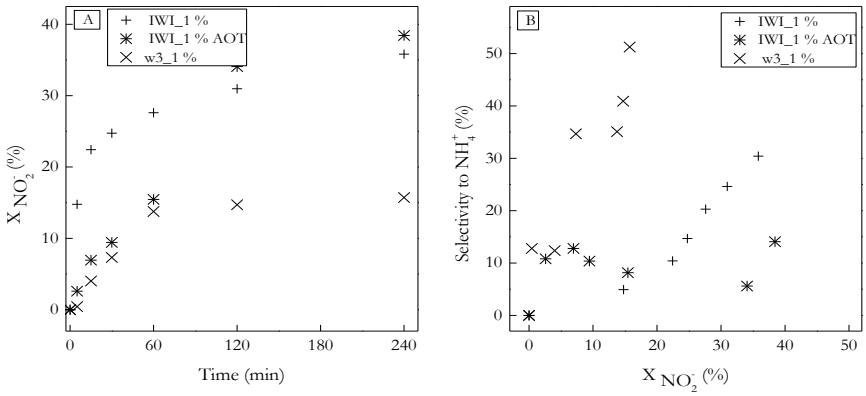

Figure 5.2. NO_2^- reduction experiments at uncontrolled pH for catalysts prepared using different procedures (7.7 mg Pd/L). **A.** NO_2^- conversion vs time. **B.** Selectivity to NH_4^+ vs NO_2^- conversion.

All the catalysts tested at uncontrolled pH exhibited relatively low NO_2^- conversion (15 – 40%). The w3_1% catalyst showed lower activity than the IWI_1%, probably due to blockage of active centres by AOT. This would take place during the synthesis of the NPs and results in Pd-AOT interactions different from those taking place when a catalyst prepared by IWI is impregnated with AOT. This view is supported by the results obtained catalyst IWI_1%AOT, where the poisoning with AOT did not produce a significant loss of activity and even showed a higher activity during the first minutes of reaction. On the other hand, the conversion rate observed for the supported NPs is higher than that previously reported for unsupported NPs [3].

The NH_4^+ selectivity was also different for catalysts IWI_1% and IWI_1%AOT, indicating that at uncontrolled pH the generation of NH_4^+ was higher for supported NPs that where poisoned by AOT during their synthesis. Therefore, shielding by AOT for the prevention of NH_4^+ generation is conditioned by the pH of the reaction medium.

The catalysts prepared by ME at w_0 = 3 were treated at different temperatures between 423 and 673 K in N_2 atmosphere to remove AOT. These temperatures were selected according to the decomposition range of AOT

observed by TGA in N_2 atmosphere (530-580 K, see appendix **Figure A.3**). Some of the catalysts were also subjected to additional reduction with H_2. The behaviour of the catalysts after thermal treatment in N_2 can be seen in **Figure 5.3 A.1** and **B.1**. It can be observed that the treatment at mild temperature (423-523 K, **Figure 5.4**) increases the activity, with a peak at 423 K. At higher temperatures the decrease in activity can be attributed to deposition of AOT decomposition products on the NPs surface and sintering. Regarding NH_4^+ selectivity, it increases substantially for the catalysts treated at the highest temperatures, where a higher removal of AOT can be expected. For these catalysts the generation of NH_4^+ is favoured even at low NO_2^- conversion. According to **Scheme 5.1**, this fact can be related to the hydrogenation and release of NO_2^- and NH_2 species adsorbed on the catalysts to produce NH_4^+.

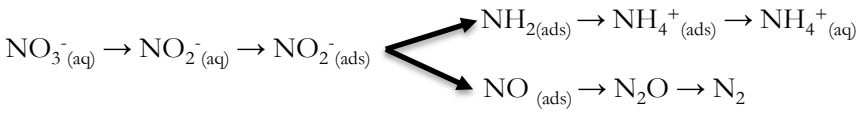

Scheme 5.1. NO_2^- reduction over Pd/Al_2O_3 as suggested by Ebbesen et al.[7] based on ATR-IR spectroscopic studies.

When the catalysts were subjected to reduction with H_2 after thermal treatment in N_2, a slight decrease of activity was observed (**Figure 5.3 A.2**). This can be due to a higher sintering of NPs. Interestingly, the selectivity to NH_4^+ was also lower. The reduction of the catalyst can modify the ratio between Pd^{n+} and Pd^0 species and also decrease the number of uncoordinated atoms on the NPs surface due annealing and sintering. This may result in a lower availability of active canters involved in the generation of NH_4^+ species [4,5].

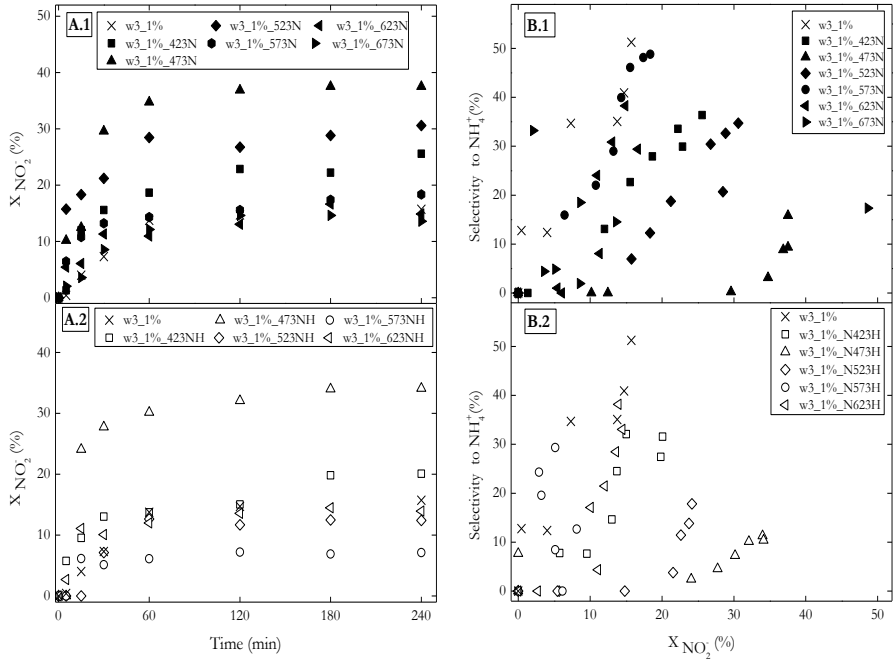

Figure 5.3. NO_2^- reduction at uncontrolled pH with catalysts subjected to thermal treatment in N_2 atmosphere (**A.1, B.1**) and thermal treatment in N_2 atmosphere followed by reduction with H_2 (**A.2, B.2**).

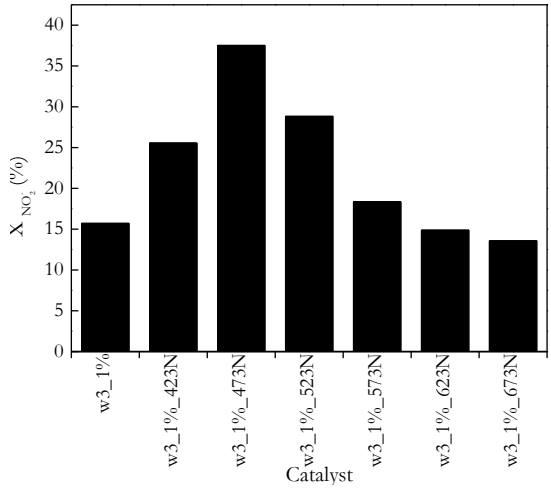

Figure 5.4. NO_2^- conversion at uncontrolled pH with catalysts subjected to thermal treatment in N_2 atmosphere (reaction time = 4 h).

With the aim of exploring the effect of the Pd loading, catalysts with different nominal loads of Pd (0.5, 1 and 2.5% wt.) were tested. **Figure 5.5** summarizes NO_2^- conversion upon reaction time for a Pd concentration in the reaction medium of 7.7 mg/L (**A.1**) and 19.25 mg/L (**A.2**). At 7.7 mg Pd/L, NO_2^- conversion range between 10 and 40 after 4 h while at 19.25 mg Pd/L conversion values within 20-80% were obtained. At the same Pd concentration in the reaction medium the conversion decreased at increasing Pd load, which can be in part related to the lower surface area of the catalysts, as shown **Table 5.2**.

Besides, the catalysts of higher nominal load showed a higher agglomeration of Pd NPs (see appendix, **Figure A.4**). In general, as the Pd nominal load in the catalysts increased, the selectivity to NH_4^+ was higher (**Figure 5.5 B.1** and **B.2**) especially at the higher concentration of Pd in the reaction medium (19.25 mg Pd/L). This increase of NH_4^+ generation with metal nominal load has also been reported by other authors [6].

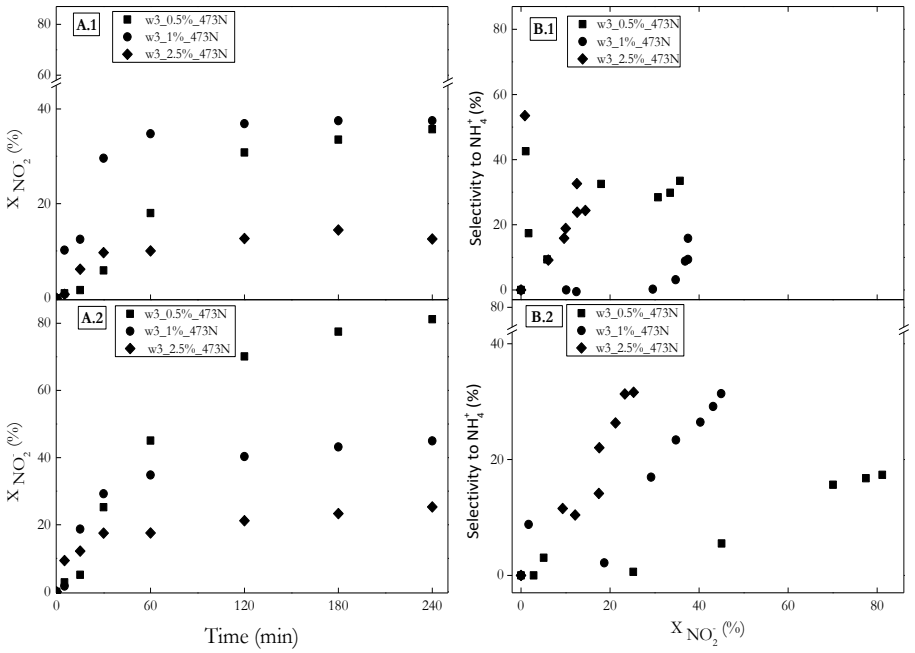

Figure 5.5. NO_2^- reduction at uncontrolled pH with catalysts of different Pd nominal load: (**A.1, B.1**) 7.7 mg Pd/L (**A.2, B.2**); 19.25 mg Pd/L.

5.2.2.2. Reaction at controlled pH

Reaction tests at controlled pH (5-6) were carried out in order to study the catalysts behaviour in a more favourable environment allowing higher activity and lower selectivity to NH_4^+. The evolution of NO_2^- conversion upon reaction time (**Figure 5.6 A.1**) shows a significantly higher reaction rate for the catalysts prepared by IWI, yielding complete NO_2^- conversion in less than 1 h. The catalysts prepared by IWI and poisoned by impregnation with AOT showed lower activity but led to complete NO_2^- conversion within the reaction time tested. It can also be observed that the catalysts prepared by ME exhibit a higher activity in the case of the NPs synthesized at w_0 = 3, i.e. those of smaller size. In *Chapter IV* [3] where unsupported NPs were prepared by ME synthesis and used as model catalysts, a faster conversion of NO_2^- was observed for the larger NPs (w_0 = 7 and 12) which was explained by the apparent structure sensitiveness caused by AOT blockage of active centres. In the current *Chapter*, a much faster NO_2^- conversion than for unsupported NPs was obtained, and the difference in activity between catalysts with NPs of different size is lower. Therefore, thanks to the immobilization of the NPs the negative effect of AOT on the activity is diminished. The control of agglomeration of NPs, which is likely to occur for unsupported ones in aqueous medium, can also play a positive role.

Figure 5.6 B.1 shows a significant generation of NH_4^+ with the catalyst prepared by IWI, delayed with respect to the reaction at uncontrolled pH, while selectivity to NH_4^+ becomes significant only at almost complete NO_2^- conversion. This has been previously observed, and explained in terms of the evolution of NH_4^+ precursor species that build up on the catalyst surface once NO_2^- is completely converted [7]. The poisoning with AOT of the IWI catalysts do not show any effect in preventing NH_4^+ formation, although it is delayed as well.

Interestingly, NH_4^+ selectivity is negligible for the catalysts prepared by ME, even at complete NO_2^- conversion. In *Chapter IV*, we reported that a low

generation of NH_4^+ was achieved for unsupported Pd NPs prepared by ME, which was attributed to the shielding effect of the AOT attached to the surface of the NPs [1]. Therefore, thanks to the immobilization of the NPs on the carbon support the activity is enhanced while the shielding effect is maintained. The negligible production of NH_4^+ at complete NO_2^- conversion denotes that building up of the nitrogen species evolving to NH_4^+ on the surface of the NPs is prevented [7]. This fact is of crucial significance since the main drawback of NO_3^-/ NO_2^- reduction is the formation of NH_4^+. The catalysts reported in the current *Chapter* could be coupled with other highly selective in the reduction of NO_3^- to NO_2^-, thus providing a useful catalytic system for the NH_4^+-free reduction of NO_3^-.

The catalysts with Pd NPs prepared by ME and subjected to thermal treatment in N_2 also yielded higher reaction rate at controlled than at uncontrolled pH (**Figure 5.3 A.2** and **Figure 5.4**). The NO_2^- conversion rate in this case is almost equivalent to that observed for IWI-based catalysts, evidencing an increase in activity due to the thermal treatment, even though AOT is not removed from the catalyst by such treatment in nitrogen atmosphere at 423-523 K (see appendix, **Figure A.5**). Changes in the sulfonate group of AOT have been reported upon thermal treatment [8], which can provoke some rearrangement of AOT on the surface of the catalyst improving the availability of the active centers. On the other hands, the removal of AOT increased the selectivity to NH_4^+ up to values equivalent to those observed for the IWI catalyst. Subsequent reduction of the Pd NPs with H_2 led to a significant decrease of the catalytic activity (**Figure 5.3 B.2**), in contrast to the small differences that were observed in the uncontrolled pH experiments. Therefore, the role of the electro-deficient Pd species and the effect of low pH may counterbalance than of NPs sintering occurring upon reduction of the catalyst.

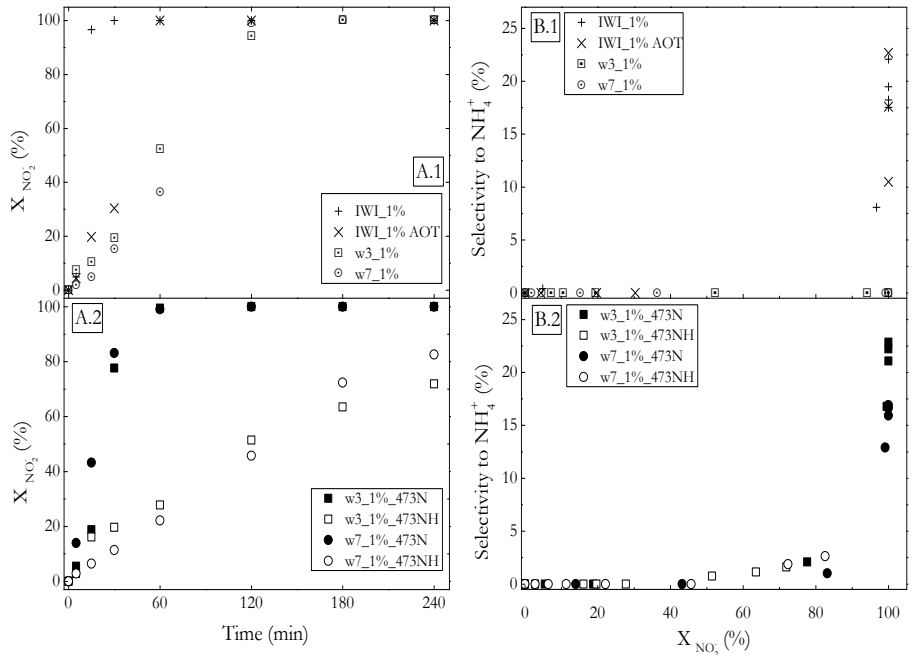

Figure 5.6. NO_2^- reduction experiments at controlled pH for catalysts subjected to thermal treatment in N_2 atmosphere (**A.1, B.1**) and thermal treatment in N_2 atmosphere followed by reduction with H_2 (**A.2, B.2**).

To learn more on the role of the AOT on catalysts activity and selectivity, alternative purification of the NPs and catalysts by washing with THF was carried out. **Figure 5.7** shows NO_2^- conversion upon reaction time at controlled pH (5-6) with those catalysts. The ones prepared with NPs washed with THF (w7 THF_1%) and by washing with THF after NPs impregnation (w7_1%THF) were more active than the equivalent catalyst washed with methanol (w7_1%). In particular, the highest reaction rate was obtained when the THF washing was performed after the impregnation of Pd NPs onto the support (w7_1%THF), suggesting that THF plays an important role on the metal-support interaction. In *Chapter IV* [3] we observed that NPs washed with THF were less active than those washed with MeOH, therefore lower removal of AOT can be expected from THF washing. Several authors have used THF to destabilize NP suspensions resulting from ME synthesis [9,10] and to enhance the interaction with the support [11]. Such

interaction would reduce the shielding effect of AOT, therefore giving rise to a higher production of ammonia.

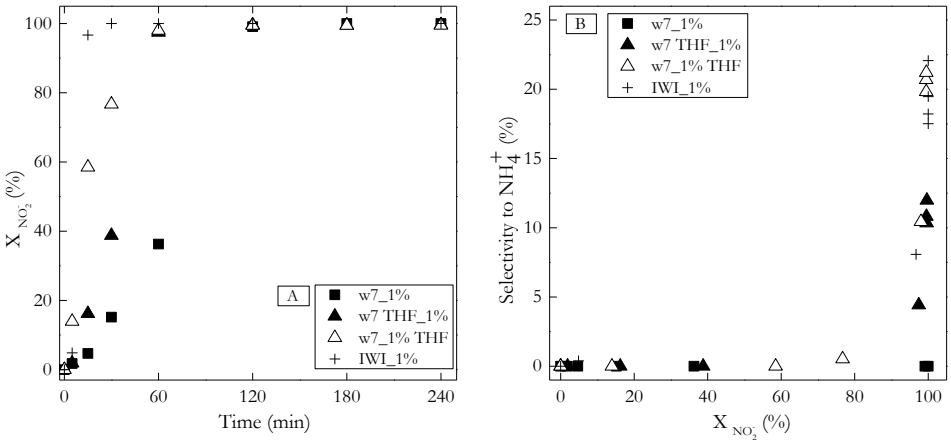

Figure 5.7. NO_2^- reduction experiments at controlled pH for IWI catalyst and catalysts purified using different solvents.

5.3. Conclusions

The catalytic reduction of NO_2^- in aqueous phase was studied as an intermediate and critical step in the reduction of NO_3^- using size-controlled Pd-AOT NPs supported on AC. Supported Pd-AOT NPs showed higher activity than unsupported ones studied in a former work. All the catalysts tested at uncontrolled pH exhibited low NO_2^- conversion, especially in the case of the catalyst synthesized via ME, and high selectivity to NH_4^+.

Pd-AOT NPs supported on AC showed complete NO_2^- conversion in the time range studied at controlled pH, although lower activity than for IWI catalysts was observed due to shielding by AOT. The thermal treatment of the catalysts increased activity due to modification and removal of AOT. Likewise, a higher reaction rate was observed for those catalysts based on Pd-AOT NPs supported AC purified with THF, showing the importance of metal-support interaction and the role of solvents in facilitating this interaction.

The catalysts based on Pd-AOT NPs showed a negligible production of NH_4^+ when used at buffered pH. The production of NH_4^+ was increased when the catalysts were subjected to thermal treatment or purification with THF, showing the role of AOT in the control of the selectivity through shielding of the metal surface and active centres. This remarkable feature opens field for the development of highly selective catalysts for the reduction of NO_3^- and other reactions.

5.4 References

[1] A.M. Perez-Coronado, L. Calvo, N. Alonso-Morales, F. Heras, J.J. Rodriguez, M.A. Gilarranz, Multiple approaches to control and assess the size of Pd nanoparticles synthesized via water-in-oil microemulsion, Colloids Surfaces A Physicochem. Eng. Asp. 497 (2016) 28–34.

[2] S. Eriksson, Preparation of catalysts from microemulsions and their applications in heterogeneous catalysis, Appl. Catal. A Gen. 265 (2004) 207–219.

[3] A.M. Perez-Coronado, L. Calvo, J.A. Baeza, J. Palomar, L. Lefferts, J.J. Rodriguez, et al., Metal-surfactant interaction as a tool to control the catalytic selectivity of Pd catalysts, Appl. Catal. A Gen. 529 (2017) 32–39.

[4] U. Matatov-Meytal, M. Sheintuch, The relation between surface composition of Pd–Cu/ACC catalysts prepared by selective deposition and their denitrification behavior, Catal. Commun. 10 (2009) 1137–1141.

[5] R. Mélendrez, G. Del Angel, V. Bertin, M.A. Valenzuela, J. Barbier, Selective hydrogenation of carvone and o-xylene on Pd–Cu catalysts prepared by surface redox reaction, J. Mol. Catal. A Chem. 157 (2000) 143–149.

[6] J. Jung, S. Bae, W. Lee, Nitrate reduction by maghemite supported Cu-Pd bimetallic catalyst, Appl. Catal. B Environ. 127 (2012) 148–158.

[7] Y. Zhao, J.A. Baeza, N. Koteswara Rao, L. Calvo, M.A. Gilarranz, Y.D. Li, et al., Unsupported PVA- and PVP-stabilized Pd nanoparticles as catalyst for nitrite hydrogenation in aqueous phase, J. Catal. 318 (2014) 162–169.

[8] W. Kiciński, M. Szala, M. Bystrzejewski, Sulfur-doped porous carbons: Synthesis and applications, Carbon N. Y. 68 (2014) 1–32.

[9] M. Bonarowska, Z. Karpinski, R. Kosydar, T. Szumelda, A. Drelinkiewicz, Hydrodechlorination of CCl4 over carbon-supported palladium-gold catalysts prepared by the reverse "water-in-oil" microemulsion method, Comptes Rendus Chim. 18 (2015) 1143–1151.

[10] M. Trépanier, A.K. Dalai, N. Abatzoglou, Synthesis of CNT-supported cobalt nanoparticle catalysts using a microemulsion technique: Role of nanoparticle size on reducibility, activity and selectivity in Fischer-Tropsch reactions, Appl. Catal. A Gen. 374 (2010) 79–86.

[11] A. Martínez, G. Prieto, Breaking the dispersion-reducibility dependence in oxide-supported cobalt nanoparticles, J. Catal. 245 (2007) 470–476.

CHAPTER VI

Carbon-supported metallic nanoparticles synthesized via incipient wetness impregnation and microemulsion for their use in the reduction of nitrate

CHAPTER VI

Carbon-supported metallic nanoparticles synthesized via incipient wetness impregnation and microemulsion for their use in the reduction of nitrate

6.1 Summary

In *Chapter V* was shown that the interaction between Pd NPs and AOT provides control of the selectivity in the catalytic reduction of NO_2^- with H_2, the intermediate step in the reduction of NO_3^- to N_2. The aim of the current *Chapter* is to study the applicability of such concept to the reduction of NO_3^-. Pd:Cu bimetallic catalysts and Pd and Cu monometallic catalysts supported on activated carbon were prepared by different methodologies, including the use of AOT at different stages of the synthesis of the catalysts. The catalytic performance was evaluated in terms of activity and selectivity in the reduction of NO_3^- with H_2. A very low activity was achieved for catalysts with Pd metal phase interacting with AOT, particularly when the synthesis of Pd NPs was carried out by the ME method. AOT seems to block the redox reaction between Pd and Cu, which leads to the oxidation of the Cu phase and the loss of activity in the first stage in the reduction of NO_2^-.

6.2. Results and discussion

Table 6.1 and **Table 6.2** summarize different bimetallic and monometallic catalysts synthesized to carry out nitrate and nitrite reduction, and the corresponding nomenclature for them.

Table 6.1. Preparation of the bimetallic catalysts.

CATALYST	PROCEDURE OF SYNTHESIS
$(Pd:Cu)_{IWI}$	Co-impregnation in order to obtain a 1 wt. % of metal.
$(Pd:Cu)_{IWI\ EXC.\ AOT}$	$(Pd : Cu)_{IWI}$ catalyst was poisoned with a solution of AOT in isooctane using an AOT/Pd mass ratio double than the one used in the ME synthesis at $w_0 = 7$.
$(Pd:Cu)_{IWI\ DEF.AOT}$	$(Pd : Cu)_{IWI}$ catalyst was poisoned with a solution of AOT in isooctane using an AOT/Pd mass ratio middle than the one used in the ME synthesis at $w_0 = 7$.
Pd_{IWI}/Cu_{IWI}	Successive impregnation in order to obtain 1 wt. % of metal. At first the Pd monometallic catalyst was prepared by IWI method. Then a defined amount of Cu precursor was added to monometallic Pd_{IWI}/C.
$(Pd:Cu)_{ME}$	Co-impregnation where Pd and Cu were chemically reduced simultaneously in ME washed with MeOH and then supported.
Pd_{ME}/ Cu_{IWI}	First, Pd monometallic catalyst via ME was synthesized. After, the Cu IWI synthesis was carried over this catalyst.
$Cu_{ME\ TT}/Pd_{ME}$	First, Cu monometallic catalyst via ME was synthesized. After, the Cu_{ME}/C was subjected to thermal treatment during 2 h under 60 $NmL.min^{-1}$ in N_2 atmosphere at 573 K ($Cu_{ME\ TT}$). After Pd NPs synthesized via ME in colloidal suspension were supported in rotary evaporator.

Table 6.2. Preparation of the monometallic catalysts using activated carbon as support.

CATALYST	PROCEDURE OF SYNTHESIS
$Pd_{IWI}+Cu_{IWI}$	Pd and Cu monometallic catalysts were prepared by IWI method.
$Pd_{IWI\ EXC.\ AOT}+Cu_{IWI}$	Pd_{IWI} catalyst was poisoned with a solution of AOT in isooctane using an AOT/Pd mass ratio double than the one used in the ME synthesis at $w_0 = 7$. After poisoning the catalyst was washed three times. Cu monometallic catalyst was prepared by IWI method.
$Pd_{ME}+Cu_{ME}$	Pd and Cu monometallic catalysts were prepared by ME method.
$Pd_{ME}+Cu_{ME\ TT}$	Pd catalyst was prepared by ME method. Cu catalyst was prepared by ME method. After, this catalyst was subjected to thermal treatment during 2 h under 60 $NmL.min^{-1}$ N_2 in atmosphere ($Cu_{ME\ TT}$).
($Pd_{ME}+Cu_{IWI}$	Pd catalyst was prepared by ME method. Cu monometallic catalysts were prepared by IWI method.
$Pd_{ME\ TT}+Cu_{IWI}$	Pd catalyst was prepared by ME method. This catalyst was subjected to thermal treatment during 2 h under N_2 atmosphere (60 $NmL.min^{-1}$)($Pd_{ME\ TT}$). Cu monometallic catalyst was prepared by IWI method.
$Pd_{ME\ TFE}+Cu_{IWI}$	Pd catalyst was prepared by ME method. In this case, the catalyst was washed with a mixture of 50% TFE+50% MeOH v/v three times instead of MeOH ($Pd_{ME\ TFE}$). El catalizador de PdME se lava con una mezcla de TFE+MeOH.
$Pd_{IWI}+Cu_{ME}$	Pd catalyst was prepared by IWI method. Cu catalyst was prepared by ME method.
$Pd_{ME}+Pd_{IWI}+Cu_{ME}$	Two Pd monometallic catalysts were prepared, one of them by ME method and the other by ME. Cu catalyst was prepared by ME method.

6.2.1. Comparison of bimetallic Pd:Cu catalysts synthesized via IWI and ME and influence of AOT

The activity and selectivity of different bimetallic Pd:Cu catalysts supported on activated carbon was studied. As a first approach, IWI catalysts prepared by co-impregnation $(Pd:Cu)_{IWI}$ and by successive impregnation of Pd and Cu (Pd_{IWI}/Cu_{IWI}) metals were tested. **Figure 6.1 A** and **B** show the evolution of NO_3^- and reaction products concentration. It can be observed that NO_3^- is adsorbed by the catalyst and it is desorbed as H_2 is introduced in the reaction system (time equal to zero). $(Pd:Cu)_{IWI}$ shows a higher activity, with a drop in NO_3^- concentration from ca. 96 to ca. 20 mg/L in 30 min. However, the higher adsorption in the case of Pd_{IWI}/Cu_{IWI} may mask partially the difference in activity.

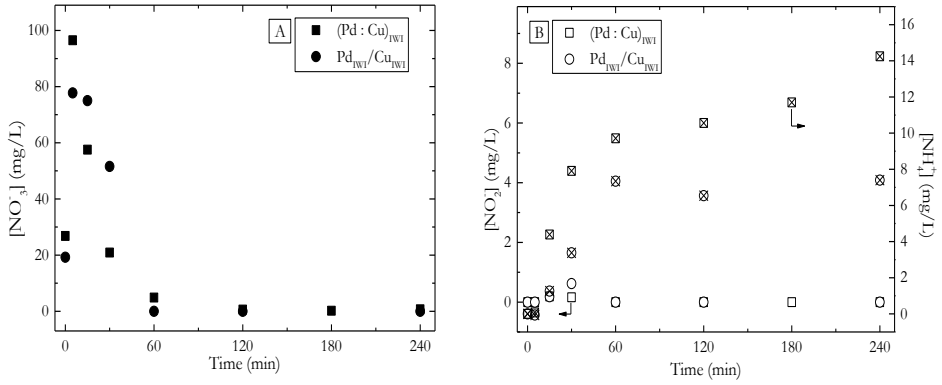

Figure 6.1. Time course of NO_3^- concentration (A) and reaction products concentration (B) (NO_2^-: open symbols, NH_4^+: crossed symbols) for IWI catalysts.

Figure 6.2 A shows the reaction results obtained for bimetallic catalysts prepared by ME and by IWI and further exposure to AOT. In both cases, the adsorption of NO_3^- is substantially lower than for IWI catalysts. Nevertheless Pd_{ME}/Cu_{IWI} catalyst shows an adsorption is slightly similar than the ones prepared via IWI, showing the AOT incorporated during the synthesis can limit the

interaction of Cu and or the support with NO_3^-. Thus, the SO_3^- at the head of AOT has a negative charge that could compete with NO_3^- or provoke NO_3^- repulsion. This competitive adsorption would be in agreement with the very strong interaction between AOT and Pd NPs reported before in *Chapter IV* [1]. Likewise, in *Chapter V* has been shown that the porosity of the catalysts decreases after impregnation of the NPs synthesized by ME due to the AOT incorporated to the support, even after purification of the NPs. The $(Pd:Cu)_{ME}$ catalyst show a very low activity in the reduction of NO_3^-. This may indicate that NO_3^- cannot reach the actives sites for reduction due to AOT blockage, which would be consistent with the lower adsorption of NO_3^-. Interestingly, in *Chapter IV* based on the reduction of NO_2^- with catalysts based on Pd NPs prepared by ME, a low activity was also observed and ascribed to the Pd-AOT interaction [1], however the activity was enhanced by purification of NPs and immobilization of NPs on carbon, thus achieving nearly total conversion of NO_2^- after 4 h as observed in the *Chapter V*. In the current study, the NPs were purified and supported but the activity remains very low. Likewise, the sites on the surface of Cu NPs, which are responsible for the reduction of NO_3^- to NO_2^-, are also blocked or are not active. The poisoning effect of AOT can be also be inferred from the loss of activity of the IWI catalysts that were exposed to AOT ($(Pd:Cu)_{IWI\ EXC.\ AOT}$ and $(Pd:Cu)_{IWI\ DEF.\ AOT}$), although in both cases the conversion of NO_3^- is slightly higher than for $(Pd:Cu)_{ME}$ catalysts. The loss of activity respect to $(Pd:Cu)_{IWI}$ is lower for the catalyst exposed to a lower AOT dose ($(Pd:Cu)_{IWI\ DEF.\ AOT}$) than the catalyst exposed to a higher AOT dose ($(Pd:Cu)_{IWI\ EXC.\ AOT}$). These catalysts also show a higher selectivity to NO_2^-, which is indicative of a lower activity of the Pd phase due to blocking by AOT. However, the selectivity to NH_4^+ is higher, showing that the selective blockage of active sites generating NH_4^+ from NO_2^- is not achieved.

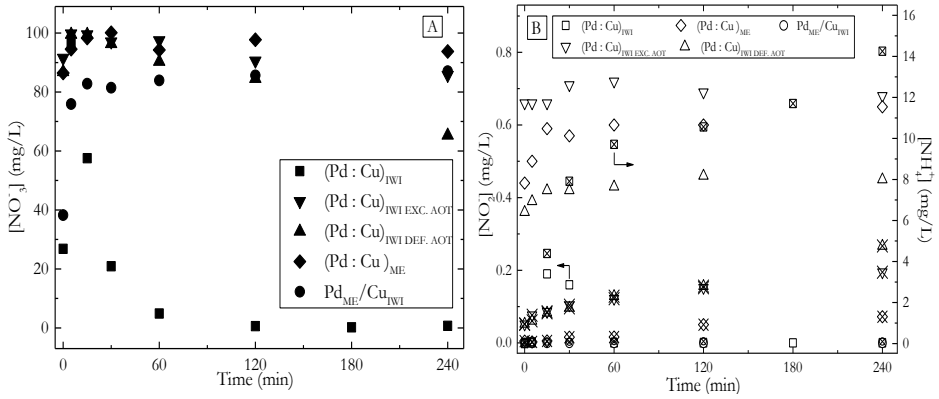

Figure 6.2. Time course of NO_3^- concentration (A) and reaction products concentration (B) (NO_2^-: open symbols, NH_4^+: crossed symbols) for ME and AOT-exposed catalysts.

6.2.2. Pd and Cu monometallic catalysts synthesized via IWI and ME

Monometallic Pd/AC and Cu/AC catalysts synthesized via IWI and/or ME were mixed to carry out NO_3^- reaction with bimetallic systems, the results are shown in **Figure 6.3**. It can be seen that NO_3^- conversion of 100% was reached after 240 min for the mixture of monometallic catalysts prepared each of them by IWI (Pd_{IWI} + Cu_{IWI}). However, when Pd_{IWI} catalyst was exposed to AOT, the activity of the mixture $Pd_{IWI\ AOT}$ + Cu_{IWI} was low. It is has been reported that the monometallic Cu catalysts are only active in NO_3^- reduction when Cu is in its reduced form [2, 3]. Thus, conversion of NO_3^- was only observed at the beginning of the reaction and then the activity declined, which can be associated to gradual oxidation of Cu simultaneous to NO_3^- conversion. To obtain an effective stabilization of Cu and maintain activity, interaction between Pd and Cu is necessary, Pd contributing to the reduction of Cu [4]. Therefore, for the $Pd_{IWI\ AOT}$ + Cu_{IWI} mixture the interaction between Pd and Cu does not seems to be possible due to blocking of Pd by AOT.

Figure 6.3 A also shows the evolution of NO_3^- concentration for the mixtures of monometallic catalysts $Pd_{IWI}+Cu_{ME}$, $Pd_{ME}+Cu_{IWI}$ $Pd_{ME}+Pd_{IWI}+Cu_{ME}$ and $Pd_{ME}+Cu_{ME}$. These mixtures of catalysts achieved NO_3^- conversion values of 94.2, 16.6 18.3 % and 3 % after 240 of reaction, respectively. The results show a decrease of activity as the proportion of Pd metallic phase interacting directly with AOT increases. The relatively high activity of $Pd_{IWI}+Cu_{ME}$ mixture and the low activity of $Pd_{ME}+Cu_{ME}$ mixture evidences that the blocking of the redox reaction between Pd and Cu is due to the interaction of AOT with Pd, and not to the interaction with Cu. On the other hand, the selectivity to NH_4^+ (**Figure 6.3 B**) is higher for catalyst mixtures with a higher proportion of Pd NPs synthesized by IWI. The activity of mixtures of Pd and Cu monometallic catalysts has been attributed to the formation of in situ bimetallic Pd:Cu catalysts due to the adsorption of the leached copper over Pd_{IWI} catalyst [2]. Therefore, when Pd catalyst was synthesized via ME, the strong interaction Pd-AOT can blockage the interaction.

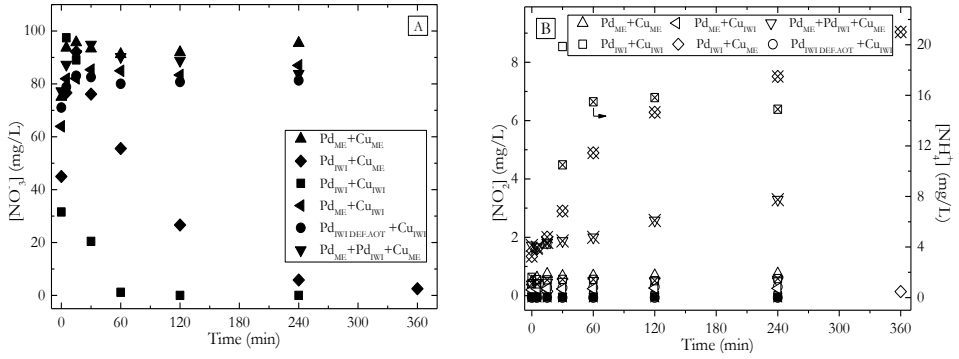

Figure 6.3. Time course of NO_3^- concentration (A) and reaction products concentration (B) (NO_2^-: open symbols, NH_4^+: crossed symbols) for ME and AOT-exposed catalysts.

6.3. Effect of the removal of AOT from catalysts

Figure 6.4 shows the evolution of NO_3^- (**Figure 6.4 A**), NO_2^- and NH_4^+ concentration (**Figure 6.4 B**) for different catalysts prepared combining different procedures to remove AOT. The first observation for these catalysts is the different adsorption of NO_3^- taking place during the first minutes of reaction. The adsorption is slightly higher for those catalysts where the Cu phase was synthesized IWI. As commented above, the AOT interacting with the surface on the metal through SO_3^- groups may compete with NO_3^- and repel it.

The catalytic activity for all the catalysts subjected to removal of AOT was low, regardless the method used, i.e. washing or thermal treatment. The low activity indicates a strong interaction between AOT and the metal phase and the insufficient removal by washing, but also that after thermal treatment AOT decomposition products remain on the surface of the catalysts. Within this set of catalysts, the mixture of monometallic catalysts Pd_{TFE}+Cu_{IWI} exhibited the highest NO_3^- conversion, showing that washing with a polar and acidic solvent such as TFE is more effective. In this sense, in *Chapter III* [1], we observed that NPs purified with a TFE+MeOH mixture showed a higher removal of AOT and the NO_3^- reaction improved leading to increase of NH_4^+ formation.

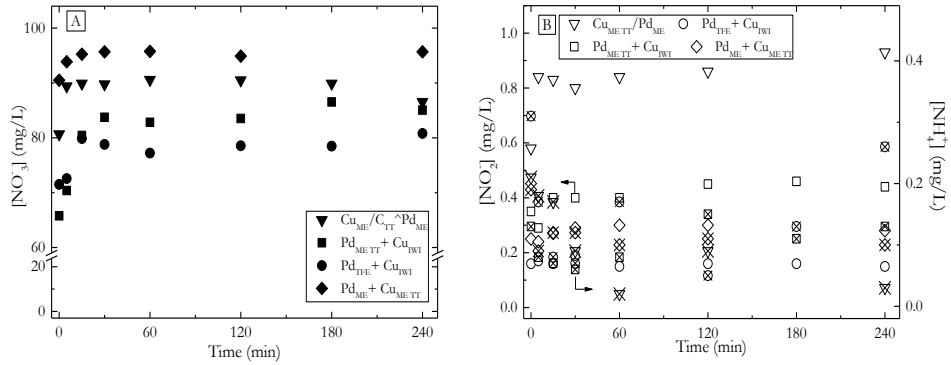

Figure 6.4. Concentration profiles of **(A)** NO_3^- and **(B)** NO_2^- and NH_4^+ as a function of time for catalyst which supported at different thermal treatment.

6.4. Nitrate and nitrite reduction

In order to explore the effect of AOT in the activity of the catalysts in the initial and intermediate stages of the reaction path, $(Pd:Cu)_{IWI\ EXC.\ AOT}$ and $Pd_{ME}+Cu_{IWI}$ catalysts were tested in NO_3^- and NO_2^- reduction. **Figure 6.5 A** shows the evolution of NO_3^-, NO_2^- and NH_4^+ concentration. As can be seen, in both experiments, the catalysts reduce NO_2^- with a high activity and a high selectivity to nitrogen, indicating that AOT does not interfere with this function of the catalyst. However, they are not active in the reduction of NO_3^-. Also, in **Figure 6.5 A** it can be observed that the NH_4^+ production for $(Pd:Cu)_{IWI\ EXC.\ AOT}$ catalyst increase with time, showing that although AOT added by impregnation reduces activity, it cannot prevent the generation of NH_4^+.

On the other hand, **Figure 6.5 B** shows the selectivity to NH_4^+. The selectivity to NH_4^+ negligible for the $Pd_{ME} + Cu_{IWI}$ catalysts even at complete NO_2^- conversion, showing that the remaining AOT fragments also contribute in some extent to blockage of active centers responsible for NH_4^+ production. This was also observed in *Chapter V*, where the negligible production of NH_4^+ at complete NO_2^- conversion was attributed to the effect of the AOT attached to the surface of the NPs. This interaction prevented the nitrogen species evolving to NH_4^+ on the surface of the NPs.

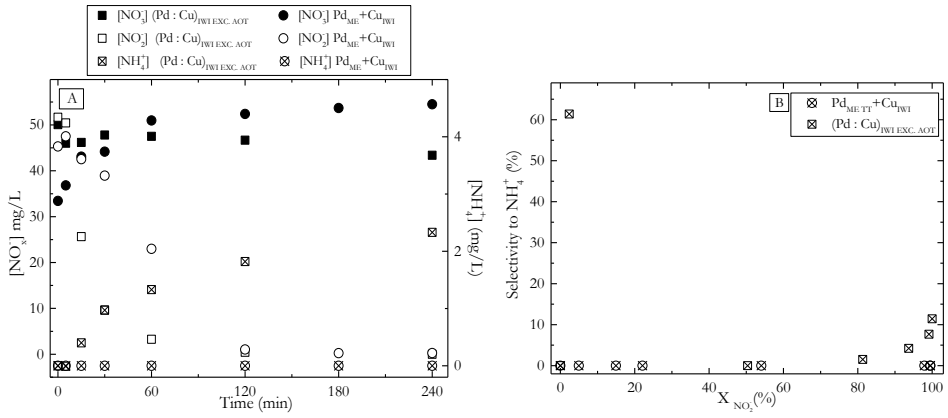

Figure 6.5. **A)** Time course of NO_3^- concentration (A) and reaction products concentration (B) (NO_2^-: open symbols, NH_4^+: crossed symbols) for ME and AOT-exposed catalysts. **B)** Selectivity to NH_4^+ for different catalysts.

In order to gain insight into the deactivation phenomena, an experiment was designed in which a pulse of NO_2^- is introduced in reactor after 60 min later that NO_3^- was added. For this runs $(Pd:Cu)_{IWI\ EXC.\ AOT}$ and Pd_{ME} + Cu_{IWI} catalyst were employed. As can be seen in **Figure 6.6 A** these catalysts were inactive in NO_3^- reduction, but 100% NO_2^- conversion was achieved after the introduction of the pulse. The catalyst $(Pd:Cu)_{IWI\ EXC.\ AOT}$ was more active and showed an activity higher than when NO_2^- was introduced in the reaction medium before bubbling H_2 (see **Figure 6.5 A**). This fact may be related to the formation of Pd-H phase over catalyst that would be available when NO_2^- is introduced as a pulse, although the excess of H_2 also lead to higher over-reduction to NH_4^+. In the case of Pd_{ME} + Cu_{IWI} catalyst the formation of NH_4^+ is negligible due to the Pd-AOT interaction.

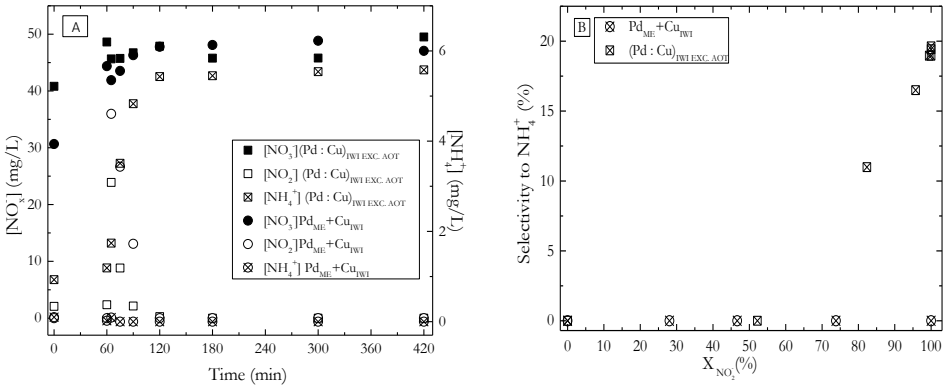

Figure 6.6. A) The concentration of NO_3^-, NO_2^- and NH_4^+ ions in the solution during the course of NO_3^- reduction and **B)** Selectivity to NH_4^+ for different catalysts: $(Pd:Cu)_{IWI\ EXC.\ AOT}$ and Pd_{ME} + $Cu_{IWI.}$

6.5 Conclusion

Bimetallic catalysts prepared by incipient wetness impregnation showed a 100 % NO_3^- conversion with a high NH_4^+ production. However, when bimetallic catalysts were synthesized by ME and by IWI using AOT in the synthesis the NO_3^- reduction was low. This may indicate that NO_3^- cannot reach the active sites for reduction due to AOT blockage. On the other hand, when physical mixtures with monometallic catalysts were tested in NO_3^- reduction, 100 % of NO_3^- conversion was reached after 240 min for the mixture of monometallic catalysts prepared each of them by IWI. However, when the physical mixture for catalysts were formed by Cu_{ME} and combined with Pd synthesized by IWI or ME the activity catalytic showed was low. Finally, NO_3^- and NO_2^- on mono and bimetallic catalyst prepared via ME and the use of AOT in the IWI synthesis experiments were carried out. These catalysts reduce NO_2^- with a high activity (100 % NO_2^- conversion) and a high selectivity to nitrogen.

In spite of the generally low NO_3^- activity of the catalysts prepared by ME, the results obtained are relevant because they allow concluded that the blocking of the redox reaction between Pd and Cu is due to the interaction of AOT with Pd, and not to the interaction with Cu.

6.6. References

[1] A.M. Perez-Coronado, L. Calvo, J.A. Baeza, J. Palomar, L. Lefferts, J.J. Rodriguez, et al., Metal-surfactant interaction as a tool to control the catalytic selectivity of Pd catalysts, Appl. Catal. A Gen. 529 (2017) 32–39.

[2] O.S.G.P. Soares, J.J.M. Órfão, M.F.R. Pereira, Nitrate reduction with hydrogen in the presence of physical mixtures with mono and bimetallic catalysts and ions in solution, Appl. Catal. B Environ. 102 (2011) 424–432.

[3] F. Epron, F. Gauthard, C. Pi, J. Barbier, Catalytic Reduction of Nitrate and Nitrite on Pt–Cu/Al 2 O 3 Catalysts in Aqueous Solution: Role of the Interaction between Copper and Platinum in the Reaction, J. Catal. 198 (2001) 309–318.

[4] J. Trawczyński, P. Gheek, J. Okal, M. Zawadzki, M.J.I. Gomez, Reduction of nitrate on active carbon supported Pd-Cu catalysts, Appl. Catal. A Gen. 409 (2011) 39–47.

CHAPTER VII

Catalytic reduction of bromate over Pd nanoparticles synthesized via water-in-oil microemulsion

CHAPTER VII

Catalytic reduction of bromate over Pd nanoparticles synthesized via water-in-oil microemulsion

7.1 Summary

Supported Pd NPs synthesized via w/o ME using the water/ AOT/ isooctane system were used as catalysts in the BrO_3^- reduction. In order to study the influence the support on the catalytic activity, Pd NPs were immobilised on different supports: activated carbon, multi-walled carbon nanotubes and titanium dioxide. Some different thermal treatments in air and nitrogen were carried out in 473-673 K range. The immobilization of Pd NPs on titanium dioxide led to higher activity than the immobilization on the carbon-based supports. Thermal treatment of the catalysts at 673 K in air removed successfully AOT and decomposition fragments, leading to a significant increase in activity. The experiments with catalysts prepared with Pd NPs supported on titanium dioxide of different size did not led to significant differences in activity. Therefore no evidence structure sensitiveness was assessed.

7.2. Results and discussion

7.2.1. Pd NPs and catalysts characterization

The textural characterization of the prepared catalysts is shown in **Table 7.1**. As can be seen, the surface area (S_{BET}) remains practically unchanged when TiO_2 or TiO_{2_773} were used as support. The adsorption-desorption isotherms indicate that both the supports and the catalysts are non-porous and the surface area correspond to external surface (see appendix, **Figure A.6**). In the case of the catalysts supported on carbon nanotubes, significant changes in the surface area were observed after impregnation of the NPs, the behaviour changed depending on the treatment applied to the carbon nanotubes. The hysteresis loop observed in the adsorption-desorption isotherms corresponds to type IV, indicating that the material is mostly mesoporous (see appendix, **Figure A.6**). The catalysts prepared with CNT_M show higher surface area and porosity in the whole mesopore range (**Table 7.1**, see appendix **Figure A.5**) for the NPs synthesized using high w_0 values, which can be ascribed to a lower amount of AOT remaining in the NPs after purification. In contrast, when Pd NPs were supported on CNT_{HNO3} the S_{BET} and the isotherms showed only slight changes with w_0, besides a significant reduction of the surface area being observed after impregnation of the NPs. This fact shows that the functional groups on the surface of the carbon nanotubes influence the interaction with the Pd-AOT system.

Table 7.1 Textural properties of the catalysts prepared by impregnation of Pd NPs synthesized using different w_c values.

w_0	TiO_2	TiO_{2_773}	CNT_M		CNT_{M_873}		CNT_{HNO3}	
	S_{BET} (m^2/g)	S_{BET} (m^2/g)	S_{BET} (m^2/g)	Vp (cm^3/g)	S_{BET} (m^2/g)	Vp (cm^3/g)	S_{BET} (m^2/g)	Vp (cm^3/g)
support	50	nd	291	1.1	338	0.87	324	0.64
3	46	nd	171	0.53	nd	nd	248	1.53
7	47	32	204	0.70	nd	nd	254	1.59
12	51	32	284	0.73	145	0.55	214	1.45

nd: not determined

In the *Chapter IV* about the reduction of NO_2^- using unsupported Pd NPs synthesized via ME with the water/AOT/isooctane system [1], we observed the

difficulty to remove AOT by purification with solvents. Furthermore, in the *Chapter V* we studied different thermal treatments to remove the surfactant from the catalysts surface, concluding that this treatment can increase the catalytic activity due to modification of the catalyst surface and the removal of AOT. This is in agreement with the results reported by Xiong et al. [2], who observed the strong interaction of AOT with the surface of NPs and the difficulty to remove AOT due to the presence of sodium and sulfonate group in the AOT molecule.

The catalysts prepared were subjected to a thermal treatment in N_2 atmosphere (473 and 673 K) and in air (573 and 673 K) to remove AOT from the catalysts. These temperatures were select according to the decomposition range of AOT observed by TGA in air and N_2 atmosphere (see appendix, **Figure A.5**). The results shown in **Table 7.2** indicate that in general, the S_{BET} increases when the catalyst was treated in air. In addition, the w12/CNT_{M_873} (380 m^2/g) and w12/CNT_{HNO3} (382 m^2/g) catalysts showed S_{BET} values very close to those of the original supports (CNT_{M_873}: 338 m^2/g; CNT_{HNO3}: 324 m^2/g), indicating the removal of AOT from the catalyst.

Table 7.2. Textural properties of the catalysts subjected to thermal treatment.

Catalyst/thermal treatment	473 K NH	673 K NH	573 K AirH	673 K AirH	
	S_{BET} (m^2/g)	S_{BET} (m^2/g)	S_{BET} (m^2/g)	S_{BET} (m^2/g)	Vp (cm^3/g)
w3/TiO_2	nd	44	nd	54	nd
w7/TiO_2	nd	nd	nd	57	nd
w12/TiO_2	nd	43	48	56	nd
w12/TiO_{2_773}	nd	nd	nd	50	nd
w12/CNT_M	290	nd	nd	380	0.86
w12/CNT_{M_873}	nd	nd	nd	291	0.71
w12/CNT_{HNO3}	nd	nd	nd	382	1.31

nd: not determined

XPS spectra were obtained in order to determine the oxidation state of Pd NPs and the changes in AOT during the thermal treatment of the catalysts (see appendix, **Figure A.7** and **Figure A.8**). **Table 7.3** summarizes the values of Pd^{n+}/Pd^0 ratio obtained from the deconvolution of the 3d region spectra of Pd XPS for the catalysts synthesized via incipient wetness impregnation (IWI) and via ME

supported on TiO_2. The presence of both electron deficient and zero-valent species was observed in all the catalyst series analysed (see **Figure A.7** and **Figure A.8** in appendix), as it has been formerly reported for Pd catalysts and NPs prepared by different procedures [3-5]. The high Pd^{n+}/Pd^0 ratio observed for $w3/TiO_2$ can be related to the important presence of AOT, affecting the reduction of NPs during the synthesis and also probably the determination of Pd^{n+}/Pd^0 ratio by XPS. After thermal treatment under air or N_2 and further reduction with H_2 ($w3/TiO_2$_673AirH and $w3/TiO_2$_673NH) a substantially lower value of the Pd^{n+}/Pd^0 ratio can be observed. This trend can also be observed for the catalysts with NPs synthesized using a w_0 of 12.

Regarding the S species, the XPS spectra (see appendix, **Figure A.9**) were fitted with a doublet according to NIST X- ray Photoelectron Spectroscopy Database [6]. The results in **Table 7.3** indicate the presence of species Pd-S, $CH_3(CH_2)S^-$, SO_3^{2-}, $-C-SO_3^{2-}$ and metal sulphate with binding energies of 161.9, 163.6, 167.4, 168.2 and 169eV, respectively. The catalyst based on NPs synthesized via ME showed a peak related to $-C-SO_3^{2-}$ species, which can be associated to the sulfonate head group of AOT. After thermal treatment with air, the intensity of this peak decreases and the peak associated to metal sulphate increases due to oxidation of the sample. In contrast, after the thermal treatment with N_2 the sulphate species were not detected and $CH_3(CH_2)S^-$ species are observed, which can be interpreted as fragmentation of the alkyl tails of AOT. In addition to this, Pd-S is observed, showing interaction between S and Pd.

Table 7.3. Pd^{n+}/Pd^{0} ratio and contribution of S species from 2p peaks for selected catalysts.

Assignment/sample	IWI/TiO_2	w3/TiO_2	w3/TiO2_673AirH	w3/TiO_2_673NH	w12/TiO_2	w12/TiO_2_673AirH
Pd^{n+}/Pd^{0}	1.3	2.85	0.36	0.06	0.57	0.24
Pd-S (161.9 eV)	-	-	-	12.9	-	-
$CH_3(CH_2)S^-$ (163.6 eV)	-	-	-	17.8	-	-
SO_3^{2-} (167.4 eV)	-	22.5	-	-	5.5	-
-C-SO_3^{2-}(168.2 eV)	-	72.3	53.9	69.3	81.2	63
Metal sulfate (169 eV)	-	5.2	46.1	-	13.3	37

7.3. Bromate reduction tests

As a first approach to BrO_3^- reduction, a blank test using CA, TiO_2 and CNT was carried out using H_2 (Blank H_2) and nitrogen (Blank N_2) to study the role of the reducing agent and adsorption on the support. As can be seen in **Figure 7.1 A**, the support without Pd NPs (Blank H_2 AC, Blank H_2 TiO_2 and Blank H_2 CNT) removes some of the BrO_3^- from the solution in the presence of H_2. This was also observed in a previous work [7] where AC was used as catalysts support for BrO_3^- reduction. Similar results were reported by Dong et al. [8] and Palomares et al. [9] when using AC and carbon nanofibers (CNF) as supports, respectively. The results in **Figure 7.1 A** show that under N_2 atmosphere, the BrO_3^- concentration remained nearly constant, as it was also observed by Restivo et al. [10] for TiO_2 and CNT. Thus, low adsorption by the support takes place and the supports contribute in some extent to the BrO_3^- reduction in the presence of H_2. On the other hand, Restivo et al. [10] observed that BrO_3^- reduction under 100 NmL·min^{-1} flow rate of H_2 using a semi-batch system and 10 mg/L of BrO_3^- loading in 200 mL solution shows activity. H_2 by itself resulted in a BrO_3^- removal of approximately 90 % after 120 min of reaction.

Figure 7.1 B compares the performance of several supported catalysts prepared by different methods and unsupported Pd NPs synthesized via ME (Pd NPs, w_0=7). As can be seen, unsupported NPs exhibited low activity in the reduction of BrO_3^- , whereas the immobilization of the NPs on AC enhanced the activity. Nevertheless, the activity in the reduction of BrO_3^- is only slightly higher than for Pd-free supports. Likewise, the catalysts prepared by IWI showed higher activity, yielding complete BrO_3^- reduction in less than 80 min for IWI/CNT and less than 15 min for IWI/TiO_2.

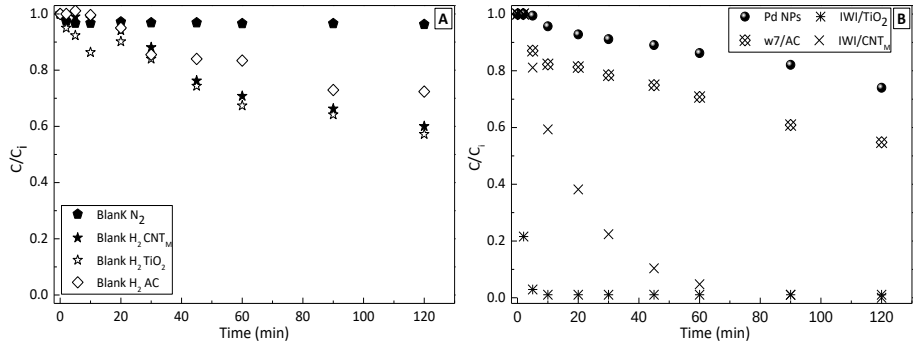

Figure 7.1. Dimensionless concentration-time course for BrO_3^- reduction experiments **A)** blank experiments with Pd-free supports and **B)** Pd catalysts prepared using different procedures.

The influence of the support on the activity of the catalysts was studied using those with Pd NPs synthesized by ME at w_0=12. The results in **Figure 7.2** indicate that the support plays an important role. Catalysts w12/TiO_2 and w12/CNT_M exhibited higher catalytic activity during the first 30 min of reaction time; however, after this time BrO_3^- concentration decreased slowly. After a reaction time of 240 min the catalyst w12/TiO_{2_773} achieved a higher BrO_3^- conversion, which can be due to the rutile crystalline structure improving the interaction of the support with the Pd-AOT NPs. The performance of this catalyst can be due to two effects i) catalyst w12/TiO_2 is more active than w12/TiO_{2_773} during the first 20-30 min of reaction, because of the stronger interaction of Pd NPs with anatase phase [11]; ii) for a longer reaction time, the performance of w12/TiO_2 catalyst declines because anatase crystalline structure is less stable than that of rutile. It is expected that the w12/TiO_{2_773} catalyst has a higher proportion of crystalline rutile due to TiO_2 treatment with air at 773 K, i.e. lower anatase:rutile ratio [12]. The lowest activity was observed for catalyst w12/CNT_{M_873}. This support was mechanically treated under ball-milling with the melamine and subjected to a thermal treatment (873 K) that promotes the thermal decomposition of the N-precursor, the products release being responsible for the incorporation of N-functionalities, namely quaternary nitrogen, pyridinic and pyrrole-type structures on the carbon surface [13]. In this way, the interaction between Pd-AOT with this

support (CNT_{M_873}) would block the active centers of the catalyst, decreasing the activity for BrO_3^- reduction. All the catalysts prepared by ME are less active than those prepared by IWI. This performance can be due to the strong interaction between the polar group of AOT ($-SO_3^-$) and Pd NPs producing blockage of the active phase of the catalyst and inhibition of BrO_3^- diffusion to the active centres. Additionally, the low activity observed for some of the catalysts studied should be related to a poor distribution of Pd-AOT NPs on the support due to interaction among them and agglomeration. Thus, supports with more favourable surface chemistry for the interaction with Pd-AOT NPs would lead to a higher distribution of the metal phase and a higher activity.

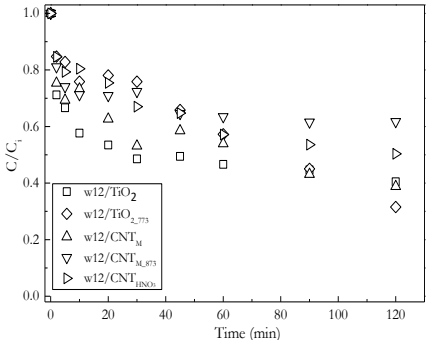

Figure 7.2. Dimensionless concentration-time course for BrO_3^- reduction experiments of w12 catalyst based on different supports.

Catalysts with NPs synthesized with different w_0 values were supported on TiO_2 to study the effect of the Pd NPs size. This support was chosen as it showed the best performance in the former tests. The Pd^{n+}/Pd^0 ratios for w_0 values of 3 and 12 can be seen in **Table 7.3**. The results in **Figure 7.3** show a significant influence of the size of the Pd NPs in the BrO_3^- reduction. The Pd NPs with the larger size (11.6 nm), i.e. synthesized via ME with w_0 = 12, led to the most active catalyst. This superior activity can be due to different factors such as i) low value of Pd^{n+}/Pd^0 ratio, which is in good agreement with the work of A.E. Palomares et al. [9] showing that the prevalence of Pd zero-valent species improves the BrO_3^- reduction rate, ii) lower amount of AOT coating the Pd NPs and iii) larger NPs

size, with higher prevalence of atoms at faces and larger crystal domains. In this sense, these results are in agreement with those reported by Chen et al. [14] who affirm that large Pd NPs (10.2 nm) are more active than the smaller ones (9.6 nm). However, in *Chapter V* was reported that the catalysts based on Pd NPs synthesized via ME can exhibit an apparent structure sensitiveness due to the shielding effect of AOT [1]. This shielding could lead to lower activity in BrO_3^- reduction, and would make not possible a study of structure sensitiveness with catalysts based on Pd NPs synthesized using AOT.

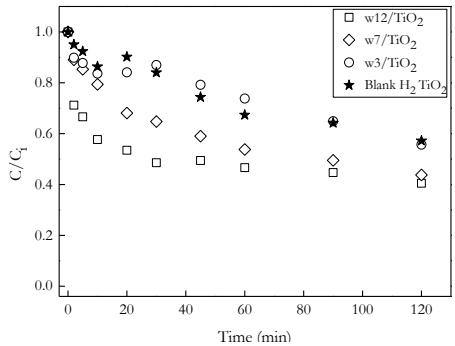

Figure 7.3. Influence of Pd NPs synthesis on BrO_3^- reduction.

To learn more on the influence of AOT and its removal on the activity of the catalysts, different thermal treatments of the catalysts were carried out. **Figure 7.4 A** shows the activity of catalysts based on Pd NPs (w_0 = 12) supported on TiO_2 and subjected to thermal treatment in air. Higher catalytic activity was obtained after the thermal treatment at 673 K than at 573 K, suggesting higher decomposition and removal of AOT. The catalysts treated at both temperatures were more active than that not subjected to thermal treatment (w12/TiO_2) (conversion 100 % vs 40 % after 120 min). Even so, they were less active than IWI/TiO_2 (**Figure 7.1 B**).

With the aim of exploring the effect of the thermal treatment in N_2 and in air, catalysts synthesized with different values of w_0 (3 and 12) and supported on TiO_2 were tested. **Figure 7.4 B** shows that the catalysts treated in N_2 at 673 K showed the lowest activity in BrO_3^- reduction (**Table 7.4**). As shown by the XPS

characterization (**Table 7.3**), during the thermal treatment with N_2 AOT was degraded to form alkyl chains linked to S and the contribution of SO_3^- groups is still high after the treatment. Therefore, the strong interaction with remaining AOT and AOT decomposition products result in lower activity of the catalyst. This is in agreement with the results reported in *Chapter V* on NO_2^- reduction, where Pd-AOT NPs subjected to thermal treatment in N_2 and H_2 showed low catalytic activity. Likewise, the catalysts with large NPs (w_0 = 12) showed higher activity than the one with small NPs (w_0 = 3) after the thermal treatment in N_2atmosphere, which can be again ascribed to higher initial AOT content and higher difficulty to remove it. On the contrary, the activity of both catalysts was identical after treatment in air at 673 K, showing that after removal of AOT, including sulfonic groups and alkyl chains linked to S, the activity increases in spite of the formation of metal sulphate species. Interestingly, after removal of AOT the catalysts with NPs synthesized using w_0 values of 3 and 12 show the same activity (**Table 7.4**) thus evidencing that the BrO_3^- reduction reaction is not structure sensitive.

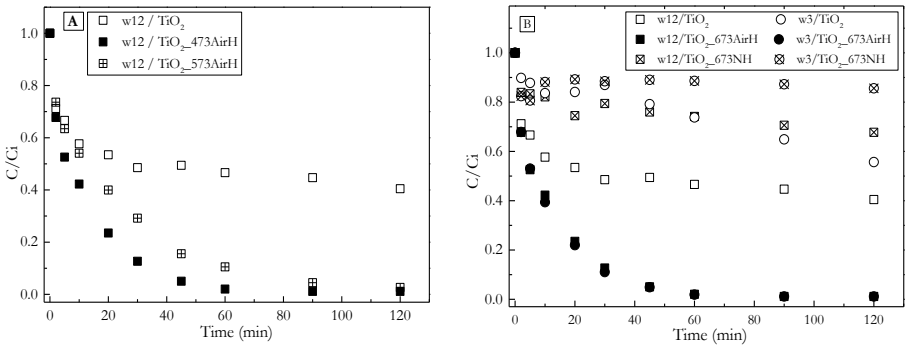

Figure 7.4. Dimensionless concentration of BrO_3^-during experiments using **A)** w12/TiO_2 catalysts subjected to thermal treatment in air at different temperature followed by reduction with H_2 and **B)** catalysts subjected to thermal treatment in N_2 or air atmosphere followed by reduction with H_2.

Table 7.4. Kinetic parameters for the reduction of BrO_3^-.

Catalyst	$k_{BrO_3^-} \cdot 10^3$ (min^{-1})	R^2
w12/TiO_2	29	0.939
w3/TiO_2	5	0.952
w12/TiO_2_573AirH	45	0.992
w12/TiO_2_673AirH	78	0.993
w3/TiO_2_673AirH	79	0.991
w12/TiO_2_673NH	2	0.978
w3/TiO_2_673NH	0.7	0.747

After optimization the thermal treatment temperature (673 K) in air atmosphere followed by reduction with H_2, this procedure was applied to catalysts based on different supports and Pd NPs synthesised using a w_0 of 12. The results obtained are presented in **Figure 7.5**, and the corresponding kinetic parameters can be seen in **Table 7.5**. The catalysts subjected to thermal treatment (**Figure 7.5**) are more active than the corresponding not heat treated samples (**Figure 7.2**). Also, a better initial activity of the catalysts subjected to thermal treatment is achieved. These results are therefore consistent with those obtained using TiO2 as support. The highest activity in BrO_3^- reduction was achieved with catalysts w12/TiO_2_AirH$_2$ and w12/CNT_M_AirH, followed by w12/TiO_{2_773}_AirH and w12/CNT_{M_873}_AirH.

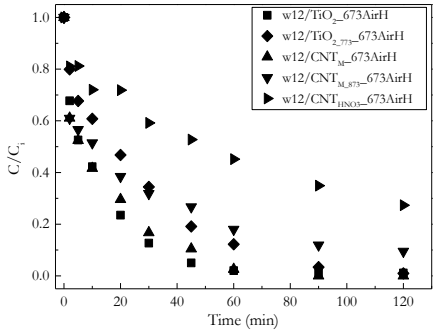

Figure 7.5. Dimensionless concentration of BrO_3^- with catalyst based on different supports subjected to thermal treatment in air atmosphere followed by reduction with H_2.

Table 7.5. Kinetic parameters for BrO_3^- reduction for catalysts synthesized with w_0 value of 12 without and with thermal treatment.

Catalyst	$k_{BrO_3^-} \cdot 10^3$ (min^{-1})	R^2
w12/TiO_2	29	0.939
w12/TiO_{2_773}	8	0.939
w12/CNT_M	16	0.981
w12/CNT_{M_873}	3	0.956
w12/CNT_{HNO3}	8	0.971
w12/TiO_2_673AirH	78	0.993
w12/TiO_{2_773}_673AirH	49	0.990
w12/CNT_M_673AirH	67	0.988
w12/CNT_{M_873}_673AirH	29	0.968
w12/CNT_{HNO3}_673AirH	17	0.998

To improve the understanding of the effect of AOT on the activity of the catalysts, the influence of the NPs preparation method was studied. As can be seen in **Figure 7.6**, the catalyst w12/TiO_2 THF was more active than the others. Pd NPs were synthesized using THF as destabilizing agent and carrying out destabilization in the presence of the support, which can avoid the agglomeration of NPs thus leading to better distribution on the support and improved activity. The use of THF as destabilizing agent and the corresponding enhancement of the interaction with the support has been reported by others [15,16]. Nevertheless, catalyst w12/TiO_2 THF is less active than w12/TiO_2_673AirH, probable because THF is a destabilizing agent but does not contribute to AOT removal.

Finally, the w12/TiO_2 THF catalyst was treated at 673 K in air and then reduced with H_2 in order to combine the methods described above. As can be seen in **Figure 7.6** and **Table 7.6**, this catalyst shows the highest activity in the reduction of BrO_3^-. However, it has to be noted that the activity only improved slightly in comparison to w12/TiO_2_673AirH catalyst, thus showing that the treatment in air is itself very effective in the removal of AOT and in the enhancement of the activity.

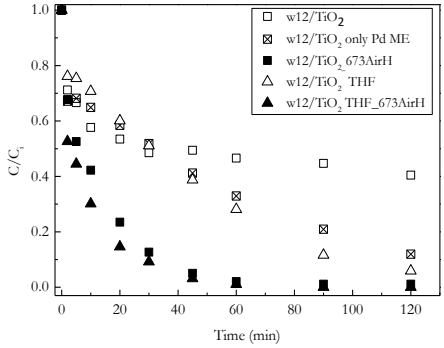

Figure 7.6. Dimensionless concentration of BrO_3^- experiments for catalysts purified using different techniques.

Table 7.6. Kinetic parameters for BrO_3^- reduction for different catalysts synthesized with w_0 value of 12.

Catalyst	$k_{BrO_3^-} \cdot 10^3$ (min^{-1})	R^2
w12/TiO_2	29	0.939
w12/TiO_2 only Pd ME	17	0.992
w12/TiO_2_673AirH	78	0.993
w12/TiO_2 THF	23	0.996
w12/TiO_2 THF_673AirH	130	0.993

7.4. Conclusions

A detailed study on the influence of the Pd NPs synthesis by ME method supported on different supports (AC, TiO_2 and CNT) as catalysts for the BrO_3^- reduction with H_2 in water was carried out. The activity of the catalysts showed the best results for the catalysts supported on N-doped CNT and TiO_2. A lower reaction time was observed for Pd NPs synthesized with w_0 equal to 3. These catalysts showed a higher amount of AOT on the catalysts surface, which led to the catalytic activity, was lower. When the catalysts with w_0 equal to 3 and 12 were subjected to a thermal treatment under air, an increase in activity leading to complete reduction of BrO_3^- was observed as a result of AOT removal. Besides, the destabilization of Pd NPs ME with THF followed by washing with methanol also

proved to be a good procedure to remove AOT. Finally, if this catalyst was treated with thermal treatment with air, this one showed the highest activity in BrO_3^- reduction.

7.5. References

[1] A.M. Perez-Coronado, L. Calvo, J.A. Baeza, J. Palomar, L. Lefferts, J.J. Rodriguez, et al., Metal-surfactant interaction as a tool to control the catalytic selectivity of Pd catalysts, Appl. Catal. A Gen. 529 (2017) 32–39.

[2] L. Xiong, T. He, Synthesis and characterization of ultrafine tungsten and tungsten oxide nanoparticles by a reverse microemulsion-mediated method, Chem. Mater. 18 (2006) 2211–2218.

[3] A.M. Perez-Coronado, L. Calvo, N. Alonso-Morales, F. Heras, J.J. Rodriguez, M.A. Gilarranz, Multiple approaches to control and assess the size of Pd nanoparticles synthesized via water-in-oil microemulsion, Colloids Surfaces A Physicochem. Eng. Asp. 497 (2016) 28–34.

[4] J.A. Baeza, L. Calvo, M.A. Gilarranz, A.F. Mohedano, J.A. Casas, J.J. Rodriguez, Catalytic behavior of size-controlled palladium nanoparticles in the hydrodechlorination of 4-chlorophenol in aqueous phase, J. Catal. 293 (2012) 85–93.

[5] C.M.A.S. Freitas, O.S.G.P. Soares, J.J.M. Órfão, A.M. Fonseca, M.F.R. Pereira, I.C. Neves, Highly efficient reduction of bromate to bromide over mono and bimetallic ZSM5 catalysts, Green Chem. 17 (2015).

[6] M. X- Ray Photoelectron Spectroscopy Database 20, Version 3.0, National Institute of Standards and Technology, Gaithersburg, http://srdata.nist.gov/XPS., (n.d.).

[7] J. Restivo, O.S.G.P. Soares, J.J.M. Órfão, M.F.R. Pereira, Metal assessment for the catalytic reduction of bromate in water under hydrogen, Chem. Eng. J. 263 (2015) 119–126.

[8] Z. Dong, W. Dong, F. Sun, R. Zhu, F. Ouyang, Reaction Kinetics, Mechanisms and Catalysis, React. Kinet. Mech. Catal. 107 (2012) 213–244.

[9] A.E.E. Palomares, C. Franch, T. Yuranova, L. Kiwi-Minsker, E. García-Bordeje, S. Derrouiche, The use of Pd catalysts on carbon-based structured materials for the catalytic hydrogenation of bromates in different types of water, "Applied Catal. B, Environ. 146 (2014) 186–191.

[10] J. Restivo, O.S.G.P. Soares, J.J.M. Órfão, M.F.R. Pereira, Catalytic reduction of bromate over monometallic catalysts on different powder and structured supports, Chem. Eng. J. 309 (2017) 197–205.

[11] J. Sá, J. Bernardi, J.A. Anderson, Imaging of low temperature induced SMSI on Pd/TiO_2 catalysts, Catal. Letters. 114 (2007) 91–95.

[12] A. Markowska-Szczupak, K. Wang, P. Rokicka, M. Endo, Z. Wei, B. Ohtani, et al., The effect of anatase and rutile crystallites isolated from titania P25 photocatalyst on growth of selected mould fungi., J. Photochem. Photobiol. B. 151 (2015) 54–62.

[13] O.S.G.P. Soares, R.P. Rocha, A.G. Gonçalves, J.L. Figueiredo, J.J.M. Órfão, M.F.R. Pereira, Easy method to prepare N-doped carbon nanotubes by ball milling, Carbon N. Y. 91 (2015) 114–121.

[14] H. Chen, Z. Xu, H. Wan, J. Zheng, D. Yin, S. Zheng, Aqueous bromate reduction by catalytic hydrogenation over Pd/Al2O3 catalysts, Appl. Catal. B Environ. 96 (2010) 307–313.

[15] M. Bonarowska, Z. Karpinski, R. Kosydar, T. Szumelda, A. Drelinkiewicz, Hydrodechlorination of CCl_4 over carbon-supported palladium-gold catalysts prepared by the reverse "water-in-oil" microemulsion method, Comptes Rendus Chim. 18 (2015) 1143–1151.

[16] M. Trépanier, A.K. Dalai, N. Abatzoglou, Synthesis of CNT-supported cobalt nanoparticle catalysts using a microemulsion technique: Role of nanoparticle size on reducibility, activity and selectivity in Fischer-Tropsch reactions, Appl. Catal. A Gen. 374 (2010) 79–86.

CHAPTER VIII

Conclusiones principales y trabajos futuros /

Main Conclusions and recommendations for future work

CHAPTER VIII

Conclusiones principales y trabajos futuros

De los trabajos descritos en los capítulos anteriores se han extraído las siguientes conclusiones:

- La relación molar agua-surfactante (w_0) es el factor que más influye sobreel tamaño de las NPs sintetizadas el método de ME. En el caso del sistema estudiado, se obtuvieron NPs de Pd de tamaño medio comprendido entre 3,8 y 11,6 nm cuando se empleó valores de la relación w_0 entre 3 y 12. La eliminación del exceso de AOT es importante para evitar la aglomeración de NPs y evaluar el tamaño de NP, particularmente para menores relaciones w_0, es decir, cuando se utiliza más AOT durante la síntesis.

- El tiempo de reacción entre la ME que contiene el precursor del metal y el agente reductor permite el control del tamaño de las NPs. Para un tiempo bajo de reacción (10 min) se obtuvieron NPs de tamaño más pequeñas y una distribución de tamaño más estrecha.

- Cuando se utilizó $NaBH_4$ como agente reductor durante la síntesis de las NPs, se obtuvieron pequeñas diferencias en el tamaño medio para la síntesis realizada con relaciones de w_0=3 (3,8 nm) y 7 (4,6 nm). Sin embargo, un rango más

amplio del tamaño de las NPs se obtuvo al usar N_2H_4 (7.1 – 9.7 nm). La relación molar agente reductor-metal también mostró cierta influencia.

- La reducción catalítica de NO_2^- realizada por NPs de Pd sintetizadas por el método de ME y sin soportar presentan una aparente sensibilidad estructural. Una mayor actividad se consiguió para las NPs de mayor tamaño. Este comportamiento se atribuyó al bloqueo debido producido por el AOT sobre las NPs de Pd estando relacionado con la fuerte interacción entre AOT y Pd NPs.

- La actividad catalítica de la reducción del NO_2^- se ve reducida cuando se emplearon NPs de Pd no soportadas sintetizadas por el método de ME. Este hecho puede deberse a que este tipo de síntesis presenta una aparente sensibilidad estructural influenciada por la interacción del AOT y las NPs. Además, este comportamiento hizo que la selectividad a NH_4^+ fuera despreciable. Por lo tanto, esta interacción entre el AOT y las NPs de Pd puede ser una herramienta muy interesante para reducir la producción de NH_4^+. Asimismo, el control de la selectividad puede estar relacionado con el bloqueo de centros activos específicos responsables de la generación de NH_4^+.

- El control del pH realizado por un sistema amortiguador de CO_2 fue ventajoso para mejorar la actividad de reducción de NO_2^- y la selectividad hacia N_2 cuando se usaron NPs de Pd sintetizadas mediante ME sin soportar y soportadas como catalizadores.

- Las NPs de Pd sintetizadas vía ME y soportadas sobre AC mostraron una mayor actividad en la reducción de NO_2^- que las no soportadas, probablemente debido a una menor aglomeración de las mismas.

- Las NPs de Pd-AOT que fueron soportadas sobre AC mostraron una selectividad insignificante de NH_4^+. Además, estos catalizadores no mostraron la liberación característica de NH_4^+ cuando se alcanzó el 100 % de conversión de NO_2. Estos resultados sugieren que el AOT que permanece en la superficie de

las NPs de Pd impide la acumulación de las especies precursoras de NH_4^+ sobre la superficie de las mismas.

- Se estudió la viabilidad de la reducción de NO_3^- mediante el empleo de las NPs de Pd-AOT soportadas, sobre la hipótesis de que estas estas NPs pudieran controlar la selectividad a NH_4^+ en la reducción de las especies de NO_2^- intermedias. Con este objetivo se probaron múltiples catalizadores bimetálicos basados en Pd. Sin embargo, cuando se emplearon catalizadores donde la fase del Pd había sido expuesta al AOT en algún punto de la síntesis del catalizador, la actividad de NO_3^- observada fue baja. Este hecho es más acentuado cuando la síntesis de las NPs de se llevaron a cabo mediante el método ME.

- La baja actividad observada para los catalizadores basados en Pd-AOT en la reducción del NO_3^- puede ser debida a que el NO_3^- no consigue alcanzar los centros activos del catalizador donde se llevaría a cabo la reducción. Este hecho se atribuyó a la obstrucción provocada por el AOT, sin embargo estos catalizadores mantuvieron su actividad en la reducción de NO_2^-. Por ello, se concluyó, que el AOT impidió la reacción redox entre el par Pd - Cu, lo que favorece la oxidación del Cu y la pérdida de actividad en la primera etapa de la reducción de NO_3^-.

- La eliminación parcial del AOT por lavado con disolventes orgánicos o tratamiento térmico aumentó la actividad en la reducción de NO_3^-, aumentando simultáneamente la selectividad a NH_4^+.

- Los catalizadores basados en NPs de Pd sintetizadas por via ME e inmovilizadas sobre AC, fueron estudiadas en la reducción de BrO_3^-. Las NPs de Pd soportadas mostraron una mejor actividad que las no soportadas. Además, las NPs de Pd soportados sobre nanotubos de carbono dopados con N, y especialmente dióxido de titanio, mostraron una mayor actividad en la reducción de BrO_3^-.

- En la reducción de BrO_3^- se mejoró sustancialmente la actividad, cuando los catalizadores fueron sometidos a tratamiento térmico. Esto se debió a la eliminación del AOT de la superficie del catalizador. Además, se observó que el tratamiento térmico en atmósfera de aire a 673 K favoreció la eliminación casi completa del AOT, mejorando la actividad de estos catalizadores.

- Las NPs de Pd de tamaños grandes, soportadas sobre TiO_2 y sometidas a tratamiento térmico con aire, para la eliminación del AOT de la superficie del catalizador, mostraron una alta actividad en la reducción de BrO_3^-. Sin embargo, no se obtuvieron resultados concluyentes con respecto a la sensibilidad estructural de los catalizadores basados en Pd-AOT para la reacción de reducción de BrO_3^-.

A través del desarrollo de esta tesis, se ha logrado una mayor comprensión de los factores que afectan a la actividad y selectividad de los catalizadores metálicos sintetizados por el sistema metal-AOT en la reducción de NO_3^-, NO_2^- y BrO_3^- en fase acuosa. Sobre la base de los conocimientos generados, se propone el siguiente trabajo de investigación futuro:

- Teniendo en cuenta los buenos resultados obtenidos en la reducción de NO_2^- con NPs de Pd-AOT NPs soportadas, se propone el desarrollo de un proceso en dos etapas. En la primera etapa, se requeriría un catalizador selectivo para la reducción de NO_3^- a NO_2^- y en la segunda etapa el catalizador basado en NPs de Pd-AOT reducirá el NO_2^- a N_2 con una selectividad muy alta.
- El estudio de la estabilidad de las NPs de Pd-AOT en reactores continuos sería de especial interés para evaluar la viabilidad del concepto de proceso en dos etapas. De la misma manera, sería de interés la aplicación a aguas reales teniendo en cuenta la influencia de la materia inorgánica y orgánica.
- Se podrían explorar diferentes tensioactivos o agentes protectores que conduzcan al control de la generación de NH_4^+ pero que permitan la interacción

entre el par redox Pd:Cu para conseguir la reducción de NO_3^-.En este camino, debería estudiarse también el papel del soporte.

- La viabilidad del control de selectividad gracias al bloqueo de los centros activos producidos por los agentes tensioactivos podrían ser de interés en otras reacciones.

CHAPTER VIII

Main Conclusions and recommendations for future work

The following main conclusions have been extracted from the work described in the former chapters:

- The water-to-surfactant (w_0) molar ratio is the most influencing factor in the synthesis of Pd NPs obtained by the ME method. In the case of the system studied, Pd NPs with a mean size range between 3.8 and 11.6 nm were obtained when values of w_0 between 3 and 12 were used. The removal of the excess of AOT is important in order to avoid agglomeration of NPs and assess NP size, particularly for lower w_0 ratios, i.e. when more AOT is used during the synthesis.

- The reaction time between the MEs containing the metal precursor and the reducing agent allows also control of the NPs size. A low reaction time (10 min) led to smaller NPs with a narrower size distribution.

- Small differences in mean size were obtained for the synthesis at $w_0 = 3$ (3.8 nm) and 7 (4.6 nm) when $NaBH_4$ was used as reducing agent, in contrast to the

broader range achieved when using N_2H_4 (7.1 – 9.7 nm). The reducing agent-to-metal molar ratio also showed some influence.

- The catalytic reduction of NO_2^- using unsupported Pd NPs synthesized by ME method exhibits apparent structure sensitiveness, with NPs of higher size leading to higher activity. This behavior can be attributed to different shielding by AOT of Pd NPs of different size, and is related to the strong interaction between AOT and Pd NPs.

- The shielding of unsupported Pd NPs by AOT reduces the catalytic activity in the reduction of NO_2^-, but leads to negligible generation of NH_4^+, which can be a very interesting tool to reduce the selectivity to NH_4^+. The control of the selectivity may be related to blocking of specific active centers responsible for the generation of NH_4^+.

- The control of pH by buffering with CO_2 was beneficial for increasing NO_2^- reduction activity and N_2 selectivity when using both unsupported and supported Pd NPs as catalysts.

- The Pd NPs synthesized via ME supported on activated carbon showed a higher activity in the reduction of NO_2^- than the unsupported ones, probably due to lower agglomeration.

- The catalyst prepared by immobilization of Pd-AOT NPs on activated carbon also exhibited a negligible selectivity to NH_4^+. In batch reactions these catalysts did not show the characteristic release of NH_4^+ at 100% NO_2^- conversion. These results also suggest that the AOT remaining on the surface of the Pd NPs prevents the accumulation on the NP surface of NH_4^+ precursor species and their further release.

- An evaluation of the applicability of the Pd-AOT NPs to the reduction NO_3^- was carried out, on the basis of the hypothesis that these NPs could control the

selectivity to NH_4^+ in the reduction of the intermediate NO_2^- species. With this purpose a number bimetallic catalysts based on Pd were tested. However, a very low activity was achieved for those with Pd metal phase interacting with AOT, particularly when the synthesis of Pd NPs was carried out by the ME method.

- The low activity in NO_3^- reduction of the bimetallic catalysts may indicate that NO_3^- cannot reach the active sites for reduction due to AOT blockage, although the catalysts did maintain the activity in the reduction of NO_2^-. AOT seems to block the redox reaction between Pd and Cu, which leads to the oxidation of the Cu phase and the loss of activity in the first stage in the reduction of NO_2^-.

- The partial removal of AOT by washing or thermal treatment increases the activity in NO_3^- reduction, but the selectivity to NH_4^+ increases simultaneously.

- Catalysts based on immobilized Pd NPs obtained by ME synthesis were also evaluated in the reduction of BrO_3^-. The activity of Pd NPs was improved respect to unsupported ones. The catalysts supported on N-doped carbon nanotubes, and especially titanium dioxide, showed a higher activity in the reduction of BrO_3^-.

- The activity of the catalysts in the BrO_3^- reduction reaction was improved substantially when they were subjected to thermal treatment due to AOT removal. A thermal treatment at 673 K in air atmosphere provided with nearly complete removal of AOT and AOT degradation fragments, hence a higher activity of the catalysts was observed.

- Large Pd NPs supported on titanium dioxide and subjected to AOT removal showed a higher activity in BrO_3^- reduction, but no conclusive results were obtained regarding the structure sensitiveness of the BrO_3^- reduction reaction.

Through this thesis, a higher understanding has been achieved on the factors that affect the activity and selectivity of metal catalysts based on metal-AOT in the reduction of NO_3^-, NO_2^- and BrO_3^- in aqueous phase. On the basis of the knowledge generated, some future research work is proposed:

- Taking into account the good results obtained in the reduction of NO_2^- with supported Pd-AOT NPs, the development of a two-step process is proposed. In the first step, a selective catalyst for the reduction $NO_3^-$to NO_2^- would be required, and in the second step the catalyst based on Pd-AOT NPs would reduce NO_2^- to nitrogen with a very high selectivity.
- The study of the stability of the Pd-AOT NPs in continuous reactors would be essential in order to assess the applicability of the concept of the two-step process. Likewise, application to real waters taking into consideration the influence of inorganic and organic matter would be of interest.
- Alternative surfactants or protective agents leading to the control of NH_4^+ generation but enabling Pd-Cu interaction should be explored in order to achieve application to NO_3^- reduction. In this sense, the role of the catalytic support should be also considered.
- The applicability of the concept of selectivity control thanks to the blockage of active centers agents could be of interest in other reactions.

APPENDIX

Appendix A. Supplementary data

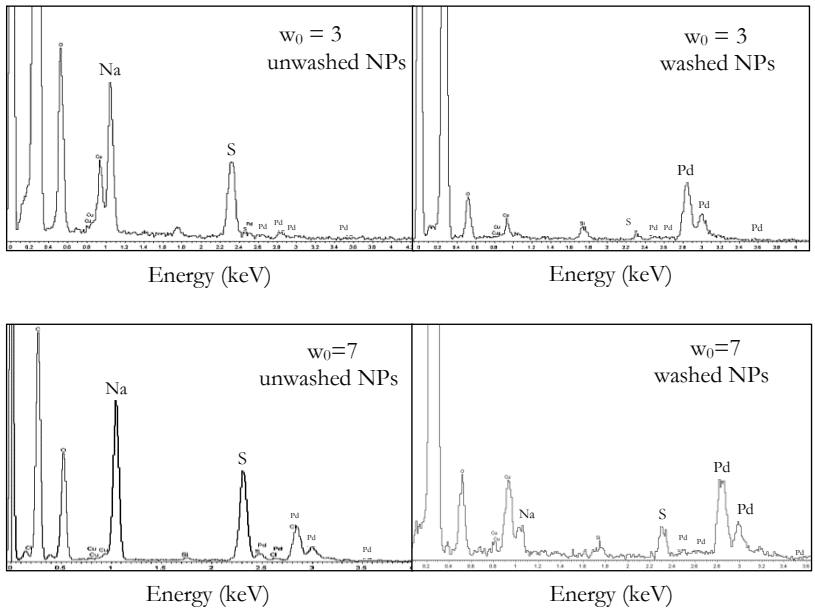

Figure A.1. EDXS profiles for unwashed and washed Pd NPs synthesized with N_2H_4/Pd = 60 mol/mol, reaction time = 10 min and w_o = 3-7.

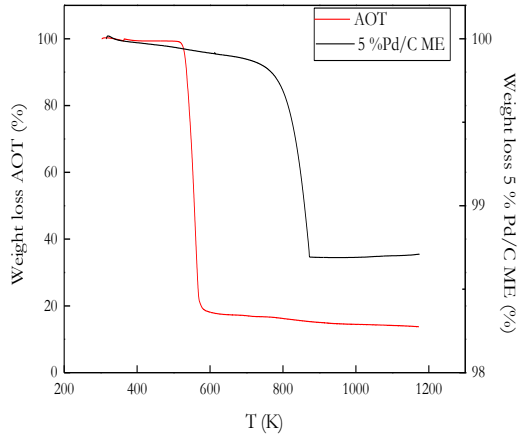

Figure A.2. Thermogravimetric analysis curves of AOT and 5 % Pd/C ME.

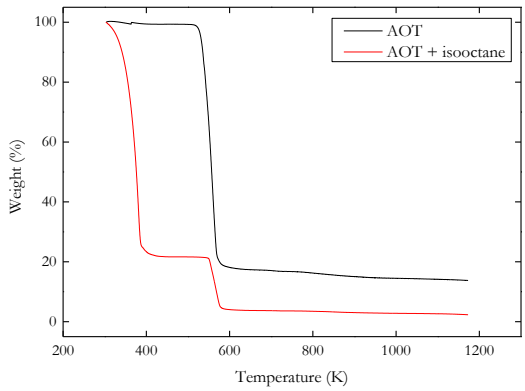

Figure A.3. Thermogravimetric analysis curves of AOT and AOT in dissolution of isooctane.

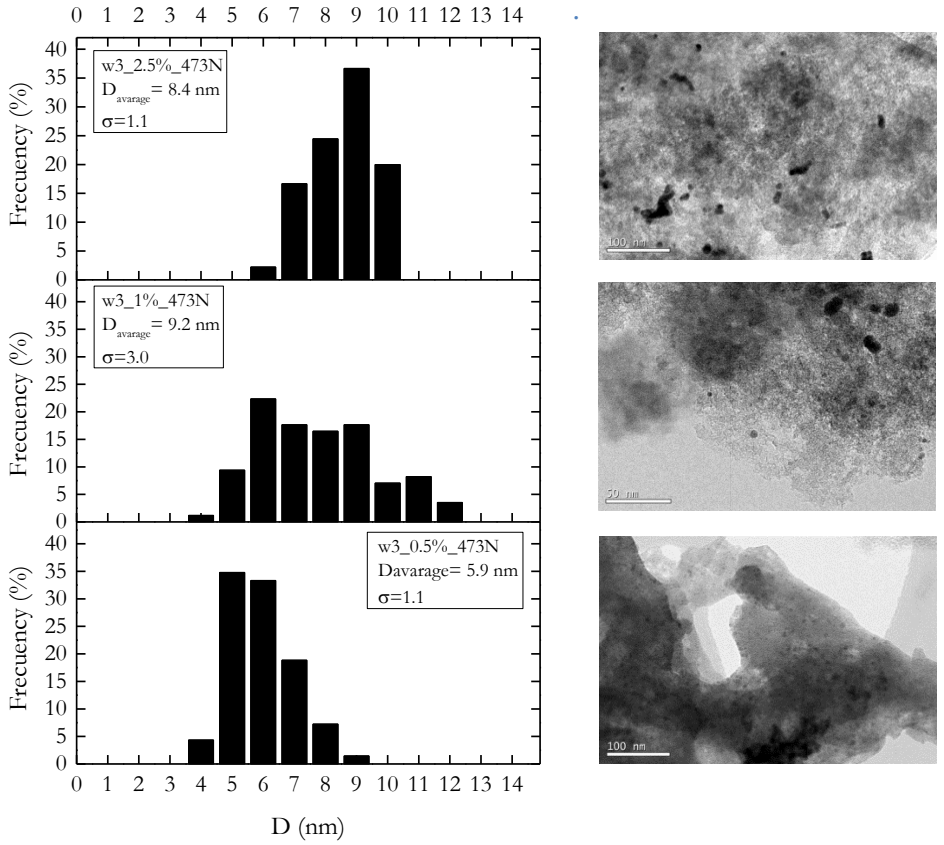

Figure A.4. Particle size distributions and TEM images of the NPs samples obtained at different weight percent of active metals on support. The relation molar water-to-surfactant used is 3.

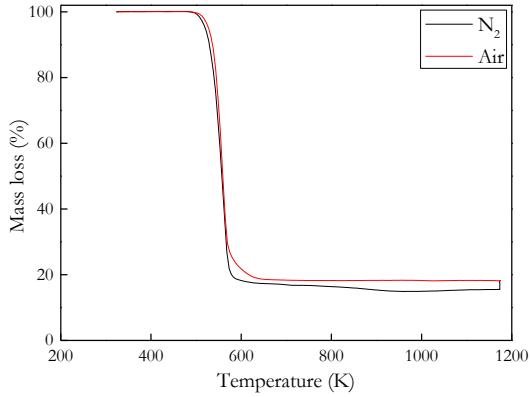

Figure A.5. Thermogravimetric analysis curves of AOT in air and N_2.

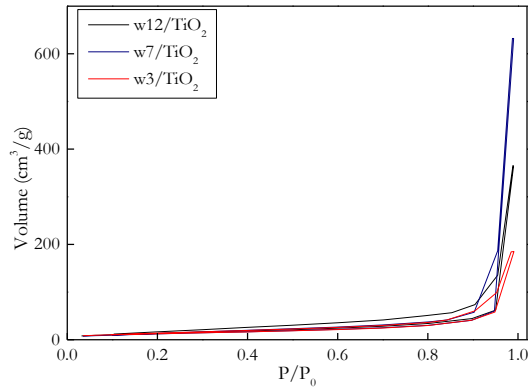

Figure A.6. N_2 adsorption-desorption isotherms of the Pd NPs supported on TiO_2.

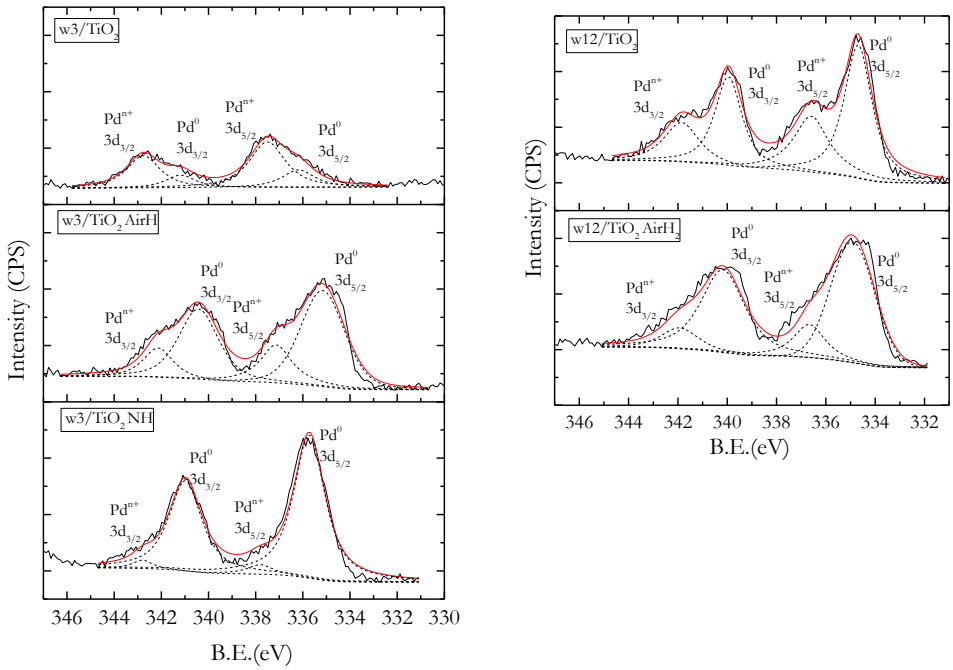

Figure A.7. XPS spectra of Pd NPs synthesized with w_0 values of 3 and 12 for Pd NPs supported on TiO_2, Pd NPs supported on TiO_2 subjected to thermal treatment under air atmosphere and afterwards reduced with H_2.

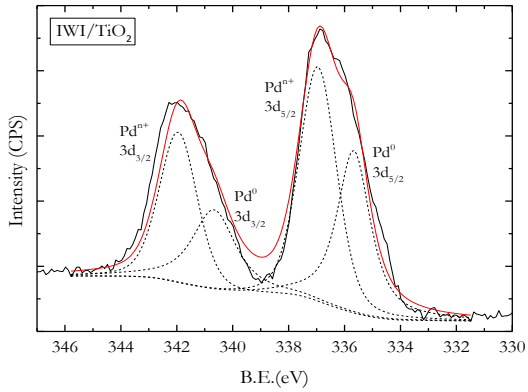

Figure A.8. XPS spectra of Pd NPs of IWI serie.

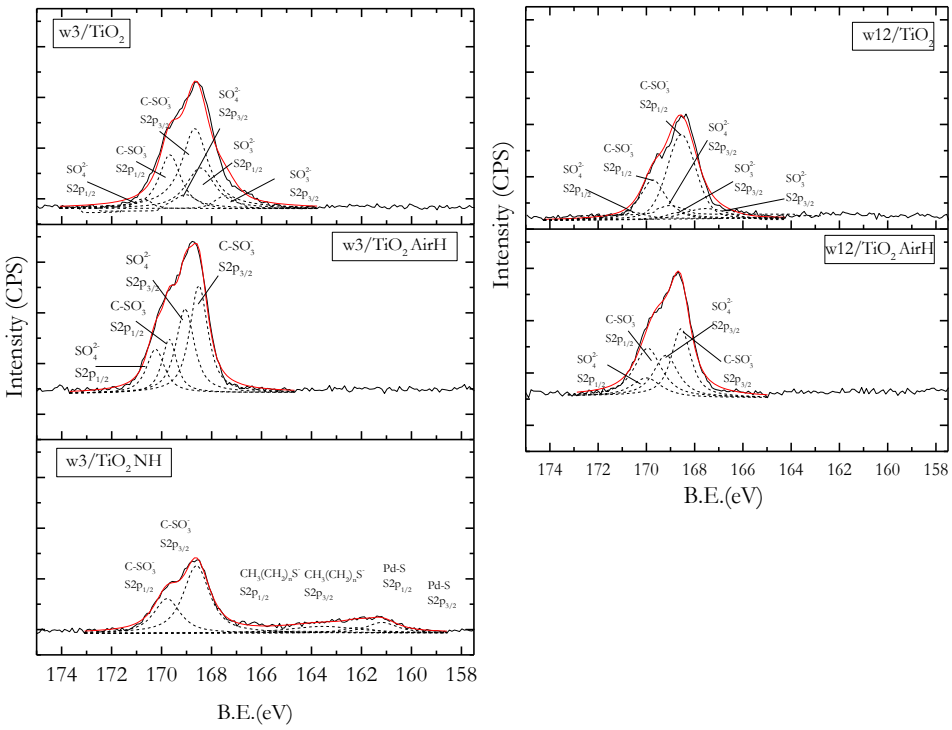

Figure A.9. XPS data for S (2p) core levels of Pd NPs synthesized with w_0 values of 3 and 12 for Pd NPs supported on TiO_2, Pd NPs supported on TiO_2 subjected to thermal treatment under air atmosphere and afterwards reduced with H2, and Pd NPs supported on TiO_2 subjected to thermal treatment under N_2.